

21663442

MICHIGAN STATE UNIVERSITY LIBRARIES



3 1293 00550 3432

**LIBRARY**  
**Michigan State**  
**University**

This is to certify that the  
dissertation entitled  
Modeling the sorption of water, and the effect of sorbed  
water on the solubility and diffusivity of oxygen in an  
amorphous polyamide.

presented by

Ruben J. Hernandez-Macias

has been accepted towards fulfillment  
of the requirements for

Ph. D. degree in Chemical Engineering

Major professor

Date February 23, 1989



**RETURNING MATERIALS:**  
Place in book drop to  
remove this checkout from  
your record. FINES will  
be charged if book is  
returned after the date  
stamped below.

MAR 13 1997	FEB 13 1997	
056	NOV 02 1997	FEB 08 2000
SEP 23 1997		FEB 14 00
AUG 28 1997	JAN 11 2000	
SEP 05 1997		
SEP 26 1997		

MODELING THE SORPTION OF WATER, AND THE EFFECT OF SORBED  
WATER ON THE SOLUBILITY AND DIFFUSIVITY OF OXYGEN IN AN  
AMORPHOUS POLYAMIDE.

by

Ruben J. Hernandez

A DISSERTATION

Submitted to

Michigan State University

in partial fulfillment of the requirements

for the degree of

DOCTOR OF PHILOSOPHY

Department of Chemical Engineering

1989

## ABSTRACT

MODELING THE SORPTION OF WATER, AND THE EFFECT OF SORBED WATER ON THE SOLUBILITY AND DIFFUSIVITY OF OXYGEN IN AN AMORPHOUS POLYAMIDE.

by

Ruben J. Hernandez

Glassy amorphous polyamides are part of a new kind of polymeric material that have excellent physical and mechanical properties. These materials are non-crystalline and show interesting mass transfer behavior with vapors and gases. In the case of Nylon 6I/6T, a totally amorphous polyamide recently developed, its interaction with water vapor affected the transport of oxygen.

Sorption, permeation, FTIR spectroscopy, density and thermal relaxation studies have been applied to describe the behavior of the system amorphous polyamide/water and amorphous polyamide/water/oxygen.

The dual-mode sorption model presented in this study was found to describe accurately the sorption of water by the amorphous polyamide, over a broad range of water activity and predicted clustering of the sorbant. The Langmuir equation was used to describe the chemisorbed solute and the

Flory-Huggins equation was used to describe the volume fraction of water that is not chemisorbed.

The sorbed molecules of water in the glassy amorphous polyamide, showed a depression in the oxygen permeability values as a function of polymer moisture content. The oxygen permeability behavior was analysed in terms of the multiplicative effect of a mobility and solubility term. The analysis of the oxygen solubility values within the polymer/water system, provided a complementary framework for the dual-mode sorption model.

Copyrighth by  
Ruben J. Hernandez Macias  
1989

To  
Natalia and  
Daniel Federico.

Let us hold the torch of Science even if it is only for a  
second.

## ACKNOWLEDGMENTS

I wish to thank the Department of Chemical Engineering, the Division of Engineering Research and the School of Packaging for offering me the support and facilities to carry out these studies.

I also want to acknowledge the grant received from E. I. DuPont de Nemours and Company Inc.

I want to thank Drs. E. A. Grulke and J. R. Giacin for continuous advise and support.

I am grateful to my Guidance Committee members Drs. K. Jayaraman, L. T. Drzal, from the Department of Chemical Engineering, and Dr. C. Talkowski from E. I. DuPont Co.

I also want to thank V. Kalankyar, Dr. P. Blatz from E. I. DuPont Co. and Dr. J. DeLong, from The Division of Engineering Research for helping to run some tests.

At last, but not least, my deepest appreciation to my parents Vicente Hernandez and Dolores Macias, and to my wife Alicia Gardiol. I could not have done it without them.

## LIST OF CONTENTS

	PAGE
LIST OF TABLES. . . . .	ix
LIST OF FIGURES . . . . .	xi
INTRODUCTION. . . . .	1
References. . . . .	7
CHAPTER I. THE EVALUATION OF THE AROMA BARRIER PROPER-	
TIES OF POLYMER FILMS. . . . .	11
INTRODUCTION. . . . .	11
Modeling Considerations. . . . .	.17
Permeability Measurements. . . . .	.20
Isostatic Method. . . . .	.20
Quasi-isostatic Method. . . . .	.25
Sorption Measurements. . . . .	27
Polymer Films. . . . .	27
Polymer Spheres. . . . .	28
Desorption Measurements. . . . .	30
Solubility Coefficient. . . . .	32
Diffusion Coefficient. . . . .	.32
METHODS. . . . .	.34
Determination of Permeation Methods. . . . .	.34
Isostatic procedure. . . . .	34
Quasi-isostatic Procedure. . . . .	37
Sorption Measurements. . . . .	.39
APPLICATIONS. . . . .	42
Quasi-isostatic Procedure. . . . .	42
Isostatic Procedure. . . . .	46

Sorption Procedure. . . . .	.47
SUMMARY. . . . .	.49
REFERENCES. . . . .	50
CHAPTER II. THE SORPTION OF WATER VAPOR BY AN AMORPHOUS	
POLYAMIDE. . . . .	56
ABSTRACT. . . . .	56
INTRODUCTION. . . . .	57
DUAL MODE SORPTION MODELS. . . . .	.58
Model for Gas Sorption in Glassy Polymers. . .	58
Models for Polar Systems at High Solute	
Activities. . . . .	.59
CLUSTERING OF SOLUTE MOLECULES. . . . .	62
Modified Dual Mode Sorption Model. . . . .	.64
EXPERIMENTAL METHODS. . . . .	65
Polymer Films. . . . .	65
Equilibrium Sorption Data. . . . .	66
Density Experiments. . . . .	66
Fourier Transform Infrared Spectroscopy. . . .	66
DSC and Dielectric Experiments. . . . .	67
RESULTS AND DISCUSSION . . . . .	.67
Equilibrium Sorption Isotherm. . . . .	67
Parameter Estimation for Equation 8. . . . .	70
Sensitivity Coefficients. . . . .	.74
Clustering Analysis. . . . .	77
Physical Evidence for Solute Binding. . . . .	.78
Relaxation Temperatures. . . . .	83
Density Data. . . . .	.84

Proposed Mechanism for Effects of Water Sorption on Physical Properties of Amorphous Polyamide. . . . .	87
LITERATURE CITED. . . . .	88
CHAPTER III. EFFECT OF WATER CONTENT ON THE SOLUBILITY, DIFFUSION AND PERMEABILITY IN NYLON 6I/6T. . . . .	93
INTRODUCTION. . . . .	93
Oxygen Permeability as Function of Polymer Water Activity. . . . .	95
Oxygen Solubility and Diffusion coefficient. . . . .	96
EXPERIMENTAL METHODS. . . . .	99
Polymer Films. . . . .	99
Equilibrium Sorption Data. . . . .	99
Oxygen Permeability Studies. . . . .	100
RESULTS AND DISCUSSION. . . . .	102
Equilibrium Sorption isotherms. . . . .	102
Calculation of Oxygen Solubility. . . . .	108
Conditions for Applying Eqn. 10 . . . . .	110
Permeability Data . . . . .	113
Oxygen Solubility. . . . .	123
Oxygen Diffusion Coefficient. . . . .	132
CONCLUSIONS . . . . .	135
SUMMARY. . . . .	136
REFERENCES. . . . .	138
APPENDIX A. . . . .	140
APPENDIX B. . . . .	149

## LIST OF TABLES

CHAPTER	TABLE		PAGE
1	1	Permeability constants and lag time diffusion coefficients for toluene in selected polypropylene based structures.	43
	2	Values for eqn.(23) obtained for the system Oxygen/Nylon 6I/6T, at 22.0°C and water activity = 0.441.	48
2	1	Models for polar system at high solute activities.	60
	2	Experimental data at 23 °C.	68
	3	Langmuir and Flory-Huggins volume fraction contributions.	73
	4	Amide I, Amide II and CH absorption frequencies.	80
	5	Intensity ratios of Amide I and Amide II with respect to CH bands.	80
3	1	Water polymer isotherm at 5 °C	103
	2	Water polymer isotherm at 23 °C	104
	3	Water polymer isotherm at 42 °C	105
	4	Values of $\chi$ , K and B as a function of temperature.	109
	5	Water activity values at the onset of cluster formation.	109
	6	Solubility of oxygen in Nylon 6I/6T as a function of pressure at 24 °C.	111
	7	Diffusion, solubility and permeability values of oxygen at 11.9 °C.	114
	8	Diffusion, solubility and permeability values of oxygen at 22.0 °C.	115
	9	Diffusion, solubility and permeability values of oxygen at 40.3 °C.	116
	10	Values of the constants for eqn. 6	123

11	Experimental and calculated solubility of oxygen at 11.9 °C.	126
12	Experimental and calculated solubility of oxygen at 22.0 °C.	127
13	Experimental and calculated solubility of oxygen at 40.3 °C.	128
APPENDIX B	Activation energy as a function of $A_w$ .	173

## LIST OF FIGURES

CHAPTER	FIGURE		PAGE
1	1	Transmission rate profile curve for toluene vapor through oriented PET at 90 ppm and 23 °C.	21
	2	Generalized transmission rate profile curve by quasi-isostatic method test.	26
	3	A plot of $M_t/M_\infty$ vs. $t^{1/2}$ for d-limonene by high density polyethylene/sealant structure at 1.5 ppm and 20.5 °C.	29
	4	Schematic diagram of the isostatic test apparatus.	35
	5	Schematic diagram of the quasi-isostatic test apparatus.	38
	6	Schematic diagram of the electrobalance test apparatus.	41
	7	Effect of penetrant concentration on the transmission of toluene vapor at 23 °C through coextruded OPP.	44
	8	Effect of penetrant concentration on the transmission of the toluene at 23 °C through biaxially oriented polypropylene.	45
2	1	Experimental sorption values and Flory-Huggins fitting.	69
	2	Experimental sorption values and Flory-Huggins fitting at low activity values.	71
	3	Best fit for the Langmuir-Flory-Huggins model.	72
	4	Sensitivity coefficients as a function of activity.	75
	5	Clustering function as a function of water activity.	76
	6	Typical FTIR spectrum of the amorphous polyamide recorded at room temperature.	79
	7	Spectrum region of Amide II as a function of activity.	81

	8	Glass transition temperatures as a function of activity.	85
	9	Density as a function of activity.	86
3	1	Oxygen permeability apparatus.	101
	2	Water sorption isotherms at 5 °C, 23 °C and 42 °C.	106
	3	Values of K and B of the Langmuir equation.	107
	4	Solubility of oxygen as a function of partial pressure at 24 °C.	112
	5	Oxygen permeability values at 11.9 °C, 22.0 °C and 40.3 °C.	117
	6	Diffusion coefficient values at 11.9 °C, 22.0 °C and 40.3 °C.	118
	7	Oxygen solubility values at 11.9 °C, 22.0 °C and 40.3 °C.	119
	8	Solubility and diffusion coefficient of oxygen at 11.9 °C.	120
	9	Solubility and diffusion coefficient of oxygen at 22.0 °C.	121
	10	Solubility and diffusion coefficient of oxygen at 40.3 °C.	122
	11	Oxygen solubility at 11.9 °C as function of $a_w$ .	129
	12	Oxygen solubility at 22.0 °C as function of $a_w$ .	130
	13	Oxygen solubility at 40.3 °C as function of $a_w$ .	131
	14	Activation energy as a function of water activity.	134
APPENDIX B		Activation energy versus pre-exponential term for the diffusion of oxygen in the amorphous nylon.	174

## INTRODUCTION

The presence of sorbed or diffusing low molecular weight penetrants in polymer solids often has a marked effect on material properties. The way in which the penetrant is sorbed and distributed within the polymeric matrix can be expected to affect the penetrant mobility, the local polymer chain segmental mobility, and related parameters such as free volume distribution and eventually, efficiency of free volume utilization [1]. Two major classes of polymer properties that are controlled by the segmental mobility of the polymer chain are the transport and mechanical properties. The mobility of polymer chains is determined by the polymer structure and its morphology, and is affected by sorbed molecules and the mode of sorption. For a given polymer structure, the transport and mechanical properties will therefore depend on the precise interaction and the sorbed penetrant.

Penetrant molecules are sorbed within the polymer in different modes [2]. The nature of interactions between penetrant and polymer is an important factor in the manner in which the molecules of penetrant are distributed within the polymeric matrix. Particular sorption modes of interest are the localization of penetrant molecules at specific polymer sites that may be more or less active, randomly

dispersed (free) penetrant molecules and sorbed-sorbed molecules resulting in clustering formation. The total penetrant sorption process will probably be the result of the combination of these three different mechanisms or sorption modes.

The specific sorption process may be described as a function of penetrant concentration or activity, temperature, and time to reach equilibrium, as well as the composition of the penetrant-polymer system. Therefore, polymer structure, availability of specific active sites of interaction in the polymer, chain stiffness or segmental mobility, plus the physico-chemical characteristics of the penetrant (gas, water or organic compounds) determine the mode and mechanisms of sorption and transport of the penetrant within the polymer.

A very common model that describes sorption of penetrants in glassy polymers was introduced by Matthes in 1944, using the concept of the dual-mode sorption mechanism [3]. He combined a Langmuir and a Henry's law type expression to describe the sorption of water by a cellulosic material. A large number of other investigators have extended the use of this model to describe the sorption of fixed gases (most of them above the critical temperature) such as  $\text{CO}_2$ ,  $\text{CH}_4$ ,  $\text{C}_2\text{H}_6$ , etc., by different polymers, [4]-[12]. This model has also

been used to correlate the sorption of mixed gases in glassy polymers [13].

Although this model based, on Langmuir and Henry equations, may well describe the sorption of gases by polymers, it actually overpredicts the sorption of vapors by polymers, and is not able to predict the cluster formation of the absorbed molecules.

Another important characteristic of this model is that Henry's law of dissolution does not distinguish solutions containing only molecules of ordinary size from those solutions of very large molecules. Flory [14-15] and Huggins [16], derived an equation for the activity coefficient of a solute in a polymer, as a function of volume fraction of the solute. At low activity values, this equation underpredicts the sorption of vapor by polymers and predicts clustering of the solute within the polymer in the whole range of solute activity.

The formation of clusters can be predicted by applying the clustering function to a specific model describing the sorption behavior of a penetrant-polymer system. The clustering function ([17], [18]) is a monotone, increasing function of the probability of finding molecules of the same kind close to one another. Orofino et al., [19], applied the clustering function to several polymer-water systems obeying Flory-Huggins thermodynamics. However, when the clustering function is applied to the Flory-Huggins model, clustering is predicted in the whole range of vapor activity.

Polyamides, as most polymeric materials, sorb both water and organic vapors. In the past years polyamide-water systems have been the subject of a number of studies, [19]-[23]. The amide function of the polymer participates in hydrogen bonding, where the hydrogen on a nitrogen atom associates with the carbonyl oxygen atom of an adjacent molecule. Such non-covalent bonds are relatively strong (8 kcal/mol), and serve to provide a cross-link network between polymer molecules. They exist in the amorphous as well as in the crystalline regions of polyamides [20]. Disruption of hydrogen bonding in the noncrystalline region is necessary for a solvent to attack polyamides and is a major factor in the mechanism of absorption of molecules that surround the polymer [24].

Puffr and Sabenda [23] suggested a mechanism of water sorption into Nylon 6 at room temperature, which involved two neighboring amide groups in water-accessible regions forming a sorption center. This sorption center could accommodate up to 3 water molecules, involving hydrogen bonding between adjacent amide groups. Additional sorbed water molecules may be accommodated via a clustering mechanism. Papir et al. [25], working also on the nature of the absorption of water in Nylon 6 confirmed the hypothesis of Puffr and Sabenda, in that two "types" of water, tightly

bound and loosely bound, can exist within the polymer matrix.

Fourier transform infrared (FTIR) spectroscopy is considered a powerful tool for polymer characterization, [27]-[28]. In the present study FTIR spectroscopy has been employed to glean information related to the nature, strength, and number of intermolecular forces occurring between sorbed water and an amorphous polyamide. The FTIR spectroscopy studies focused specifically on the detection of possible changes in hydrogen bonding between N-H and carbonyl groups. This was done by observing the vibrational modes of the amide group, consisting of the Amide I and Amide II bands, as a function of polymer water content.

In recent years, a totally amorphous polyamide has been developed, the 6I/6T (70/30) amorphous nylon [29]. Preliminary studies on the effect of water sorption on the barrier properties of this polymer showed atypical behavior, as compared to semicrystalline nylons under the same conditions. For example, oxygen permeability in Nylon 66 increases as a function of moisture content of the polymer, while it showed a decrease in the amorphous nylon 6I/6T. Further, the tensile modulus for Nylon 66 decreases as a function of moisture content, while the tensile modulus for the amorphous nylon increases with increase in moisture content. The intriguing behavior of the water-nylon systems

has made evident the need of a model that would provide a more quantitative description of the mechanism of the sorption process of water by polar polymers. The thrust is also to look for a model that may be used to explain the sorption and diffusion behavior of organic vapor penetrants in polar polymer. This is important not only for theoretical but also for practical reasons. Most polymer materials are normally exposed to vapors (water or organic) and the interaction that takes place affects the performance of such polymer as is the case for example, in polymer composites or product-package interactions.

The present research work has addressed, therefore, two major objectives:

I. To complete an experimental description of the equilibrium sorption process of the binary system water-amorphous polyamide, and to describe the experimental behavior of the diffusion and solubility of oxygen within the system water-amorphous polyamide.

II. To develop a theoretical framework for interpreting the mechanism of sorption equilibrium of the binary system water-polymer, and of the three components system oxygen-water-polymer. It is expected that the conclusions of this work will be valid to describe the equilibrium sorption of organic compounds-polymer systems.

## REFERENCES

1. Sfirakis, A. and C. E. Rogers, Effects of Sorption Modes on the Transport and Physical Properties of Nylon 6, *Polym. Eng. Sc.*, 20, 4, 294-299 (1980).
2. Rogers, C. E., Physics and Chemistry of the Organic Solid State, Vol II, Chapter 6, Interscience, N. Y. (1965).
3. Matthes, A., Zur Theorie des Quellungsvorganges an Gelen, *Kolloid-Z. Z.*, 108, 79-94 (1944).
4. Michaels, A. S., W. R. Veith and J. A. Barrie, Diffusion of Gases in Polyethylene Terephthalate, *J. Appl. Phys.*, 35, (1), 13-65 (1963).
5. Veith, W. R. and J. A. Eilenberg, Gas Transport in Glassy Polymers, *J. Appl. Polym. Sc.*, 16, 945-954 (1972).
6. Veith, W. R., J. M. Howell and J. H. Hsieh, Dual Sorption Theory, *J. Membr. Sc.*, 1 (1976) 177-220.
7. Koros, W. J., and D. R. Paul, Transient and Steady State Permeation in Polyethylene Terephthalate, *J. Polym. Sc. Phys. Ed.*, 21, 441-465 (1983).

8. Kulkarni, S. S. and S. A. Stern, The Diffusion of CO<sub>2</sub>, CH<sub>4</sub>, C<sub>2</sub>H<sub>4</sub> and C<sub>3</sub>H<sub>8</sub> in Polyethylene at Elevated Pressures, J. Polym. Sc. Phys. Ed., 21, 441-465 (1983).
9. Barrie, J. A. and P.S. Sagoo, The Sorption and Diffusion of Water in Epoxi Resins, J. Membr. Sc., 18 (1984) 197-210.
10. Barrer, R. M., Diffusivities in Glassy Polymers for the Dual Mode Sorption Model, J. Membr. Sc., 18 (1984) 25-35.
11. Koros, W. J., R. T. Chern, V. Stannett and H. B. Hopfenberg, A Model for Permeation of Mixed Gases and Vapors in Glassy Polymers, J. Polym. Sc. Phys. Ed., 19, 1513-1530 (1981).
12. Uragami, T., H. B. Hopfenberg, W. J. Koros, D. K. Yang, V. Stannett and R. T. Chern, Dual-Mode Analysis of Subatmospheric-Pressure CO<sub>2</sub> Sorption and Transport in Kapton H Polyimide Film, J. Polym. Sc. Phys. Ed., 24, 779-792 (1986).
13. Koros, W. J., Model for Sorption of Mixed Gases in Polymers, J. Polym. Sc. Phys. Ed., 18, 981-992 (1980).

14. Flory, P. J., Thermodynamics of High Polymers Solutions, J. Chem. Phys., 10, 51 (1942).
15. Flory, P. J., Principles of Polymer Chemistry, Cornell University Press, Ithaca, NY, (1953).
16. Huggins, M. L., Thermodynamic Properties of Solutions of Long-Chain Compounds, Ann. NY Acad. Sci., 42, 1 (1942).
17. Zimm, B. H. and J. L. Lundberg, Sorption of Vapors by High Polymers, J. Phys. Chem., 60, 425-428 (1956).
18. Lundberg, J. L., Clustering Theory and Vapor Sorption by High Polymers, J. Macrom. Sci. Phys., B3 (4), 693-711 (1969).
19. Orofino, T. A., H. B. Hopfenberg and V. Stannett, Characterization of Penetrant Clustering in Polymers, J. Macrom. Sci. Phys., B3 (4), 777-788 (1969).
20. Cannon, C. G., Spectrochim. Acta, 16, 302 (1960).
21. Starkweather, H. W., The Effect of Water on Some Properties of Oriented Nylon, J. Macrom. Sci. Phys., B3 (4), 727-736 (1969).

22. Skirrow, G. and Young K. R., Sorption, Diffusion and Conduction in Polyamide-Penetrant systems: I. Sorption Phenomena, *Polymer*, 15, 771-776 (1974).
23. Puffr, R. and J. Sabenda, On the Structure and Properties of Polyamides: XXVII. The Sorption of Water in Polyamides. *J. Polym. Sc. Part C*, 16, 79-93 (1967).
24. Kohan, M. I., Nylon Plastics, J. Wiley, N.Y. (1973).
25. Papir, Y. S., Kapur, S., C. E. Rogers and E. Baer, Effect of Orientation, Anisotropy, and Water Vapor on the Relaxation Behavior of Nylon 6 From 4.2 to 300 °K, *J. Polym. Sc. A-2*, 10, 1305 (1972).
26. Koenig, J. L., Fourier Transform Infrared Spectroscopy of Polymers, *Advances in Polymer Science*, 54, 87 (1984).
27. Painter, P. C., M. M. Coleman and J. L. Koenig, Theory of Vibrational Spectroscopy with Application in Polymers, J. Wiley, N. Y. (1981).
28. Siesler, H. W. and K. Holland-Moritz, Infrared and Raman Spectroscopy of Polymers, M. Dekker Inc. N. Y. (1980).
29. Blatz, P. and C. Talkowski, Personal Communication (1987).

## CHAPTER I

### THE EVALUATION OF THE AROMA BARRIER PROPERTIES OF POLYMER FILMS\*\*

Key Words: Aroma barrier, organic penetrants, diffusion, sorption, permeability, barrier polymer films, polypropylene, high density polyethylene.

#### INTRODUCTION

The shift from absolute barrier type packages, such as cans and bottles, to semi-permeables polymeric packaging systems has created a need to develop a better understanding of the transport of gases, vapors, and other low molecular weight moieties through polymer films. The transport of permeants such as oxygen, carbon dioxide and water vapor through polymer structures has been the subject of numerous investigations, and standard test methods are available for determining transmission rates for these permeants (ASTM E96-66, ASTM D3985-81).

---

\*\* This review paper was published in the Journal of Plastic Film and Sheeting. Volume 2, 187-211 (1986).

In contrast, while the transport of organic penetrants through packaging materials have been the subject of several recent investigations, there is a paucity of data available in this area.

This paper will, therefore, focus on the various procedures developed for quantifying the rate of diffusion of organic penetrants through barrier membranes and describe in detail the specific procedure employed in the studies reported.

Pye et al. (1976) described a continuous or isostatic procedure for measuring the diffusivity properties of polymer membranes that employed two gas chromatographs connected to a cell. One chromatograph was equipped with flame ionization detection and the second was based on a thermal conductivity cell. This was achieved by incorporating gas sampling valves in the carrier gas stream. With multiple detectors, the authors were able to study the diffusion of gases as well as organic vapors through polymer films. The system described by Pye et al. also included a gas and organic vapor mixture generating apparatus.

Niebergall et al. (1978) also described a method for determining the diffusivity values of the various organic penetrant/barrier film systems based on the isostatic procedure of test. The apparatus developed by these authors was designed to allow measurement of transmission rates for mixtures of organic vapors through barrier structures as

function of penetrant concentration, temperature and relative humidity.

Zobel (1982) has also reported an isostatic method for measuring the permeability rate of films to organic vapors at low penetrant concentrations and, in recent articles, described a modification of the previous procedure which incorporated an absorption/desorption cycle, Zobel (1984, 1985).

An isostatic procedure was described by DeLassus (1986), who studied the transport of d-limonene vapor through a series of polymer films typically used for food packaging. The author employed techniques on photoionization and atmospheric pressure ionization, Caldecourt and Tou (1985), for quantifying the permeation rate of d-limonene through the respective test films. Hernandez (1984) and Baner et al. (1986) also employed an isostatic procedure for determining the diffusion coefficient from permeability data of organic penetrants through polymer membranes. Analysis of permeated vapor was based on a gas chromatographic technique with flame ionization detection. Smith and Adams (1981) and Pasternak (1970) also reported permeability studies using a continuous flow or isostatic method.

Hilton and Nee (1978) developed an accumulation or quasi-isostatic test method for determining the permeability of organic vapors through barrier films, where the polymer film was mounted in a permeability cell above a reservoir of liquid permeant. The permeant vapor which has diffused

through a barrier film accumulates in the low concentration chamber of the test cell and was quantified by a gas chromatographic technique. A similar procedure for determining the permeability of organic vapors through barrier films was reported by Murray and Dorschner (1983). In a more recent publication, Murray (1985) expanded on this procedure and reported a number of examples for which the test apparatus was employed to determine the relative permeation rates of organic vapors through barrier structures. These methods are limited, however, to determining the transmission rates and permeability constant values at only one concentration given by the saturation equilibrium vapor pressure of the liquid penetrant at a given temperature.

Gilbert et al. (1983) also evaluated the barrier properties of polymeric films to various organic penetrants by a quasi-isostatic test procedure. To provide a constant concentration or partial pressure gradient, wherein the net movement for the penetrant is from high partial pressure to low partial pressure, these authors continually flowed a penetrant vapor stream through the high concentration chamber of the permeability cell. Baner et al. (1984) described a test apparatus based on the quasi-isostatic procedure for determining the diffusion of organic penetrant through polymer films, and also employed the continuous flow of organic vapor through the high concentration cell chamber

to assure a constant vapor gradient. A chromatographic method was developed for the permeation rate measurements. Peterlin (1975) has studied the concentration dependence of the diffusion and permeability coefficient in a homogeneous membrane.

In addition to the permeation methods described above, the transport of small molecules in polymers can also be evaluated by absorption-desorption methods. Fujita (1961) has described the general behavior of sorption and permeability of organic vapors. Bischoff et al. (1984) have studied the effect of the polymer molecular orientation on the sorption of toluene by high density polyethylene (HDPE). Applying a successive sorption method, Choy et al. (1984) studied the sorption and diffusion of toluene vapor in oriented polypropylene (OPP) film of varying draw ratios. By this method the authors obtained values of the diffusion coefficient ( $D$ ), solubility ( $S$ ) and permeability ( $P$ ) of the polymer, as well as information on the structure and molecular dynamics of OPP as a function of draw ratio. Berens (1978) described vapor sorption studies on polyvinyl chloride (PVC) powders as a mean of studying the transport of low molecular weight organic molecules in glassy polymers. For a detailed review of the sorption method for measuring the sorption and diffusion coefficients of small molecules in polymers, the reader is referred to Berens (1978) and references cited therein.

Baner (1986) applied the sorption equilibrium method by using a electrobalance to study the sorption and diffusion of toluene vapor in OPP and Saran (trademark of the Dow Chemical Company for its polyvinylidene chloride and copolymers) film samples as a function of penetrant concentration.

Knowledge of the diffusion, solubility and permeability of organic penetrants through polymer structures has both theoretical and practical importance. In terms of theoretical importance, such studies can aid developing a better understanding of the mechanism of diffusion of organic penetrants through polymer membranes and particularly for the case of permeant molecules that have strong interaction with the polymer. The diffusion and solubility of organic penetrants will be of practical importance for example in the case of packaged goods, when product quality is related to the transfer of organic vapors when polymers materials are used. For example, the aroma barrier properties of a package system are important, since the retention of product aroma constituents and the exclusion of sensorially objectionable organic molecules from the package external environment contribute to the keeping quality and, thus, the shelf life of the product. Further, knowledge of the aroma barrier properties of polymeric packaging materials can provide a mean of designing and/or selecting a barrier structure for a specific end use application.

Knowing solubility data for essential flavor ingredients in certain polymers is of paramount importance in avoiding the effect of "flavor scalping". For example, d-limonene, a common flavor component present in foods has a relative high solubility in HDPE, Mohny et al., (1986). Since the flavor compounds are normally present in low concentration in the foodstuffs, there is a potential risk to "lose" aroma constituent due to absorption by the package polymeric material.

#### MODELING CONSIDERATIONS

Diffusion (D) and solubility (S) coefficients are usually determined by observing the change in weight (increase or decrease) of a polymer sample during a sorption process. Such a process can involve the absorption or the desorption of low molecular weight moieties by the polymer sample. Diffusion and permeability (P) values can be obtained from permeability experiments where the transport of a permeant through a polymer membrane is continually monitored (isostatic procedure) or by quantifying the amount of the penetrant that has passed through the film and accumulated as a function of time (quasi-isostatic procedure). The basic equations for describing the diffusion process are Fick's first and second law of diffusion (Crank, 1975).

$$F = - D \frac{dc}{dx} \quad (1)$$

and

$$\frac{dc}{dt} = \frac{d}{dx} \left[ D \frac{dc}{dx} \right] \quad (2)$$

Where F is the flux or the rate of transfer of penetrant per unit area, expressed as a mass of diffusant per unit area per time; c is the concentration of the penetrant in the film, expressed in the same unit of mass of diffusant per unit of volume or mass of the polymer; D is the mutual diffusion coefficient, in unit of (length)<sup>2</sup>/time; t is time and x is the length in the direction in which the transport of the penetrant molecules occurs. To obtain the flux F, or the diffusion coefficient D, equation (1) or (2) must be solved together with the initial and boundary conditions associated with the experiment to give the desired values.

Solution to eqn. (2), and respective initial and boundary conditions, can be performed analytically or numerically to calculate D. In the first case a power-series of solutions usually arises when solving for the unsteady state case.

In this paper, simplified equations related to the first approximation of the power-series are presented (Crank, 1975). It should be noted that when the diffusion coefficient is calculated using these equations, only approximated values will be obtained. More accurate estimation of this parameter  $D$ , can be carried out by using, for example, a non linear maximum likelihood sequential method based on the Gauss linearization method (Beck and Arnold, 1977).

To relate the concentration of the penetrant in the polymer, (solubility), to the penetrant concentration in the gas or vapor phase in equilibrium with the polymer, Henry's law is assumed

$$c = S.p \quad (3)$$

Where  $p$  is the partial pressure of the penetrant in the gas phase and  $S$  is the solubility coefficient of the penetrant into the polymer. The partial pressure of the penetrant is further related to the penetrant concentration in the gas phase through, for example, the ideal gas law. Application of the ideal gas law is justified when the concentration of the diffusant in the gas phase is lower than one atmosphere.

The diffusion coefficient  $D$ , can be independent or, a function of the penetrant concentration  $c$  in the polymer. In the latter case, the diffusion coefficient would not be constant but would be concentration dependent. In either case, it is assumed that the diffusion process is fickian. If the diffusion coefficient is time dependent, the diffusion process is said to be non-fickian (Meares, 1965).

### Permeability Measurements

#### Isostatic Method

A representative transmission rate profile curve for describing the transport of a permeant through a polymer membrane by an isostatic method is shown in figure 1. From such an experiment, diffusion and permeability coefficient values are obtained, and while the specific experimental configuration may vary among investigators, the basic equations describing the permeation phenomenon are similar. Solution of eqn. (1) depend on the boundary conditions of the experiment, in this case given by:

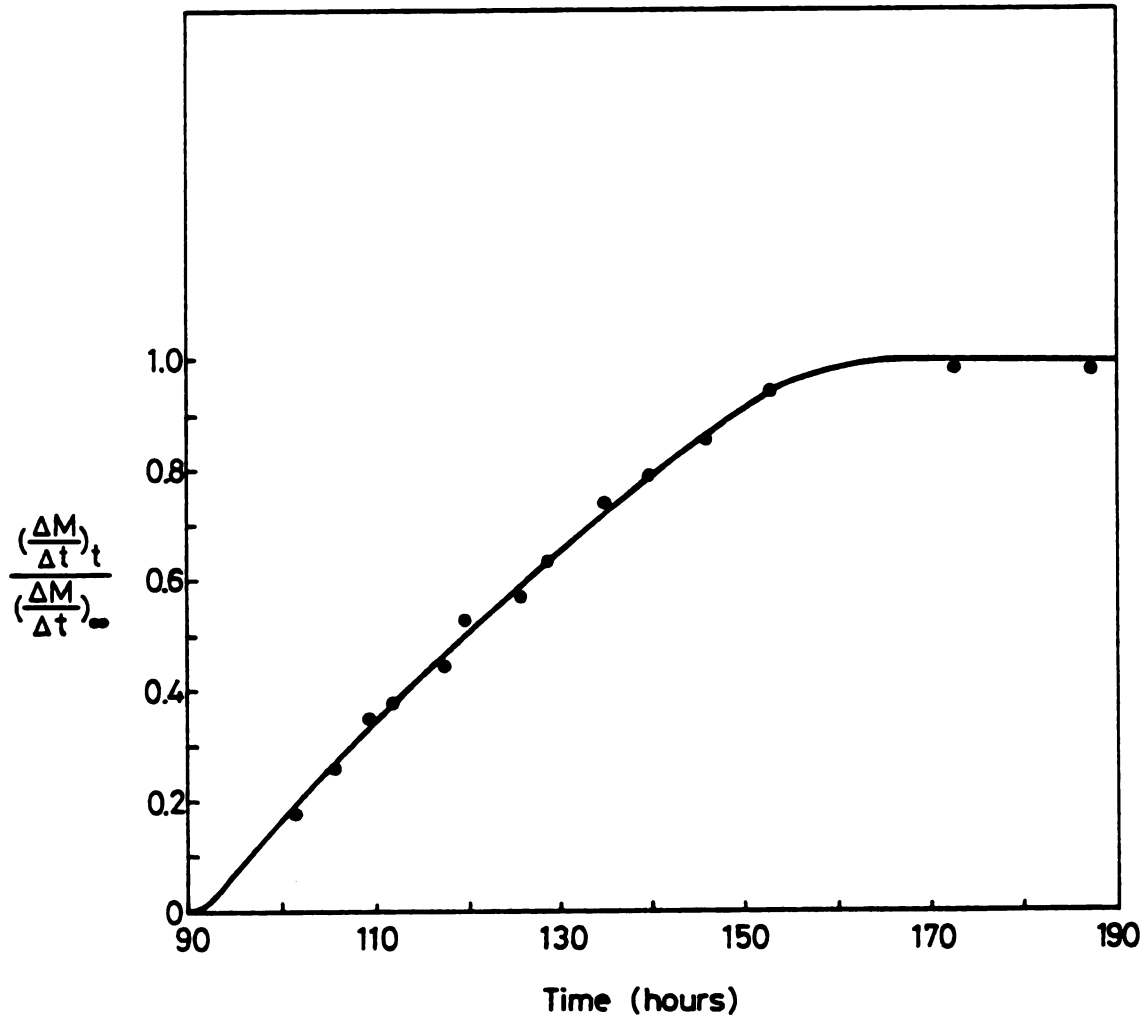


Figure 1. Transmission rate profile curve for toluene vapor through oriented polyethylene terephthalate (PET) at 90 ppm and 23 C (thickness of the film was  $3.49 \times 10^{-5}$  m, crystallinity 27%).

$$\begin{aligned}
c &= c_0 & \text{at } x &= 0 & t &= 0 \\
c &= 0 & \text{at } x &= L & t &> 0 \\
c &= c_2 \frac{L-x}{L} & \text{at } 0 < x < L & t &= \infty
\end{aligned} \tag{4}$$

where  $L$  is the thickness of the film,  $c_0$  is the concentration at  $x = L$  in equilibrium with the permeant flow. These B.C. represent the change from one steady state,  $t = 0$  and  $c_1$ , to the final  $c_2$  at  $t = \infty$ , with the partial pressure of the permeant on the downstream side of the membrane always kept at zero since pure gas nitrogen is continuously flowed.

A solution of eqn. (1) subject to boundary conditions given by eqn. (4) was presented by Pasternak et al. (1970) and is given as a first approximation in Equation (5)

$$\frac{\left( \frac{\Delta M}{\Delta t} \right)_t}{\left( \frac{\Delta M}{\Delta t} \right)_\infty} = \left[ \frac{4}{\sqrt{\pi}} \right] \left[ \frac{L^2}{4Dt} \right]^{1/2} \exp \left[ -\frac{L^2}{4Dt} \right] \tag{5}$$

where  $(\Delta M/\Delta t)_t$  and  $(\Delta M/\Delta t)_\infty$  are the transmission rate of the penetrant at time  $t$  and at steady state, respectively. For each value of  $(\Delta M/\Delta t)_t/(\Delta M/\Delta t)_\infty$  a value of  $l^2/4Dt$  can be calculated, and by plotting  $4Dt/l^2$  as a function of time, a straight line is obtained. From the slope of this graph,  $D$  is calculated by substitution in eqn. (6).

$$D = \frac{(\text{slope}) \times l^2}{4} \quad (6)$$

Smith and Adams (1981) used this method to study the effect of the tensile deformation on gas permeability in glassy polymers. From a different general expression for  $(\Delta M/\Delta t)_t/(\Delta M/\Delta t)_\infty$ , Ziegel et al. (1969) derived equation (7), to solve for  $D$ :

$$D = \frac{l^2}{7.199 t_{1/2}} \quad (7)$$

where  $t_{1/2}$  is the time required to reach a rate of transmission  $(\Delta M/\Delta t)_t$  equal to half the steady state  $(\Delta M/\Delta t)_\infty$  value.

DeLassus (1985) applied eqn. (7) to calculate the diffusion coefficient of limonene vapor for different polymer films typically used for food packaging.

The permeability coefficient  $P$ , can be calculated from the isostatic method by substitution in eqn. (8)

$$P = \frac{a.G.f.l}{A.b} \quad (8)$$

where

$a$  = calibration factor to convert detector response to units of mass of permeant/unit of volume [(mass/vol.) /signal units]

$G$  = response units from detector output at steady state (signal units)

$f$  = flow rate of sweep gas conveying penetrant to detector (volume/time)

$b$  = driving force given by the concentration or partial pressure gradient (pressure or concentration units).

### Quasi-Isostatic Method

In this method, the permeated gas or vapor is accumulated and monitored as a function of time. A generalized transmission rate profile curve describing the transport of permeant through a polymer membrane by the quasi-isostatic method is shown in Figure 2. As shown, the total quantity of penetrant to have transmitted through the film is plotted as a function of time. Barrer (1939) presented a solution of equation (2) for this specific set of experimental conditions, which allowed determination of D,

$$D = \frac{l^2}{6\theta} \quad (9)$$

where  $\theta$  is the intersection of the projection of the steady-state portion of the transmission curve and is called the lag time. The steady-state permeability coefficient P can be determined from the quasi-isostatic method by substitution into eqn. (10).

$$P = \frac{y \cdot l}{A \cdot b} \quad (10)$$

where y is the slope of the straight line portion of the transmission rate curve (mass/time).

By plotting  $\log [t^{1/2} (\Delta M/\Delta t)_t]$  as a function of  $1/t$ , it is possible to obtain information about the concentration dependency of the diffusion coefficient.

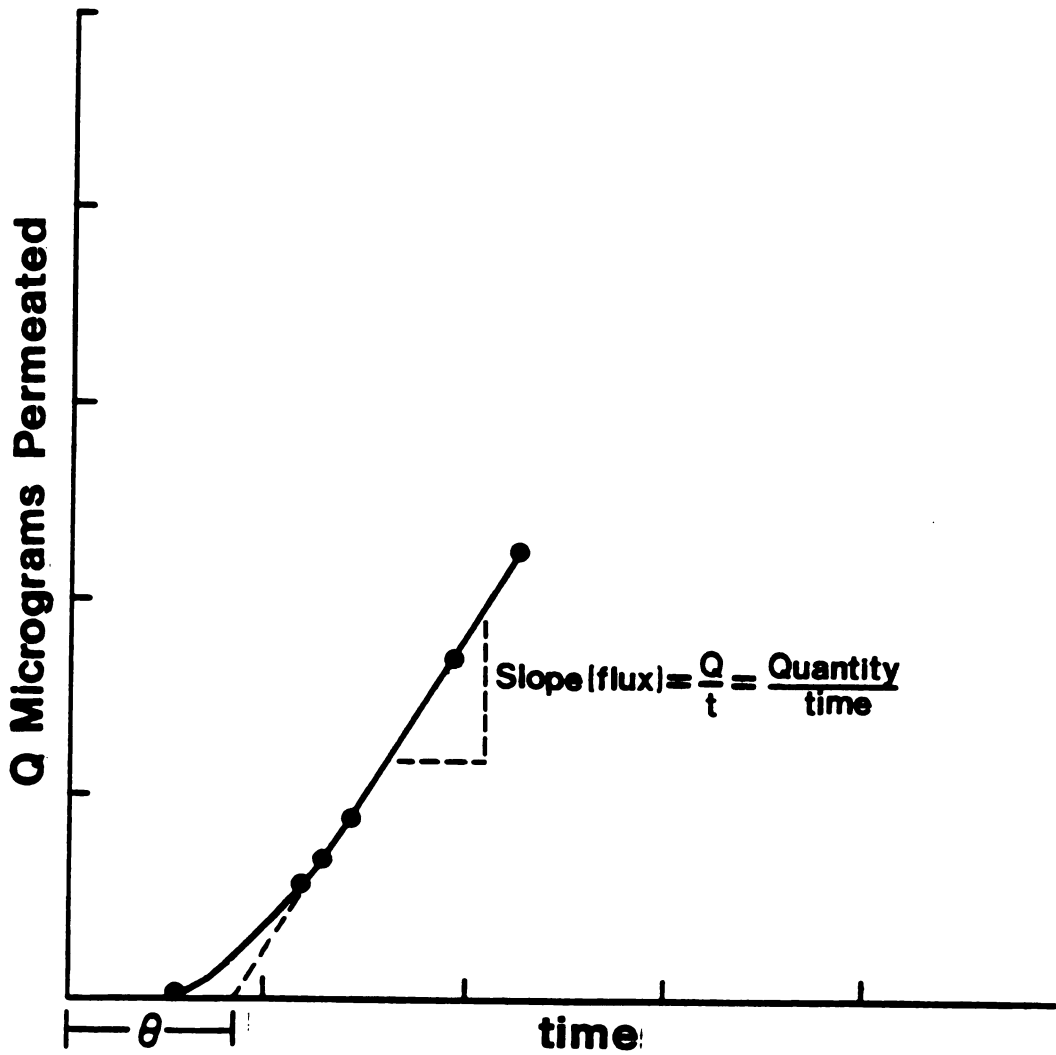


Figure 2. Generalized transmission rate profile curve by quasi-isostatic method test.

## Sorption Measurements

### Polymer Films

Sorption experiments are usually carried out at equilibrium vapor pressure, using a gravimetric technique in an apparatus that records continually the gain or the loss of weight by a test specimen as a function of time. A recording electrobalance (Cahn Instrument Co., Cerritos, California) is commonly used for such studies.

The diffusion equation that describes appropriately the sorption of penetrant by a polymer sample in film or sheet form for large time is described by Crank (1975), and taking the first two terms of the serie solution, eqn. (11) is obtained,

$$\frac{M_t}{M_\infty} = 1 - \frac{8}{\pi^2} \left[ \exp\left(\frac{-D.t.\pi^2}{L^2}\right) + \frac{1}{9} \exp\left(\frac{-9D.t.\pi^2}{L^2}\right) \right] \quad (11)$$

where  $M_t$  and  $M_\infty$  are the amount of penetrant sorbed by the polymer film sample at time  $t$  and the equilibrium sorption uptake after infinite time, respectively; and  $L$  is the thickness of the sample.

The sorption diffusion coefficient  $D_s$  can be calculated by a non-linear regression analysis of the above equation or approximated by setting  $M_t/M_\infty$  equal to 0.5 and solving for  $D_s$  to obtain,

$$D_s = \frac{0.049 \cdot L^2}{t_{1/2}} \quad (12)$$

where  $t_{1/2}$  is the half sorption time or the time required to attain the value  $M_t/M_\infty$ .

A graphical representation of eqn. (11) and data from an experimental sorption process are shown in figure 3, where values of  $M_t/M_\infty$  are plotted as a function of square root of time,  $t^{1/2}$ .

In the early stage of the diffusion process, the uptake by a film is described by,

$$\frac{M_t}{M_\infty} = 4 \left( \frac{Dt}{L^2} \right)^{1/2} \left[ \frac{1}{\pi^{1/2}} + 2 \operatorname{ierfc} \frac{1}{(2Dt)^{1/2}} \right] \quad (13)$$

### Polymer Spheres

The ratio of the amount of vapor absorbed at any time  $t$  over the equilibrium sorption uptake at infinite time  $M_t/M_\infty$  for polymer samples of spherical geometry and of diameter  $d$  is given by the expression:

$$\frac{M_t}{M_\infty} = 1 - \frac{6}{\pi^2} \left[ \exp\left(\frac{-D \cdot t \cdot \pi^2}{d^2}\right) + \frac{1}{4} \exp\left(\frac{-16D \cdot t \cdot \pi^2}{d^2}\right) \right] \quad (14)$$

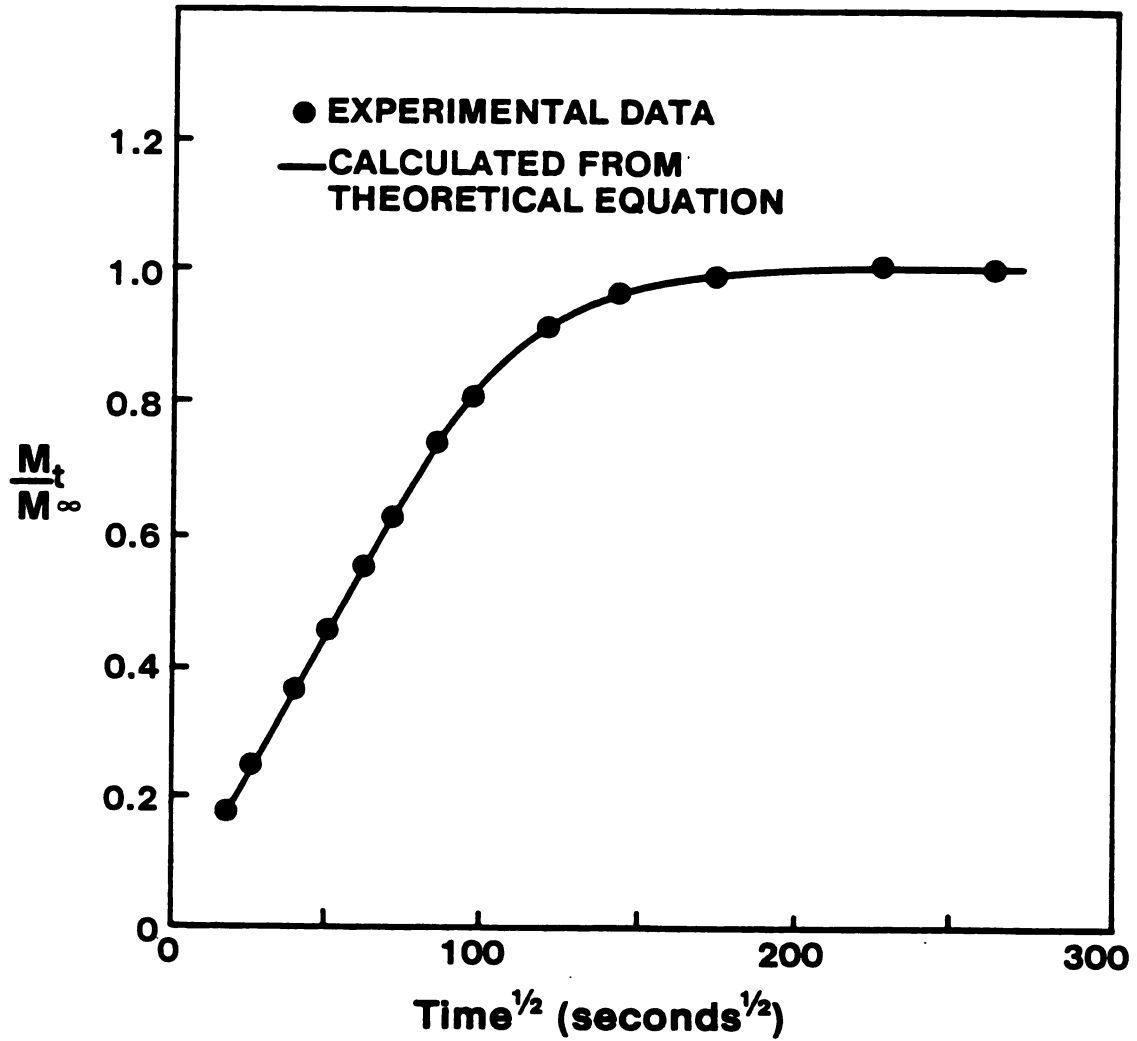


Figure 3. A plot of  $M_t/M_\infty$  vs.  $t^{1/2}$  for d-limonene by high density polyethylene/sealant lamination (thickness,  $4.8 \times 10^{-5}$  m); vapor concentration 1.5 ppm; temperature 20.5 C.

which is the first two terms of the serie solution presented by Crank (1975). The diffusion coefficient is also readily obtained from eqn.(14) by setting  $M_t/M_\infty$  equal to 0.5 to give the expression,

$$D_s = 7.45 \times 10^{-3} \frac{d^2}{t_{1/2}} \quad (15)$$

Berens (1977, 1978) conducted absorption experiments to study the characteristics of the transport of vinyl chloride monomer in polyvinyl chloride (PVC) using powdered polymer samples. Application of equations (14) and (15) showed that the PVC powder particles could be treated as spheres.

#### Desorption Measurements

When desorption experiments are performed and the value of the mass transfer coefficient of the moiety in the gas phase is negligible, eqns. (11) and (14) can also be applied to the desorption process by considering the loss of the penetrant at any time  $t$  and the amount of penetrant loss after infinite time as  $M_t$  and  $M_\infty$ , respectively.

The diffusion coefficient for the desorption process  $D_d$  is given by:

$$D_d = 0.049 \frac{l^2}{t_{1/2}} \quad (16)$$

for film samples and, for polymer samples of spherical geometry by:

$$D_d = 0.00745 \frac{d^2}{t_{1/2}} \quad (17)$$

When  $D_s$  and  $D_d$  are different the diffusion coefficient may be better represented by the average of these two values.

However, when the mass transfer coefficient of the diffusing molecule in the gas phase cannot be neglected the power-series of solution must include this parameter, Crank (1975). The expression that includes only the leading term of the solution for the above boundaries conditions is given by:

$$\frac{M_t}{M_\infty} = 1 - \frac{2L \cdot \exp(-B \cdot D \cdot T/l^2)}{B^2(B^2 + L^2 + L)} \quad (18)$$

where

$$B \cdot \tan(B) = L$$

and

$$L = L \cdot k \cdot D$$

$k$  is the mass transfer coefficient in the gas phase. A simplified method to solve for both the diffusion and the mass transfer coefficients has been presented by Han et al. (1986), but the numerical solution presented by the authors is probably incorrect.

## Solubility Coefficients

The solubility coefficient  $S$  is readily calculated from absorption experiments by substitution into the expression

$$S = \frac{M_{\infty}}{w \cdot b} \quad (19)$$

where  $S$  is expressed as mass of vapor sorbed at equilibrium per mass of polymer per unit of driving force concentration or penetrant partial pressure.  $M_{\infty}$  is the total amount (mass) of vapor absorbed by the polymer at equilibrium for a given temperature,  $w$  is the weight of the polymer sample under test, and  $b$  is a value of the penetrant driving force in units of concentration or pressure.

## Diffusion coefficients

Implicit in the expression to calculate  $D$  is the assumption that the diffusion coefficient is independent<sup>of</sup> of the concentration of the penetrant. However, unlike the transport of less-interactive penetrants (such as oxygen or nitrogen), the molecular transport of most organic vapors show non-ideal diffusion and solubility behavior due to their ability to interact with, and swell the polymeric matrix. Since those effects is a function of the concentration of the vapor, both  $D$ ,  $S$ , and also  $P$  are function of the penetrant concentration.

Nevertheless, these equations can also be applied when the polymer sample swells and the thickness changes as the vapor enters the film. As Crank and Park (1968) showed,  $\bar{D}$  (the mean diffusion coefficient) can be related to the variable diffusion coefficient  $D$  by the approximation

$$\bar{D} = \frac{1}{C_0} \int_0^C D \, dc \quad (20)$$

where the range of concentration goes from zero to  $C_0$ . A graphical or numerical derivation of  $\bar{D}C_0$  versus  $C_0$  gives a first approximation of the relationship between  $D$  and  $C$ . In many cases, this first approximation may be sufficiently accurate. However, successively better approximation can be obtained.

When the diffusion process is dependent upon the time necessary for polymer molecule chain reaccommodation, the diffusion coefficient is considered non-fickian. Such non-fickian behavior of the diffusion process is usually determined by experimentation. For example, the plots for permeation and sorption data exhibiting non-fickian behavior are different from those presented in Figures 1-3. There is not available a general theory for predicting the non-fickian behavior. Readers interested in this subject are referred to Fujita (1961), Meares (1965) and Crank and Park (1968) and references found therein.

## METHODS

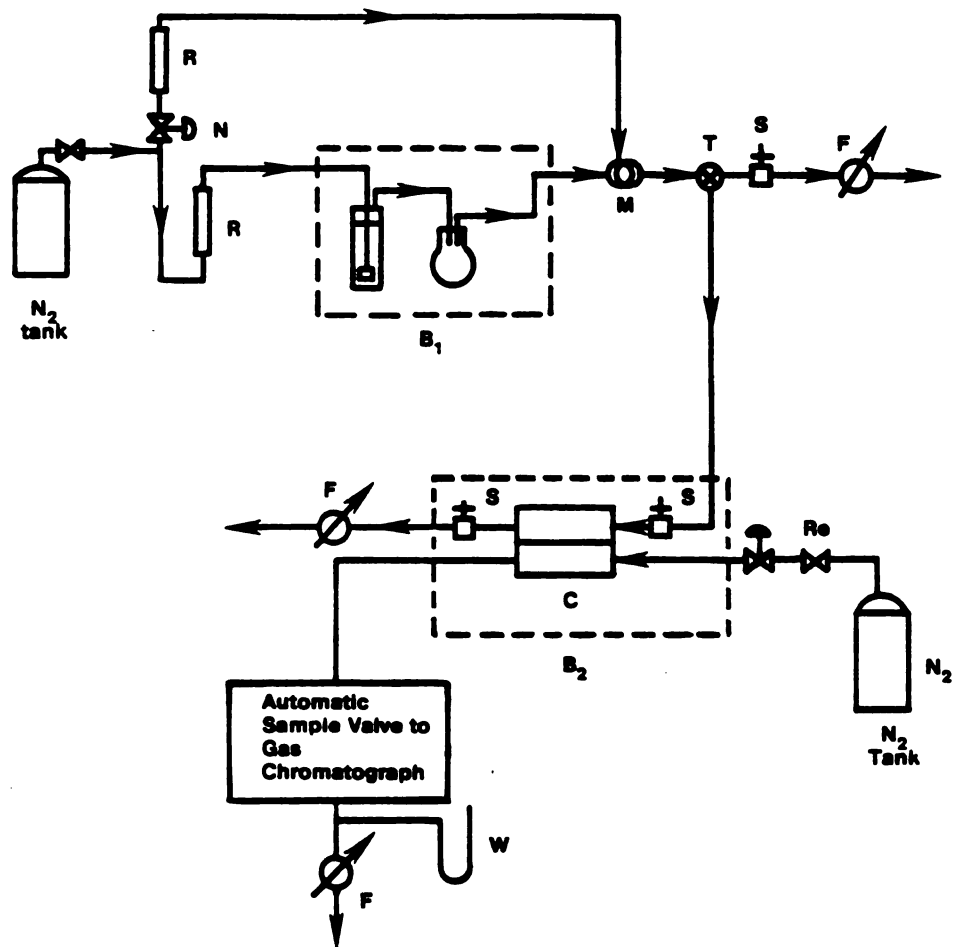
Determination of permeation rates

## Isostatic Procedure

A schematic diagram of the isostatic test apparatus is shown in Figure 4.

The test system allows for the continuous collection of permeation data of a molecule (gas or organic vapor), through a polymer membrane from the initial time zero to steady state conditions, as a function of temperature and permeation concentration. The permeability cells are of our own design and consist of two stainless steel chambers, with the upper and lower cell chambers each being equipped with a gas sampling port and inlet and outlet valves. The film to be tested is placed between the two stainless steel plates forming the cell, with the two cell chambers each leaving a volume of 5 cc. The surface area of the film exposed to the permeant is  $50 \text{ cm}^2$ . Hermetic isolation of the chambers from the environment is achieved by the compression of overlapping Viton "O" rings on the film.

The assembled cell and film is placed horizontally in a constant temperature bath. A constant concentration of permeant vapor is continually flowed through the upper (high concentration) cell chamber. Concurrently a constant flow of inert gas (nitrogen) is passed through the lower cell chamber removing permeant vapor at a constant rate and conveying it to the detector apparatus.



- B<sub>1</sub>** - Water bath, generation of permeant vapor phase diluted in Nitrogen  
**B<sub>2</sub>** - Water bath ( $\pm 0.1^\circ\text{C}$ )  
**C** - Cell  
**F** - Gas flow bubble meter  
**M** - Mixing device  
**N** - Needle valve  
**R** - Rotameter  
**Re** - Regulator  
**S** - Sample port  
**T** - Three way valve  
**W** - Water manometer

Figure 4. Schematic diagram of the isostatic test apparatus

This detection system consist of a gas chromatograph, equipped with a flame ionization detector, interfaced to the permeability cell via a computer controlled gas sampling valve. At preselected time intervals the concentration of penetrant in the carrier stream flowing through the low concentration chamber is determined and the the flow is monitored continually until steady state conditions are attained. Values of  $\Delta M/\Delta t$  can be then calculated for each time. The diffusion and permeability coefficient values are then computed by substitution into eqns. (6) and (8).

A constant concentration of permeant vapor is produced by bubbling nitrogen gas through liquid permeant. This is carried out by assembling a vapor generator consisting of a glass gas washing bottle containing the organic liquid, and a fritted dispensor tube. The concentration obtained in this way can be adjusted to a required value by mixing it with a pure gas carrier steam. Before being directed to the permeation cell the vapor stream is passed through a glass reservoir to damp perturbations in the concentration. The vapor generator system is mounted in a constant temperature bath. As shown, flow meters were used to provide a continous indication that a constant rate of flow is mantained. Gas flow are regulated using needle valves. Prior to initiate a run, care is taken to purge the lower cell chamber, the capillary tubing and the sampling valve of residual permeant vapor.

## Quasi-Isostatic Procedure

Figure 5 represents a schematic diagram of the quasi-isostatic permeation test apparatus. The permeability cell, constructed of stainless steel (or aluminium), is comprised of two cell chambers and a hollow center ring. Each cell chamber have a volume of 50 cc; the volume of the center cavity is approximately 50 cc. The area of the film exposed to the permeant is 50 cm<sup>2</sup>. In operation, two test films are placed between the center ring and each of the cell chambers. Isolation of the interior of the chamber from the environment is achieved by using a Viton "O" ring on each of the side of the center ring providing a Viton/film/metal contacting surfaces seal. Each cell chamber and the center ring are equipped with an inlet and outlet valve and a sampling port. The films to be tested are mounted in the permeability cell and the cell is assembled. The constant concentration flow of permeant is flowed through the center ring. As showed in Figure 5, to perform simultaneously multiple runs, several cells can be attached to a dispensing manifold. Each permeant stream running into each cell may have a different concentration value.

During the diffusion process, the change in penetrant concentration in the accumulation cell chamber is determined by gas chromatography. At predetermined time intervals an aliquot (.5 ml) of head space is removed from the cell

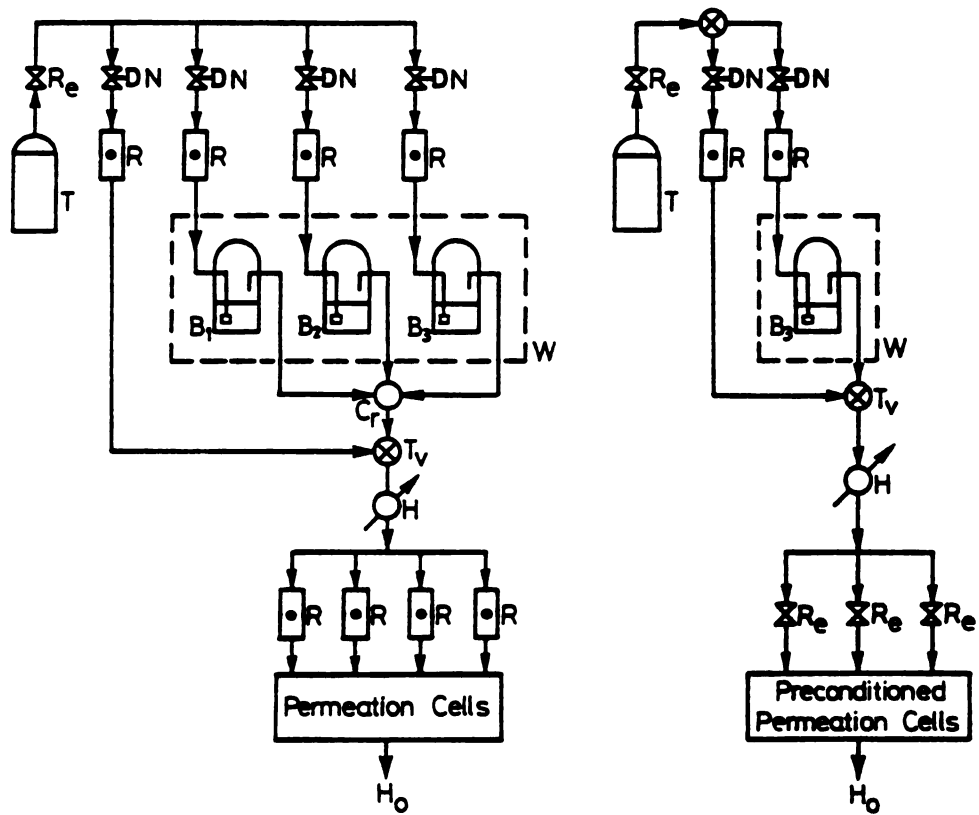


Figure 5. Schematic diagram of the quasi-isostatic test apparatus

chamber with a gas tight syringe and injected into the gas chromatograph. To keep the pressure constant inside the cell, 0.5 ml of pure nitrogen is re-injected into the cell. Further, to ensure a quasi-constant driving force of the permeant through the film during each run, the permeant concentration in the low concentration cell is not allowed to exceed 1-2% of the permeant concentration at the center ring.

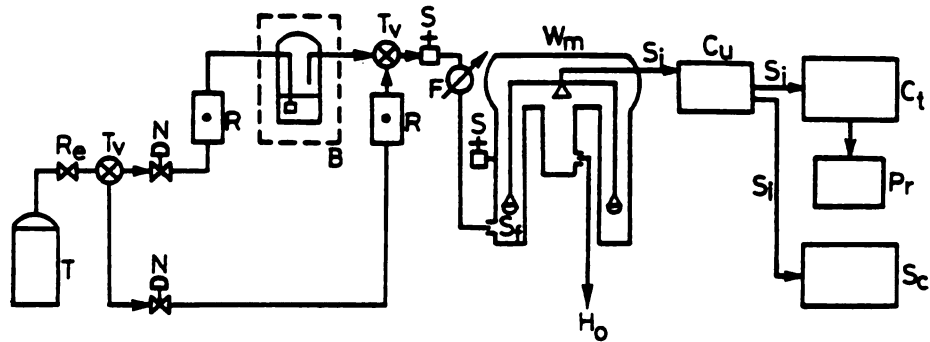
To determine the diffusivity and the permeability values, the increase in penetrant quantity in the accumulation chamber is plotted as a function of time and the resultant transmission rate profile is related to the permeability of the film sample. The time lag is obtained as the intercept on the time axis of the steady rise portion of the penetrant-time plot. By using eqn. (9) the diffusion coefficient can be determined from the lag time values. The lag time diffusion coefficient for laminated structures is considered to be an effective diffusion coefficient value, being the result of the combination of different diffusion coefficients of the respective individual layers.

#### Sorption Measurements

Sorption measurements can be carried out on a Cahn electrobalance (Cahn Instruments Inc. Cerritos, California). The electrobalance is maintained in a constant temperature environment.

A sample film between 25 and 100 mg is normally used for sorption experiments, and the sensibility of the apparatus is around 1 microgram. A schematic diagram of the test system is shown in Figure 6. The test system allows for the continuous collection of sorption data of an organic or water vapor by a polymer film from the initial time zero, when the film is first exposed to the vapor, to the steady state condition, when the equilibrium is reached.

As shown, the polymer film sample to be tested is suspended directly from one of arm of the electrobalance and a constant concentration of penetrant vapor is continually flowed through the sample tube (hang-down tube), such that the polymer sample is totally surrounded by the vapor. A constant concentration of penetrant vapor is produced by the same procedure as explained before. The gain in weight of the sample due to penetrant sorption is monitored continually until the gain is zero at equilibrium. To determine  $D$  and  $S$ , the ratio of the amount of penetrant vapor absorbed at any time and the equilibrium sorption uptake at infinite time,  $M_t/M_\infty$ , is plotted as a function of time. For film samples, the diffusion coefficient  $D_s$  is determined by proper substitution into eqn. (12), and the solubility coefficient into eqn. (19).



- |                                                                                  |                                                       |
|----------------------------------------------------------------------------------|-------------------------------------------------------|
| <b>B</b> - Water bath, generation of permeant<br>Vapor phase diluted in Nitrogen | <b>R</b> - Rotameter                                  |
| <b>C<sub>t</sub></b> - Computer terminal                                         | <b>R<sub>e</sub></b> - Regulator                      |
| <b>C<sub>u</sub></b> - Control unit                                              | <b>S</b> - Sample port                                |
| <b>F</b> - Gas flow bubble meter                                                 | <b>S<sub>f</sub></b> - Sampling film                  |
| <b>H<sub>o</sub></b> - Hood                                                      | <b>S<sub>c</sub></b> - Strip chart                    |
| <b>N</b> - Needle valve                                                          | <b>S<sub>i</sub></b> - Electrical input/output signal |
| <b>P<sub>r</sub></b> - Printer                                                   | <b>T<sub>v</sub></b> - Three way valve                |
| <b>T</b> - Nitrogen tank                                                         | <b>W<sub>m</sub></b> - Cahan electrical balance       |

Figure 6. Schematic diagram of the microbalance test apparatus.

## APPLICATIONS

## Quasi-Isostatic Procedure

A limited number of penetrant/polymer film combinations have been studied using the quasi-isostatic procedure and test apparatus described above. Interested readers are referred to Baner et al. (1986) and Baner (1986) for detailed summary of these findings. In this review two examples are presented on the diffusion of toluene vapor through polypropylene based structures:

- 1) Two ply coextruded Oriented Polypropylene,  $2.3 \times 10^{-5}$  m (0.9 mil) thick; and
- 2) Two side acrylic heat seal coated, biaxially oriented polypropylene,  $2.4 \times 10^{-5}$  m (.93 mil) thick.

Those films were supplied by Mobile Chemical Corporation and were identified as Bicolor 90 and Bicolor 310 respectively. The results are presented in Table 1 and Figures 7 and 8.

As shown, the permeation behavior of the films had an initial non-steady state period followed by steady state constant flow portion. The shape of the curve indicated that the diffusion process was Fickian even at the higher concentration values.

The results of these studies clearly showed the flux or permeability rate to be affected drastically by the level of vapor concentration.

TABLE 1. Permeability and lag time diffusion coefficients for toluene vapor in selected polypropylene based structures.

Film Structure	Toluene Concent. (ppm)	Temp. (°C)	Flux (mg/hr.m <sup>2</sup> )	Lag Time (min)
Bicor 90	28	22	6.0	54
	33	22	17.0	96
	74	22	900	24
	84	22	900	24
Bicor 310	39	22	.02	--
	73	22	23	1920
	88	22	400	108
	120	22	2200	36

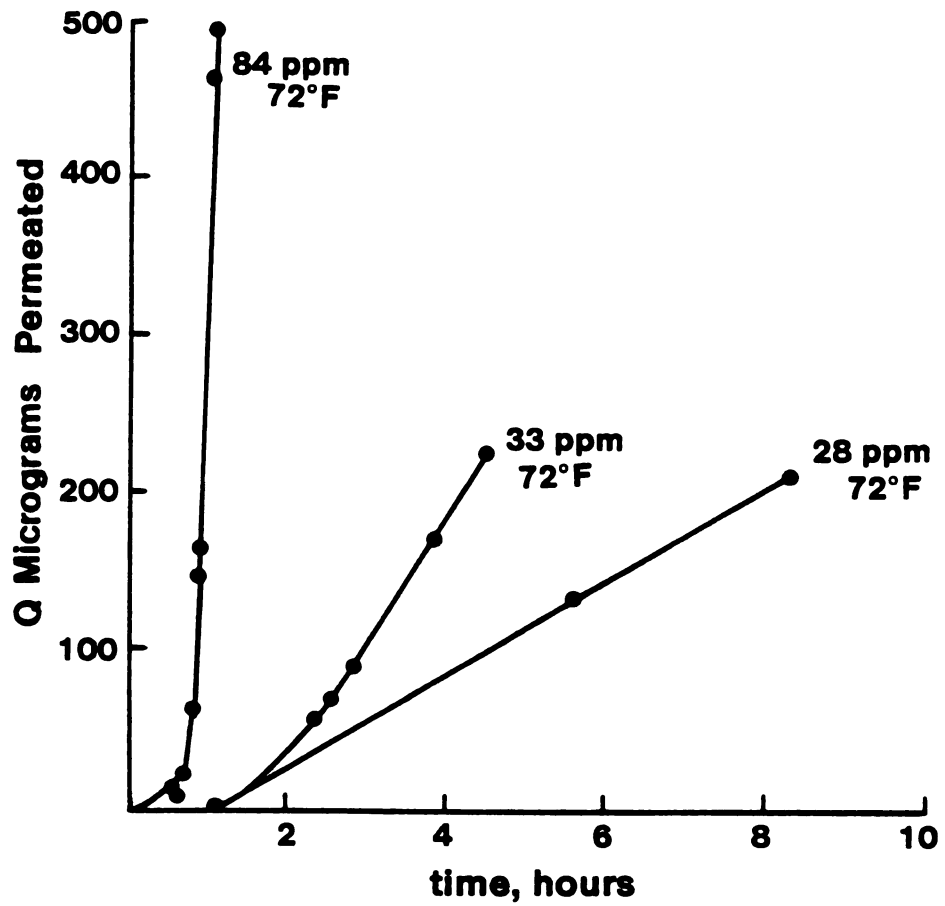


Figure 7. Effect of penetrant concentration on the transmission of toluene vapor at 23.0 C through coextruded OPP.

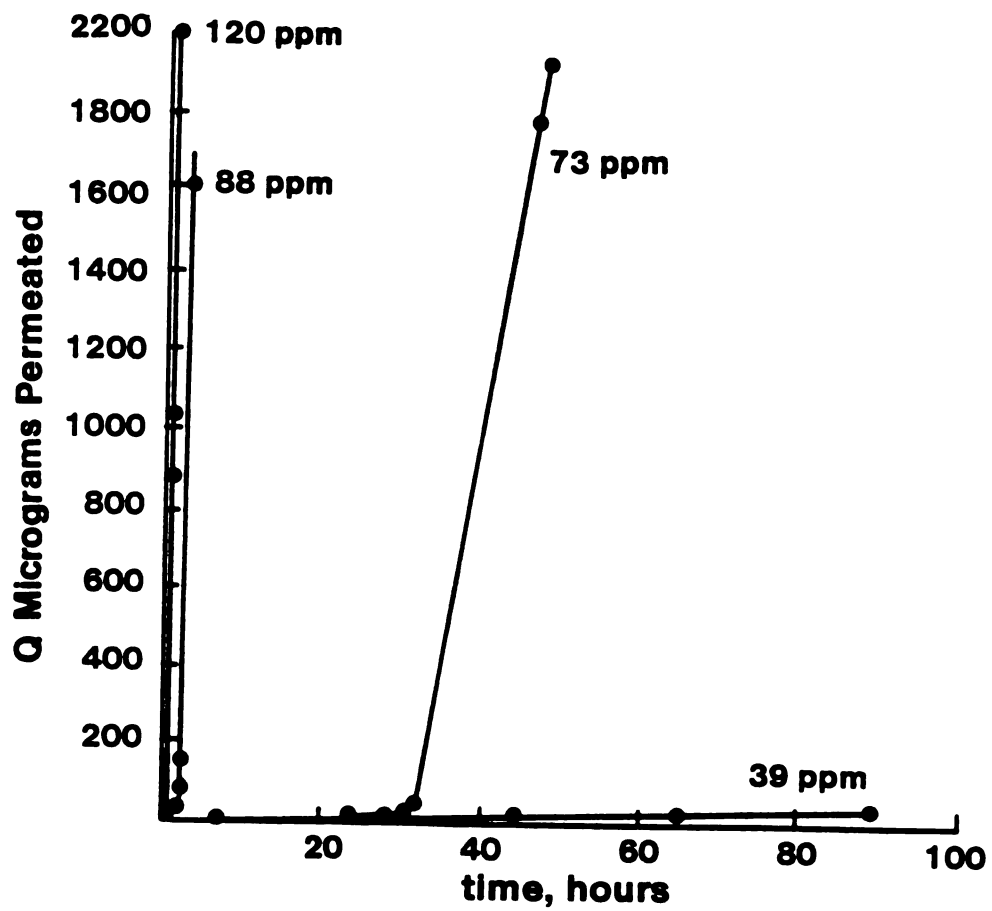


Figure 8. Effect of penetrant concentration on the transmission of toluene at 23.0°C through biaxially oriented polypropylene acrylic coated.

Since the change of the lag time values are not equally affected, it may be suggested that sorption behavior of the toluene into the polypropylene structure, as a function of concentration, is a dominant phenomenon. This behavior is normally related to configurational changes and alteration of the polymer chain conformational mobility.

#### Isostatic Procedure

Equation (5) can be written as:

$$A = X^{1/2} \cdot \exp(-X) \quad (21)$$

where

$$A = \frac{\sqrt{\pi}}{4} \frac{\left(\frac{\Delta M}{\Delta t}\right)_t}{\left(\frac{\Delta M}{\Delta t}\right)_\infty} \quad (22)$$

and

$$X = \frac{l^2}{4Dt}$$

To solve the non-linear equation (22), the Newton Raphson method can be used, Chapra and Canale (1985). In this case, eqn. (22) is written as,

$$G = X^{1/2} \exp(-X) - A = 0 \quad (23)$$

A iteration calculation method for eqn. (23) can be implemented to solve for X, Hernandez (1984).

This procedure can be applied to both organic vapors and gases.

In Table 2 data are shown for the permeation of oxygen through an amorphous polyamide.

The diffusion coefficient is calculated from the slope of a linear regression analysis of  $l/X$  versus time. For the values shown in Table 2,  $D$  was  $6.73 \times 10^{-10}$   $\text{cm}^2/\text{sec}$ , and the correlation coefficient was .998.

#### Sorption procedure

Shown in Figure 3 is a plot of  $M_t/M_\infty$  vs.  $t^{1/2}$  for d-limonene sorption by a laminate structure made of High Density Polyethylene (HDPE) and a sealant (blend of ethylene vinyl acetate/surlyn ionomer/polubutylene). The sorption experiment was carried out at vapor concentration of 1.5 ppm (mg/l). Also shown in Figure 3 is the sorption profile obtained by substitution into eqn. (11), the diffusion coefficient was calculated by eqn. (12). As seen, good agreement was obtained between the experimental and calculated sorption curve, supporting the theory that at low penetrant concentration the diffusion process is fickian. Mohny et al. (1986) have shown, however, that for HDPE at d-limonene concentration higher than 5 ppm there is an onset of non-fickian relaxation controlled sorption, which results in an uptake larger than the expected. Similar sorption behaviors has been described by Berens (1977), Bagley and Long (1958) and Fujita (1961).

TABLE 2. Values for eqn. (23) obtained for the system  
Oxygen/Nylon 6I/6T, at 22.0°C and water activity = 0.441.

---

Time (min)	Flow Percent	1/X
30	.56	.611
33	.63	.676
36	.67	.727
39	.72	.794
42	.76	.852
45	.79	.912
48	.81	.960
51	.83	1.006
54	.86	1.078
57	.87	1.108
60	.89	1.165
63	.90	1.218
66	.91	1.247

---

For the sorption process of HDPE/sealant laminate film sample and d-limonene vapor concentration of 1.5 ppm, calculations gave a  $D = 4.3 \times 10^{-10} \text{ cm}^2/\text{sec}$  and a solubility coefficient,  $S = 7.6 \times 10^{-3} \text{ g}$  of limonene per gram of polymer structure.

#### SUMMARY

For penetrant such as organic vapors which can exhibit physicochemical interactions with a polymer matrix, the diffusion coefficient  $D$ , solubility  $S$ , and permeability  $P$  should be determined experimentally in order to describe accurately the mass transfer behavior of penetrant /barrier system. Concentration and time dependent processes should be also considered when dealing with organic penetrants.

In terms of practical applications, the loss of volatile aroma compounds from a polymeric package system can be the result of both sorption and permeation process and both mechanism must be considered for the prediction of changes in the quality of a packaged product.

## REFERENCES

1. ASTM Designation E96-66, Standard Method of Test for Water Vapor Transmission of Materials in Sheet Form.
2. ASTM Designation D3985-81, Standard Method of Test for Oxygen Gas Transmission Rate Through Plastic Film and Sheeting Using A Coulometric Sensor.
3. Bagley, E. and Long, F.A., "Two-Stage Sorption and Desorption of Organic Vapor in Cellulose Acetate," J. Am. Chem. Soc., 77:2172(1958).
4. Baner, A.L., Hernandez, R.J., Jayaraman, J., and Giacin, J.R., "Isostatic and Quasi-Isostatic Methods for Determining the Permeability of Organic Vapors Through Barrier Membranes," in Current Technologies in Flexible Packaging. ASTM STP 912(1986).
5. Baner, A.L., "Diffusion and Solubility of Toluene in Polymeric Films," Presented at the 13th Annual IAPRI Symposium, Oslo, Norway (May, 1986).
6. Beck, J.V. and Arnold, K.J., Parameter Estimation in Engineering and Science, John Wiley and Son, New York, NY (1977).

7. Barrer, R.M., "Permeation, Diffusion and Solution of Gases in Organic Polymers," Trans. Faraday Soc., 35:628 (1939).
8. Berens, A.R., "Diffusion and Relaxation in Glassy Polymer Powders: 1. Fickian Diffusion of Vinyl Chloride in Poly (Vinyl Chloride), Polymer, 18:697 (1977).
9. Berens, A.R., "Analysis of Transport Behavior in Polymer Powders," J. Membrane Science, 3:247 (1978).
10. Bischoff, M. and Everer, P., "Effect of Orientation on the Sorption of Toluene by High Density Polyethylene," J. of Membrane Sci. 23:333 (1984).
11. Caldecourt, V. and Tou, J., "Atmospheric Pressure Ionization Mass Spectrophotometric and Photoionization Techniques for Evaluation of Barrier Film Permeation Properties," TAPPI Proceedings, Polymers, Laminations and Casting Conference, 441 (1985).
12. Chapra, S.C. and Canale, R.P., Numerical Methods for Engineers, McGraw-Hill Book Company (1985).
13. Choy, C.L., Leung, W.P., and Ma, T.L., "Sorption and Diffusion of Toluene in Highly Oriented Polypropylene," J. Polymer Science: Polymer Physics Edition, 22:707 (1984).

14. Crank, J. and Park, G.S., Diffusion in Polymers, Academic Press, New York, NY (1968).
15. Crank, J., The Mathematics of Diffusion, 2nd Edition, Clarendon Press, Oxford, England (1975).
16. DeLassus, P., "Transport of Unusual Molecules in Polymers Films," TAPPI Proceedings, Polymers, Laminations and Coating Conference, 445 (1985).
17. Fujita, J., "Diffusion in Polymer-Diluent Systems," Fortsch-Hochpolym-Forsch, 3:1 (1961).
18. Gilbert, S.G., Hatzidimitriu, E., Lai, C., and Passy, N., "Studies on Barrier Properties of Polymeric Films to Various Organic Aromatic Vapors," Instrumental Analysis of Food, 1:405 (1983).
19. Han, J.K., Miltz, J., Harte, B.R., Giacin, J.R. and Gray, J.I., "Loss of 2-tertiary-butyl-4-methoxy phenol (BHA) from High Density Polyethylene Film," Polymer Engineering and Science (1986) .
20. Hernandez, R.J., "Permeation of Toluene Vapor Through Glassy Poly(ethylene) Terephthalate Films," M.S. Thesis, Michigan State University, East Lansing, MI 48824-1223 (1984).

21. Hilton, B.W. and Nee, S.Y., "Permeability of Organic Vapors Through Packaging Films," *Ind Eng. Chem. Prod. Res. Dev.*, 17(1):80 (1978).
22. Meares, P., "Transient Permeation of Organic Vapors Through Polymer Membranes," *J. Appl. Polymer Sci.*, 9:917 (1965).
23. Mohny, S., Hernandez, R.J., Giacini, J.R., and Harte, B.R., "The Aroma Permeability of Packaging Films and Its Relationship to Product Quality," Presented at 13th Annual IAPRI Symposium, Oslo, Norway (May, 1986).
24. Murray, L.J. and Dorschner, R.W., "Permeation Speeds Tests, Aids Choice of Exact Material," *Package Engineering*, March:76 (1983).
25. Murray, L.J., "An Organic Vapor Permeation Rate Determination for Flexible Packaging Materials," *J. Plastic Film and Sheeting*, 1:104 (1985).
26. Niebergall, W., Humeid, A., and Blochl, W., "The Aroma Permeability of Packaging Films and Its Determination by Means of a Newly Developed Measuring Apparatus," *Lebensm. Wiss U. Technol.*, 11(1):1 (1978).

27. Pasternak, R.A., Schmimscheimer, J.F., and Heller, J., "A Dynamic Approach to Diffusion and Permeation Measurements," J. Polymer Sci. Part A-2, 8:467 (1970).
28. Peterlin, A., "Dependence of Diffusive Transport on Morphology of Crystalline Polymers," J. Macromol. Sci. Phys., B11(1):57 (1975).
29. Pye, D.G., Moehr, M.M., and Panar, M., "Measurement of Gas Permeability of Polymers, II. Apparatus for Determination of the Permeability of Mixed Gases and Vapors," J. Applied Polymer Sci., 20:1921 (1976).
30. Smith, T.L. and Adam, R.E., "Effect of the Tensile Deformation on Gas Transport in Glassy Polymer Films," Polymer, 22(3):299 (1981).
31. Ziegel, K.D., Frensdorff, H.K., and Blair, D.E., "Measurement of Hydrogen Isotope Transport in Poly(Vinyl Fluoride) Films by Permeation Rate Method," J. Polymer Sci., Part A-2, 7:809 (1969).
32. Zobel, M.G.R., "Measurement of Odour Permeability of Polypropylene Packaging Films at Low Odourant Levels," Polymer Testing, 3:133 (1982).

33. Zobel, M.G.R., "Aroma Barrier Properties of Coextruded Films," Presented at COEX'84 in Proceedings of the 4th Annual International Conference and Exhibition on Coextrusion Markets and Technology, September 19-21, Princeton, NJ (1984).
  
34. Zobel, M.G.R., "The Odour Permeability of Polypropylene Packaging Film," Polymer Testing, Vol. 5, No. 2:153 (1985).

## CHAPTER II

### The Sorption of Water Vapor by an Amorphous Polyamide \*\*

#### ABSTRACT

The dual-mode sorption model presented here was found to describe accurately the sorption of water vapor by an amorphous polyamide at 23° C over a broad range of water activity. The Langmuir equation is used to calculate the volume fraction of chemisorbed solute and the Flory-Huggins equation is used instead of Henry's Law to calculate the volume fraction of water which is not chemisorbed. This model describes the data over the range of water activities from zero to one and predicts clustering of the sorbant. Fourier Transform Infrared (FTIR) spectroscopy data and dielectric measurements of the gamma relaxation temperature suggest that the water binds to amide groups at low water activities. This physical evidence of binding corresponds well with the predictions of the Langmuir factor of the sorption model.

---

\*\* Paper submitted to the Journal of Membrane Science.

## INTRODUCTION

An amorphous polyamide recently has been synthesized and characterized [1]. This polymer is made from hexamethylenediamine and a mixture of isophthalic and terephthalic acid. The random placement of these isomers in the polymer chain prevents crystallization of the material. Preliminary studies on the effect of water sorption on the barrier properties of this amorphous polymer show atypical behavior, compared to semicrystalline polyamides. For example, oxygen permeability increases as a function of moisture content in Nylon 66 (a semicrystalline polyamide) but decreases as a function of moisture content in amorphous material. The tensile modulus decreases with moisture content in Nylon 66 but increases with moisture content in the amorphous material [1].

The intriguing behavior of the amorphous polyamide system in the presence of water demonstrates the need for equilibrium models which describe sorption phenomena well over a wide solute activity range. Improved models are needed for binary systems and hopefully can be extended to describe ternary systems (non-condensable gas - water - polymer) in order to interpret and control barrier properties. This study models the sorption phenomena of water vapor into amorphous polyamide as the first step in describing the effects of water on the barrier and mechanical properties of this polymer.

DUAL MODE SORPTION MODELS

**Model for Gas Sorption in Glassy Polymers**

Sorption of gases, such as helium, nitrogen, oxygen, carbon dioxide, and methane above their critical temperature, into glassy polymers has been studied by many researchers. The dual mode sorption model proposed by Michaels et al [2] is the most widely used model for analyzing these data. This model assumes that the solute molecules in the glassy polymer consist of freely diffusing and bound species which are in dynamic equilibrium with the medium. The solubility of the freely diffusing species is represented by Henry's Law and the solubility of the bound species is described by a Langmuir type adsorption isotherm. Local equilibrium between the freely diffusing and the bound species is maintained throughout the polymer matrix [3]. The model is:

$$C = C_D + C_H = k_D p + \frac{C_H' b}{1 + b p} \quad (1)$$

where  $C$  is the total solubility of sorbant in the polymer,  $C_D$  and  $C_H$  are the solubilities due to Henry's law and Langmuir sorption,  $k_D$  is the Henry's law constant,  $b$  is the hole affinity constant,  $C_H'$  is the hole saturation constant and  $p$  is the pressure. The plot of the penetrant solubility,  $C$ , as a function of pressure for eqn 1 is always monotonically convex to the pressure axis.

This model has been used to describe the solubility of gases in glassy polymers, and in glassy, polar polymers as well. Uragami et al [4] studied

the sorption and equilibrium for  $\text{CO}_2$  in a polyimide film for pressures up to 0.78 atmospheres. Chern et al [5] applied eqn 1 to the permeability of  $\text{CO}_2$  through Kapton polyimide for pressures up to 16.3 atmospheres. Koros and Sanders [6] described a bicomponent sorption process by the dual mode sorption model ( $\text{CO}_2/\text{C}_2\text{H}_4$  and  $\text{CO}_2/\text{N}_2\text{O}$  in poly(methyl methacrylate)). Henry's law is an adequate description of the solubility for many gases, although it may fail at high solute activities.

#### **Models for Polar Systems at High Solute Activities**

Solutes below their boiling point (such as organic solvents and water at room temperature) often exhibit an inflection point in the solubility versus pressure curve. For these cases, eqn. 1 does not describe the data well over the activity range,  $0 < a_1 < 1$ , and usually underpredicts the actual solubility values at high activities. This lack of agreement has been explained as a "positive deviation" of the Henry's law caused by the swelling of the polymer network as the penetrant is sorbed. It is postulated that the network swelling exposes more binding sites and increases the sorption level of the penetrant synergistically [3].

Table 1 lists some recent data sets for polar systems at high solute activities and models used to describe the solute solution factor ( $C_D$  of eqn. 1) for these data. The Henry's Law description of solute solution has been modified to include a concentration effect [8], [10]. In the case of vinyl chloride/poly(vinyl chloride), the new term has been related to the Flory-Huggins equation. Berens [9] reported that this equation adequately

Table 1. Models for Polar Systems at High Solute Activities

System	Solution Factor	Comment	Ref.
H <sub>2</sub> O/Polyacrylonitrile	$k_d \exp(\sigma c) p$	data of [7]	[8]
Vinyl Chloride/Poly- (vinyl Chloride)	Flory-Huggins <sup>1</sup>	fits for $0 < a_1 < 1$	[9]
	$k_d \exp(\sigma c) p$	data of [9]	[10]
	$\sigma = 2(1+\chi)A$		
H <sub>2</sub> O/Kapton <sup>2</sup>	$k_d p$		[11]
H <sub>2</sub> O/Nylon 6 <sup>3</sup>	Flory-Huggins <sup>1,4</sup>	fit by authors	[12]
H <sub>2</sub> O/Epoxy <sup>5</sup>	$k_d p$	hysteresis	[13]
H <sub>2</sub> O/Epoxy <sup>6</sup>	$k_d = \exp(1+\chi)$	two Langmuir factors	[14]

1 - Flory-Huggins model only, no Langmuir term

2 - Registered trademark, E.I. du Pont de Nemours and Company, for a aromatic polyether diimide.

3 - trademark of E.I. duPont de Nemours, Inc.

4 - best fit model as determined by authors of this work.

5 - TGDDM/DDS epoxy resins (MY720, Ciba-Geigy, Ltd.)

6 - DBEBA/TETA (Epikote 828, Shell, Italy) and TBDDM/DDS (Araldite MY720 Ciba-Geigy, Ltd.)

described his data. For high molecular weight polymers, the Flory-Huggins expression [15-17] is:

$$\ln a_1 = \ln V_1 + \frac{V_2}{V_1} + \chi \frac{V_2^2}{V_1} \quad (2)$$

where  $\chi$  is the interaction parameter. Although eqn. 2 does not provide the most accurate description of the thermodynamic performance of polymer solutions, it does contain most of the essential features which distinguish such solutions [18]. Eqn. 2 usually fits equilibria data over a wider range than Henry's law. For example, sorption data of toluene in poly(vinyl chloride) is well fit by the Flory-Huggins equation especially for  $0.5 < a_1 < 1.0$  [19].

Sfirakis and Rogers [12] studied the sorption of vapors by Nylon 6 but did not present a mathematical model to describe the sorption process. However, this data set can be fit to eqn. 2 with a  $\chi$  value of 1.88. The Henry's Law term seems adequate for fitting the water/Kapton data. Either hole filling or chemisorption might be occurring in the polyimide for the Langmuir contribution, as Kapton is known to hydrogen bond with water. Water is known to hydrogen bond with a variety of epoxies and the dual mode sorption model describes some data well [13]. Apicella et al [14] tested the hole-filling hypothesis with an epoxy system by sorbing water between 0 and 60 atm. Two Langmuir factors were needed to model these data: one for chemisorption (probably to hydroxyl or secondary amine groups) and one for sorption into holes. The use of eqn. 2 to describe solvent solution seems an obvious extension of the work summarized in Table 1. The constant describing solute solution is usually determined at high solute

pressures. It would be desirable to develop criteria for determining how to choose the constants.

### CLUSTERING OF SOLUTE MOLECULES

Self-association of the solute to form clusters has been used to explain a number of transport phenomena occurring in polar systems. For example, the clustering of water molecules in polyacrylonitrile coincides with a maximum in the diffusion coefficient [20]. Clustering could reduce the effective mobility of water since the size of the diffusing group increases. A similar effect has been reported for Kapton by Yang et al [11]. The authors calculated the clustering of water by differentiation of a fourth order polynomial fit. Puffr and Sebenda [21] reported the clustering of water in several polyamides. Skirrow and Young [22] described the clustering of water, methanol and propanol in Nylon 6 by plotting  $a_1/V_1$  versus  $a_1$ . In Nylon 6, clustering has been associated with a change in the diffusion coefficient [12]. Aronhime et al [23] reported clustering of water in epoxy resins. It would be useful to predict the onset of clustering by direct analysis of the model used to describe the solute sorption.

The clustering function developed by Zimm and Lundberg [24-25] has been used with binary systems in equilibrium to give a measure of the tendency of like molecules to cluster. Their clustering function,  $G_{11}/V_1$ , is:

$$\frac{G_{11}}{V_1} = -v_2 \frac{\delta (a_1/V_1)}{\delta a_1} - 1 \quad (3)$$

where  $V_1$  is the volume fraction of the solute,  $V_2$  is the volume fraction of the polymer, and  $a_1$  is the solute activity. When  $G_{11}/V_1$  is greater than -1, the solute is expected to cluster.

Equation 1 is not written in a convenient form for the analytical determination of the derivative in eqn 3. Popular methods for evaluating the clustering function are either fitting activity versus volume fraction data with polynomials and taking their derivatives or doing a numerical differentiation of the data. Equation 1 can be rearranged to express the concentration,  $C$ , as volume fraction and to express the Henry's law and Langmuir contributions in terms of activity:

$$V_1 = V_1^H + V_1^L = K_D a_1 + \frac{K a_1}{1 + B a_1} \quad (4)$$

where  $V_1^H$  and  $V_1^L$  are the Henry's law and Langmuir volume fraction contributions,  $K_D = k_D p_s$ ,  $K = C_H' f b p_s$ ,  $B = b p_s$ ,  $p_s$  is the saturation vapor pressure of the solute and  $f$  is a conversion factor. Applying eqn 3 to eqn 4 gives:

$$\frac{G_{11}}{V_1} = -V_2 \frac{V_1 - [K_D a_1 + K a_1 / (1 + B a_1)^2]}{V_1^2} \quad (5)$$

Since the term in brackets is always less than  $V_1$ ,  $G_{11}/V_1$  is always less than -1 for the range,  $0 < a_1 < 1$ . Therefore, a system which follows Henry's law solubility and Langmuir binding should not have clustering.

The clustering function for the Flory-Huggins equation has been derived previously [26] and is:

$$\frac{G_{11}}{V_1} = \frac{2\chi}{1 - 2\chi V_1} > -1 \quad (6)$$

for a constant value of  $\chi$ . eqn 6 always predicts clustering in the range,  $0 < V_1 < 1/2\chi$ . The equation is not defined at the upper limit of the range ( $V_1 = 1/2\chi$ ), which is the spinodal point indicating phase separation.

Neither the conventional dual mode sorption model or the Flory-Huggins model with a constant value for  $\chi$  correctly describe the apparent clustering in the systems mentioned above (Table 1).

#### Modified Dual Mode Sorption Model

In this study, eqn 1 has been modified by using the Flory-Huggins equation to describe non-specific solution rather than Henry's law. This modification should allow the model to fit over the activity range,  $0 < a_1 < 1$ . Other choices for the solution model are possible, but the Flory-Huggins equation is relatively simple to apply. Because the non-specific sorption term is nonlinear, the complete model can have an inflection point and should predict clustering somewhere over the range of activity values. For convenience, the modified dual mode sorption model is expressed in terms of volume fractions and solute activity:

$$V_1 = V_1^{FH} + V_1^L \quad (7)$$

wh

fr

fo

7

I

where  $V_1^{FH}$  refers to the Flory-Huggins contribution to the solute volume fraction. Since eqn 2 is nonlinear, it is convenient to determine the value for  $V_1^{FH}$  by numerical methods, such as the Newton-Raphson technique and eqn 7 becomes:

$$V_1 = FH(a_1, \chi) + \frac{K a_1}{1 + B a_1} \quad (8)$$

The clustering function based on eqn. 8 is:

$$\frac{G_{11}}{V_1} = \frac{V_2}{V_1^2} \left[ \frac{K a_1}{(1+B a_1)^2} + \frac{V_1^{FH}}{1-V_1^{FH}(1+2\chi V_2^{FH})} \right] - \frac{1}{V_1} \quad (9)$$

Equation 9 predicts clustering for some values of the constants but is undefined when:

$$1 - V_1^{FH} (1 + 2 \chi V_2^{FH}) = 0 \quad (10)$$

This occurs when  $V_1$  is 1.0 (pure solvent) or  $1/2\chi$  (phase separation).

## EXPERIMENTAL METHODS

### Polymer Films

The amorphous polyamide used in this study was provided by E. I. du Pont De Nemours and Company. The polymer was synthesized from hexamethylene diamine and a mixture of 70/30 isophthalic and terephthalic acids. The random placement of the acid isomers in the polymer chain prevents

crystallization. No evidence of a crystalline melting point was found for this polymer.

#### Equilibrium Sorption Data

Equilibrium sorption data was taken on polymer films using a Cahn Electrobalance Model RG. A stream of nitrogen adjusted to specific values of water activity provided the source of water vapor in equilibrium with the polymer films. The apparatus and operation are described elsewhere [27]. Closed containers with salt solution to provide selected values of water activity were also used. The experiments were conducted at room temperature. The film samples, of  $2.93 \times 10^{-5}$  m thickness (1 mil), were dried under vacuum at  $100^{\circ}$  C before each run.

#### Density Experiments

Film densities were determined in a density gradient column with the gradient made of toluene and carbon tetrachloride.

#### Fourier Transform Infrared Spectroscopy

The sample for infrared analysis was prepared by casting a thin film onto a zinc sulfide (ZnS) crystal from a 2% solution with 1,1,1,3,3,3-hexafluoro-2-propanol (Kerr Company, Novi, Michigan). After evaporation of the solvent at room temperature, the sample was dried in a vacuum oven at  $100^{\circ}$  C to remove residual solvent and water. The sample was then equilibrated with water vapor at selected water activity values. After

attaining equilibrium, the sample was immediately covered with another crystal of ZnS and transferred to the instrument.

#### Differential Scanning Calorimetry and Dielectric Experiments

Film samples were prepared for these analyses by vacuum drying at 100° C and equilibrating with the vapor over salt solutions to give selected water activities.

### RESULTS AND DISCUSSION

#### Equilibrium Sorption Isotherm

Sorption equilibrium values of water weight fraction and volume fraction in the amorphous polyamide at 23° C are presented in Table 2. Experimentally determined and calculated densities for the water-polymer solution also are presented. Isotherm data was obtained over a wide activity range ( $0.046 < a_1 < 0.96$ ) in order to provide a good test of the modified dual mode sorption model. Figure 1 shows the sorption isotherm for water in the amorphous polyamide. The solid curve through the data is the Flory-Huggins equation (eqn 2) with a  $\chi$  value of 1.632. The value of the interaction parameter was calculated by using a Box-Kanamazu modification of the Gauss method of minimization of sum of squares for nonlinear models [28]. This model represents the data at high activities very well.

Table 2. Experimental Data

Temperature: 23C

Water Activity	Uptake Weight	Uptake Percent	Experim. Density	Calcul. Density	Weight Fraction	Volume Fraction
0.0000	0.00000	0.0000	1.1938	1.1938	0.00000	0.00000
0.0460	0.00470	0.4700	---	1.1939	0.00468	0.00560
0.0560	0.00657	0.6572	---	1.1940	0.00653	0.00781
0.0720	0.00752	0.7520	---	1.1941	0.00746	0.00893
0.0800	0.00787	0.7870	1.1938	1.1942	0.00781	0.00935
0.0900	0.00836	0.8360	---	1.1943	0.00829	0.00992
0.1100	0.00938	0.9380	---	1.1944	0.00929	0.01113
0.1550	0.01211	1.2110	---	1.1950	0.01197	0.01433
0.1890	0.01290	1.2900	---	1.1955	0.01274	0.01526
0.2520	0.01670	1.6700	---	1.1964	0.01643	0.01970
0.2690	0.01596	1.5960	---	1.1967	0.01571	0.01884
0.3080	0.02200	2.2000	1.1975	1.1973	0.02153	0.02583
0.4100	0.03040	3.0400	1.1986	1.1989	0.02950	0.03545
0.4400	0.03568	3.5680	---	1.1993	0.03445	0.04142
0.5650	0.04180	4.1800	---	1.2008	0.04012	0.04829
0.5800	0.04580	4.5800	---	1.2009	0.04379	0.05272
0.5850	0.04340	4.3400	---	1.2010	0.04159	0.05007
0.6350	0.05050	5.0500	1.2012	1.2014	0.04807	0.05789
0.7350	0.06190	6.1900	1.2017	1.2019	0.05829	0.07022
0.7900	0.07110	7.1100	---	1.2020	0.06638	0.07998
0.8600	0.07870	7.8700	---	1.2021	0.07296	0.08791
0.8800	0.08200	8.2000	1.2022	1.2022	0.07579	0.09132
0.9630	0.09000	9.0000	1.2022	1.2024	0.08257	0.09951

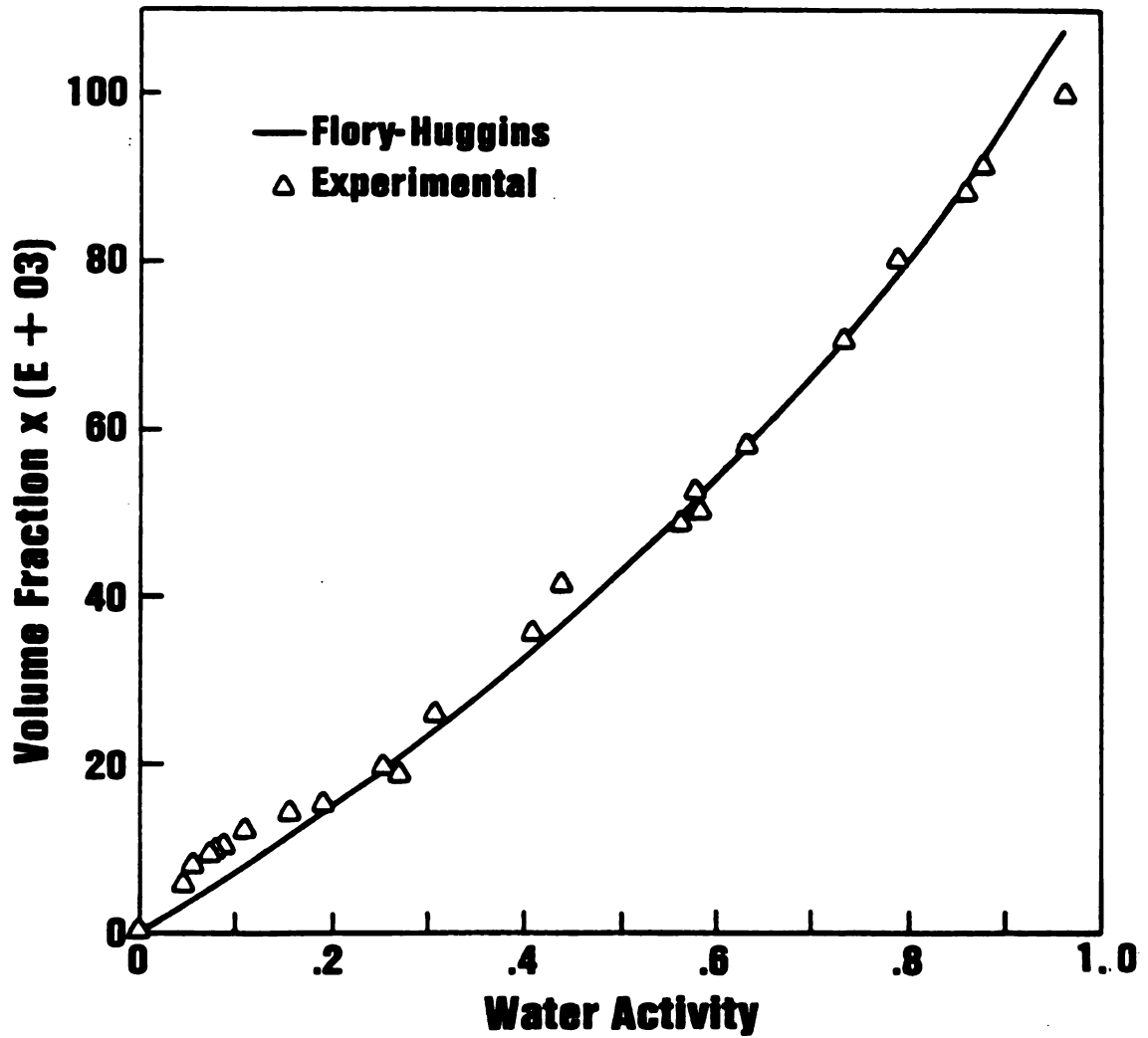


Figure 1. Experimental sorption values and Flory-Huggins fitting.

### Parameter Estimation for Equation 7

Parameter values estimated for eqn 7 were sensitive to the method used to determine them. A nonlinear regression method was used to determine the values of the three parameters simultaneously. This resulted in Langmuir coefficients with a high amount of error and a fit using eqn 7 which was no better than the fit using eqn 2. The least squares technique was not sensitive to deviations between the data and the model at low activities. However, the deviation of eqn 2 from the data is systematic. Figure 2 shows an expanded view of the low water activity data and the underprediction of eqn 2.

An alternative parameter estimation method gave coefficients with lower error. The data for  $a_1 > 0.4$  were used to determine a range of  $\chi$  values which could represent this portion of the curve.  $\chi$  should be between 1.6 and 1.85 to minimize the least square error for this data set. The data for  $a_1 < 0.4$  were used to determine the Langmuir coefficients. The nonlinear regression method gave the coefficients and the  $R^2$  parameter for a set of  $\chi$  values in this range. The  $R^2$  value was plotted as a function of  $\chi$  to find the best estimates of the parameters. Figure 3 shows eqn 8 as the solid curve ( $\chi = 1.7$ ,  $K = 0.395$  and  $B = 95.2$ ) and the complete data set. Table 3 shows the contribution of the Langmuir and Flory-Huggins factors to the solute volume fractions over the activity range. At low activities, the Langmuir contribution is high compared to the Flory-Huggins contribution and at  $a_1 = 0.4$ , it is just over 10% of the total volume fraction of solute. The Langmuir contribution is nearly constant (> 90% of its maximum value) at activities greater than 0.11 and the curve at high water activities should be insensitive to the values of the Langmuir coefficients. Therefore, the estimation method is consistent with the parameter values.

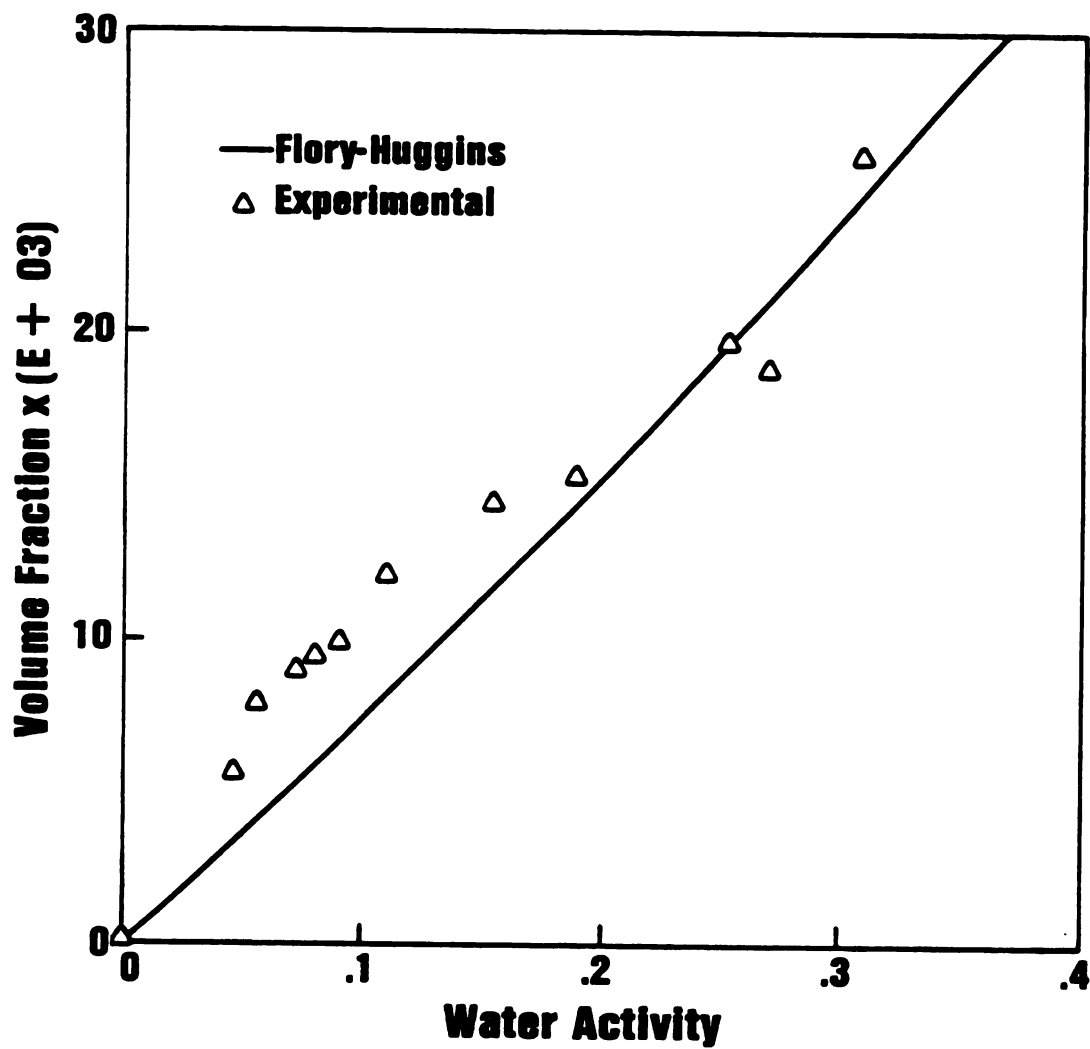


Figure 2. Experimental sorption values and Flory-Huggins fitting at low activity values.

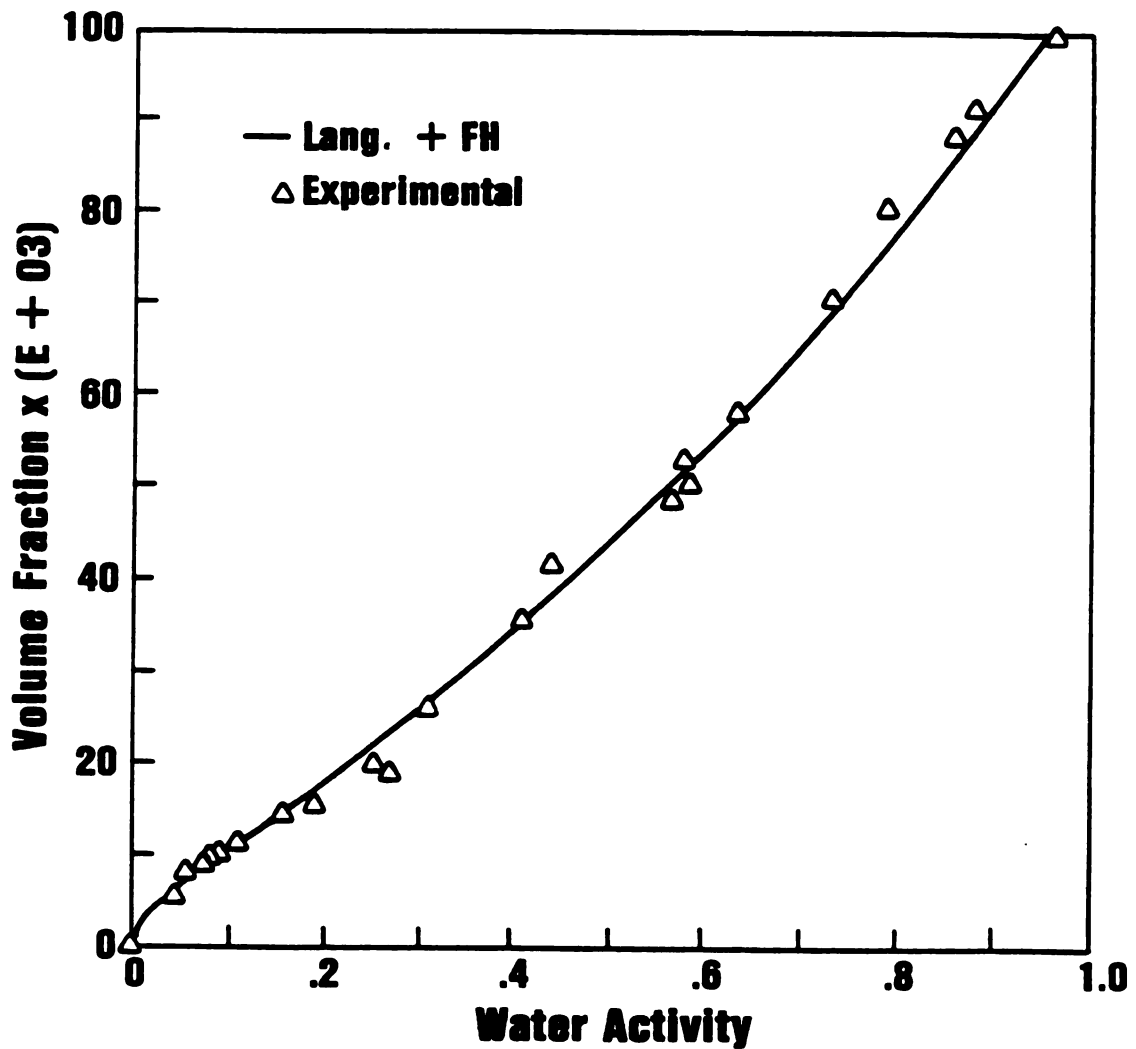


Figure 3. Best fit for the Langmuir-Flory-Huggins model. Values of the parameters are  $\chi = 1.70$ ,  $K = .385$  and  $B = 95.15$ .

Table 3. Langmuir and Flory-Huggins volume fraction contributions.

$\chi = 1.7$   
 $k = .384707$   
 $B = 95.14954$

Activity	Lang.	F-H	Total
0	0	0	0
.01	1.971345E-03	6.740509E-04	2.645396E-03
.02	2.650418E-03	1.352126E-03	4.002545E-03
.03	2.994228E-03	2.034278E-03	5.028507E-03
.04	3.201902E-03	2.72056E-03	5.922462E-03
.046	3.291226E-03	3.134332E-03	6.425558E-03
.056	3.404285E-03	3.827329E-03	7.231615E-03
.072	3.528178E-03	4.945029E-03	8.473208E-03
.08	3.573699E-03	5.508051E-03	9.081749E-03
9.000001E-02	3.62041E-03	6.215795E-03	9.836204E-03
.11	3.690574E-03	7.644741E-03	1.133531E-02
.155	3.786443E-03	1.09277eE-02	1.471418E-02
.189	3.830196E-03	1.347346E-02	1.730366E-02
.252	3.881311E-03	1.834934E-02	2.223065E-02
.269	3.891157E-03	1.970243E-02	2.359359E-02
.308	3.909771E-03	2.287032E-02	2.678009E-02
.41	3.942132E-03	3.161252E-02	3.555465E-02
.44	3.94886E-03	.0343221	3.827096E-02
.565	3.969349E-03	4.640153E-02	5.037088E-02
.58	3.971223E-03	4.794643E-02	5.191766E-02
.585	3.971826E-03	4.846641E-02	5.243823E-02
.635	3.977355E-03	5.381052E-02	5.778788E-02
.735	3.986187E-03	6.538535E-02	6.937154E-02
.79	3.990099E-03	7.234575E-02	7.633585E-02
.86	3.994368E-03	8.194831E-02	8.594268E-02
.88	3.995463E-03	8.486796E-02	8.886342E-02
.963	3.999531E-03	9.799333E-02	.1019929

### Sensitivity Coefficients

Sensitivity coefficients indicate the magnitude of the change of a function due to perturbation in the values of its parameters [28].

Sensitivity coefficients for eqn 8 are given by the first derivative of the volume fraction with respect to  $\chi$ , B and K.

$$X_K = \frac{\delta V_1}{\delta K} = \frac{a_1}{1 + B a_1} \quad (11)$$

$$X_B = \frac{\delta V_1}{\delta B} = \frac{-K a_1^2}{(1 + B a_1)^2} \quad (12)$$

$$X_\chi = \frac{\delta V_1}{\delta \chi} = \frac{V_1^{FH} V_2^{FH}}{2 v_1^{FH} - 1} \quad (13)$$

where  $X_K$ ,  $X_B$ , and  $X_\chi$  are the sensitivity coefficients of K, B and  $\chi$ . These coefficients were evaluated as a function of activity,  $a_1$ , at the optimum values of K, B, and  $\chi$  and the results are plotted in Figure 4.

For  $a_1 > 0.1$ ,  $X_\chi$  changes with activity while  $X_K$  and  $X_B$  are essentially constant. For high activity values, it will be difficult to distinguish between K and B parameters. At low activity values, they are non-linear dependent and better estimates for them can be obtained. The results shown in Figure 4 suggest that a simultaneous search for the three parameters will be difficult over the entire activity range, that high activity data will be insensitive to K and B, and that the best estimates for K and B will be obtained at low activity values. Eqs. 11-13 give a protocol for evaluating the method of determining the constants and are an improvement over the

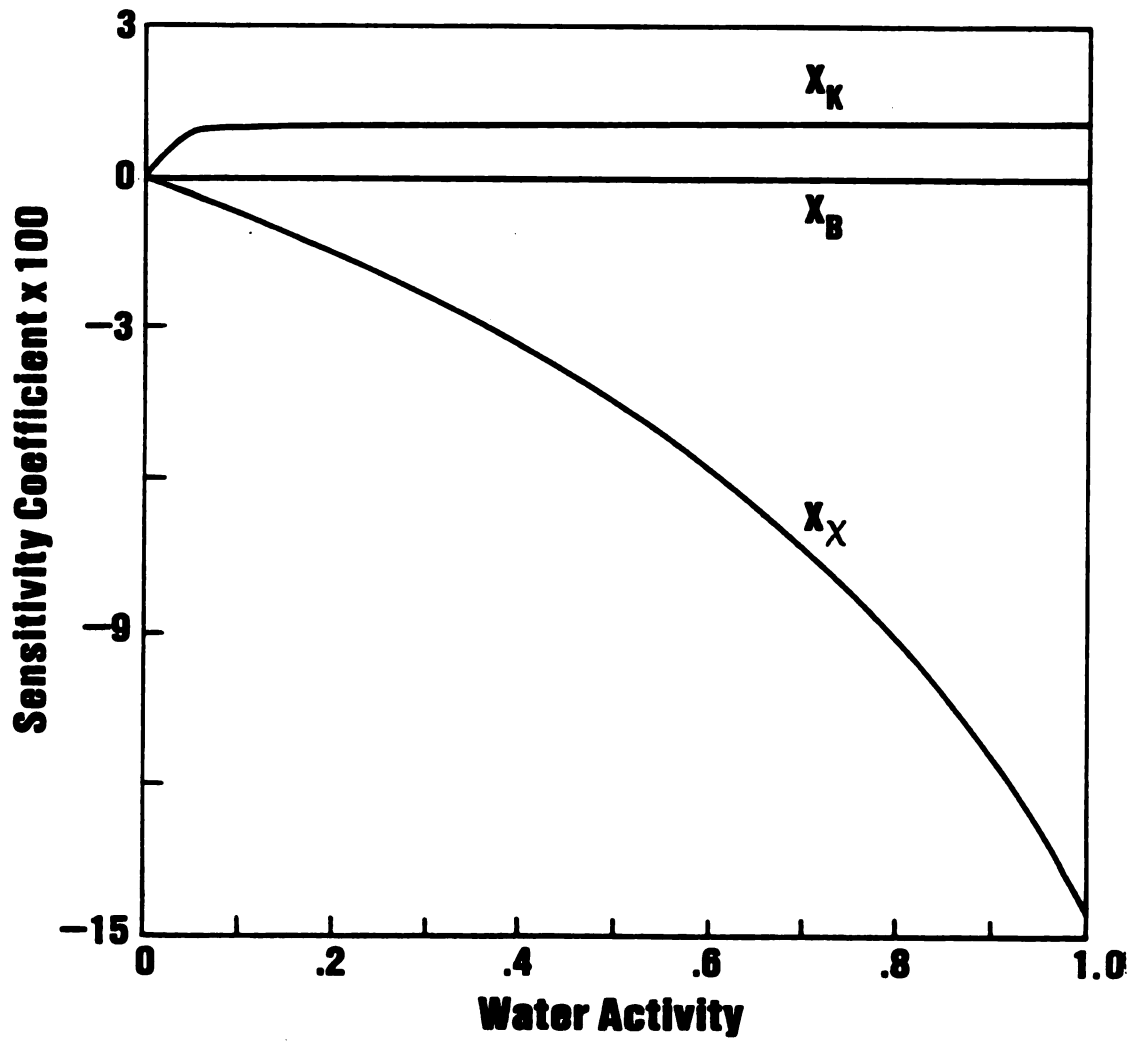


Figure 4. Sensitivity coefficients as a function of activity.

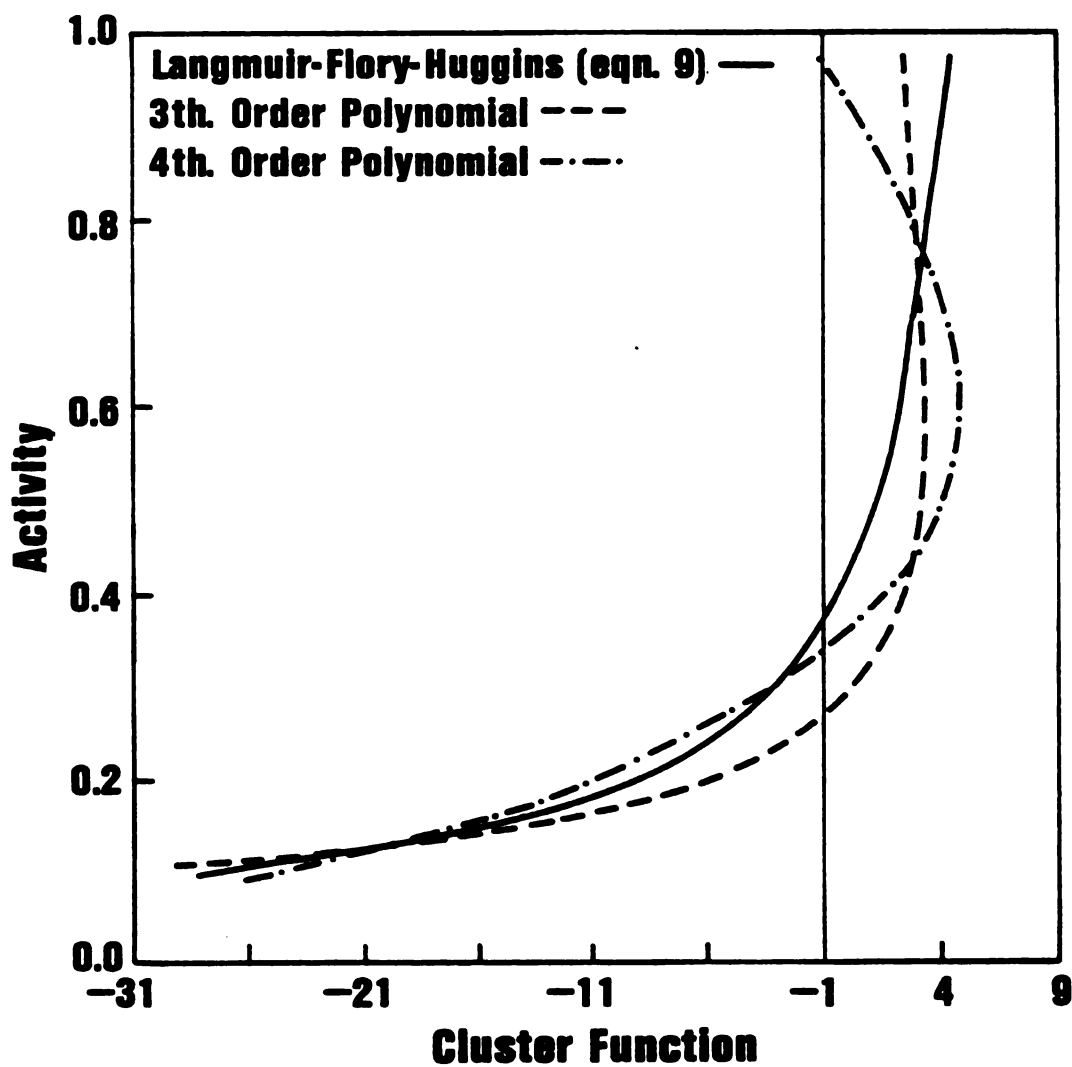


Figure 5. Clustering function as a function of activity.

suggestion that the constant(s) for the solution phenomenon should be determined when the solute partial pressure is much larger than the Langmuir affinity constant,  $b$  [10].

### Clustering Analysis

Equation 9 and polynomial expressions were used to compute the clustering function for the water sorption data. The polynomial expressions fit the data with similar least square errors. Both expressions approached but did not pass through the zero activity-zero volume fraction point, and neither expression replicated the S-shaped curve of the data. Figure 5 shows the clustering function estimated from two polynomial fits (third and fourth order) and the modified dual mode sorption model. All three equations predict clustering ( $G_{11}/V_1 > -1$ ) but differ in the solute activity at which this should occur. The fourth order polynomial predicts clustering in the activity range,  $0.34 < a_1 < 0.96$ . The third order polynomial predicts clustering for  $a_1 > 0.27$  but the clustering function does go through a maximum at  $a_1 = 0.60$ . There is no obvious physical explanation for why clustering should decrease, or disappear, at high water activities.

Equation 9 predicts clustering at  $a_1 = 0.38$  and the function is increasing monotonically over the whole activity range.

### Physical Evidence for Solute Binding

The Langmuir isotherm was derived based on chemisorption of a chemical species to a specific binding site characterized by a single activation energy. Solute sorption described by this isotherm for the water-polyamide solution might result in observable changes in physical properties of the polymer, particularly if the water is associated with a specific group on the polymer backbone. One obvious possibility is water interaction with the amide group. FTIR spectroscopy studies were done to detect possible changes in hydrogen bonding between N-H and carbonyl groups by observing the vibrational modes of the amide group (Amide I and Amide II bands).

The Amide I mode includes contributions from C=O stretching, C-N stretching and C-C-N deformation vibrations. The Amide II band includes N-H plane bending, C-N stretching and C-C stretching vibrations. Figure 6 shows a typical FTIR spectrum taken at room temperature over the range, 800-4000  $\text{cm}^{-1}$  for a cast polyamide sample. The Amide I and Amide II modes occur at 1640 and 1541  $\text{cm}^{-1}$ , respectively, for the dry sample and are the most intense bands. The frequency scale and the relative intensity of the Amide I and Amide II modes were internally calibrated with reference to the  $\text{CH}_2$  stretching band at 2858  $\text{cm}^{-1}$ . Table 4 lists the absorption frequencies, and Table 5 lists the intensity ratios for the Amide I and Amide II bands of the sample recorded as a function of water volume fraction and activity. The frequency of the  $\text{CH}_2$  stretching band, which served as the internal calibration band, is presented for reference. Figure 7 shows the absorption

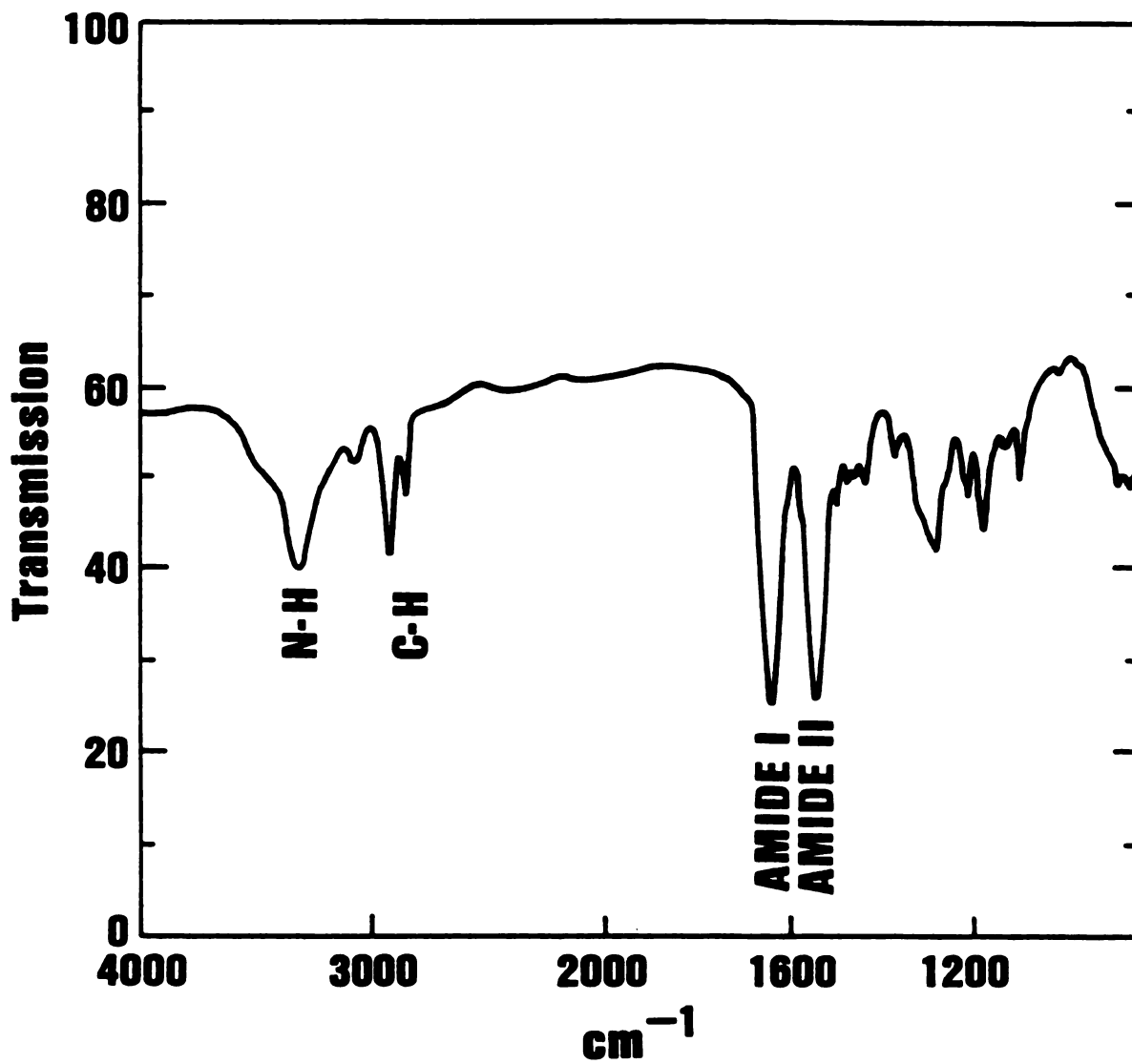


Figure 6. Typical FTIR spectrum of the amorphous polyamide recorded at room temperature.

Table 4. Amide I, Amide II and CH absorption frequencies.

Activity	CH Peak	Amide I	Amide II
0	2858	1640	1541
0.08	2858	1640	1545
0.308	2858	1641	1545
0.56	2858	1641	1545
0.88	2858	1641	1546

Unite:  $\text{cm}^{-1}$

Table 5. Intensity ratios of Amide I and Amide II with respect to CH bands.

ACTIVITY	AMIDE I / C-H	AMIDE II / C-H
0	1.77	5.47
0.08	1.78	5.44
0.308	1.87	5.11
0.56	1.80	5.43
0.88	1.84	5.14

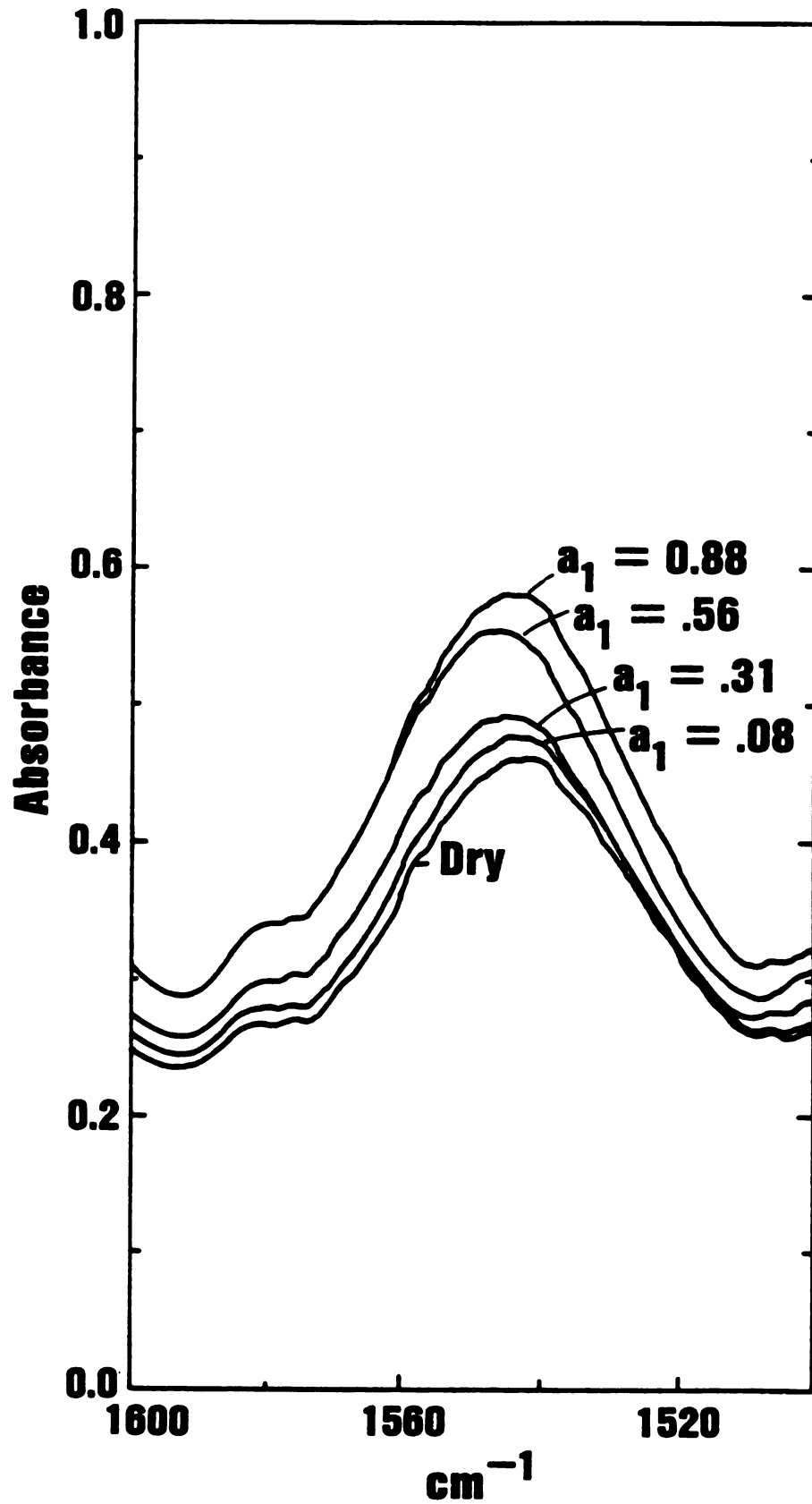


Figure 7. Spectrum region of Amide II as a function of activity.

region from 1500 to 1600  $\text{cm}^{-1}$  (Amide II mode) as a function of  $a_1$ . The spectrum are displayed on an absolute absorbance scale.

The Amide I band remained essentially constant at 1640  $\text{cm}^{-1}$  as did its intensity. The peak maxima of the Amide II band shifted to higher frequency, 1541 to 1546  $\text{cm}^{-1}$ , over the range, 0% to 9.1%, water volume fraction. The intensity ratio of the Amide II band remained essentially constant. The shift of the Amide II band to higher frequency with increasing water content is consistent with an increase in the average hydrogen bond strength [29]. These data suggest that the water does not change the hydrogen-bonding strength of the carbonyl group but does change the hydrogen bonding strength of the N-H group. The shift in the Amide II band is completed at the water activity at which 90% of the Langmuir sites would be filled (Table 3).

In linear, aliphatic homopolyamides there is essentially 100% hydrogen bonding, as evidenced by the absence of bands in the infrared spectra above 3300  $\text{cm}^{-1}$  [30]. In structurally irregular copolymers, such as amorphous polyamide, both the N-H stretching region and the Amide II region can be resolved into "free" and hydrogen bonded stretching modes. Skranovek et al [29] resolved the N-H stretching region into three components: a "free" N-H mode, a hydrogen-bonded N-H stretching mode and an Amide II mode. The Amide I band was resolved into a "free" and hydrogen-bonded carbonyl mode.

Most of the first water molecules sorbed form hydrogen bonds with the "free" N-H groups of the amorphous polyamide. This would be an exothermic process and should have a single activation energy associated with it. The formation of these new hydrogen bonds should have a negligible enthalpic effect [21],[31]. The extent of disruption of the self-association of polyamide neighboring groups by water molecules is not known. Both the

model and the FTIR data suggests that chemisorption has been completed at activities well below those at which clustering occur.

At a water activity of 0.08 (where the Langmuir sites are 89% saturated), the total amount of chemisorbed water is only 4% of the total water volume fraction. This amount corresponds to  $3.34 \times 10^{-3}$  g of water per gram of polymer, or one molecule of water per 22 repeating units of the polymer. Each repeat unit contains 2 amide groups so only 2.3% of the amide groups available form hydrogen bonds with water.

#### Relaxation Temperatures

Several relaxation temperatures have been described for semicrystalline polyamides. Papir et al [31] related the gamma relaxation peak ( $140^{\circ}\text{K}$ ) of Nylon 6 to the movement of methylene and polar groups. Sfirakis and Rogers [12] reported that the gamma peak for the Nylon 6-water system was affected by water concentration. The change in intensity of the gamma peak with changing water concentration leveled off at a concentration corresponding to the apparent onset of water clustering. The gamma relaxation temperature was measured via the dielectric constant at 1 kHz. The gamma peak of the amorphous polyamide was  $173^{\circ}\text{K}$  in the dry state. The peak was not observed for samples equilibrated at  $a_1 > 0.08$ . The difference could be due to the interaction of water with the amide group decreasing the units available to participate in the relaxation process.

Data for the alpha relaxation temperature (glass transition temperature) were obtained by DSC measurements. The effect of sorbed water on  $T_g$  is shown in Figure 8, where  $T_g$  values are plotted with water volume fraction. There is an apparent change in slope of  $T_g$  with activity near  $a_1 = 0.40$ . A similar trend was observed on  $T_g$  versus water volume fraction obtained from the dielectric experiments. The slope change occurs near the activity at which clustering is predicted. A similar trend was observed by Sfirakis and Roger [12] for the change in the  $\gamma$  peak intensity for the system water-nylon 6.

#### Density Data

Figure 9 shows the change in total density with water activity. The amorphous nylon solution becomes more dense as water is added. This is the opposite effect expected from a mixing rule depending on additive molar volume fractions. A similar result has been reported for an epoxy system [32]. Notice that there is little change in density below water activities of 0.1, where the Langmuir coefficients suggest that chemisorption (or "hole filling") is essentially completed. It is interesting to point out that the permeability of this amorphous nylon to oxygen decreases by a factor of 2 for films at water activities greater than 0.10 compared to a sample from which water has been removed. An inflection point occurs in the density curve near the water activity range ( $0.30 = a_1$  at the maximum of  $d\theta/da_1$  for these data) over which clustering is predicted to begin. The water activity at this inflection point is similar to that near the apparent change in  $T_g$  vs  $a_1$  curve (Fig. 8).

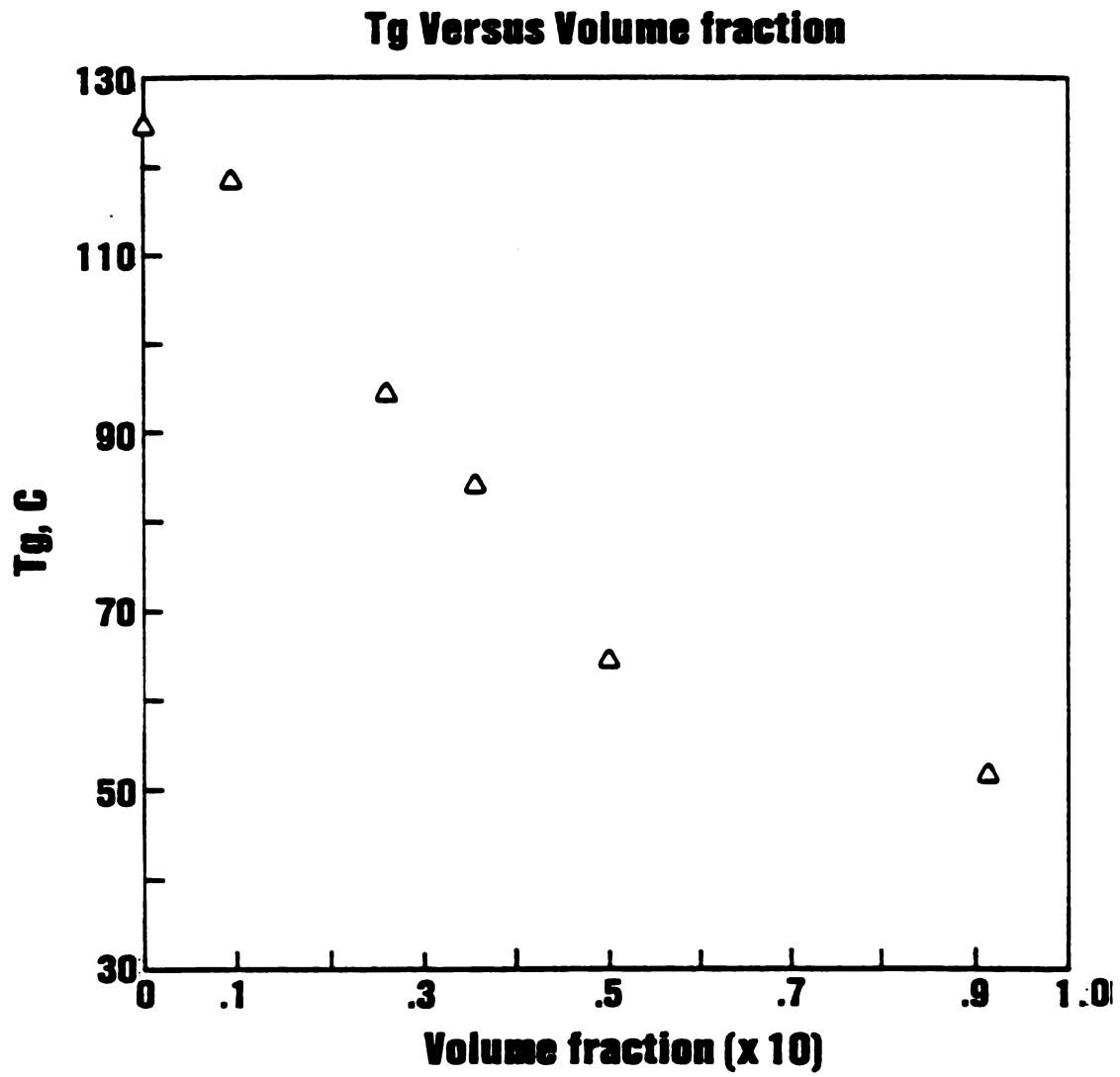


Figure 8. Glass transition temperature as a function of activity.

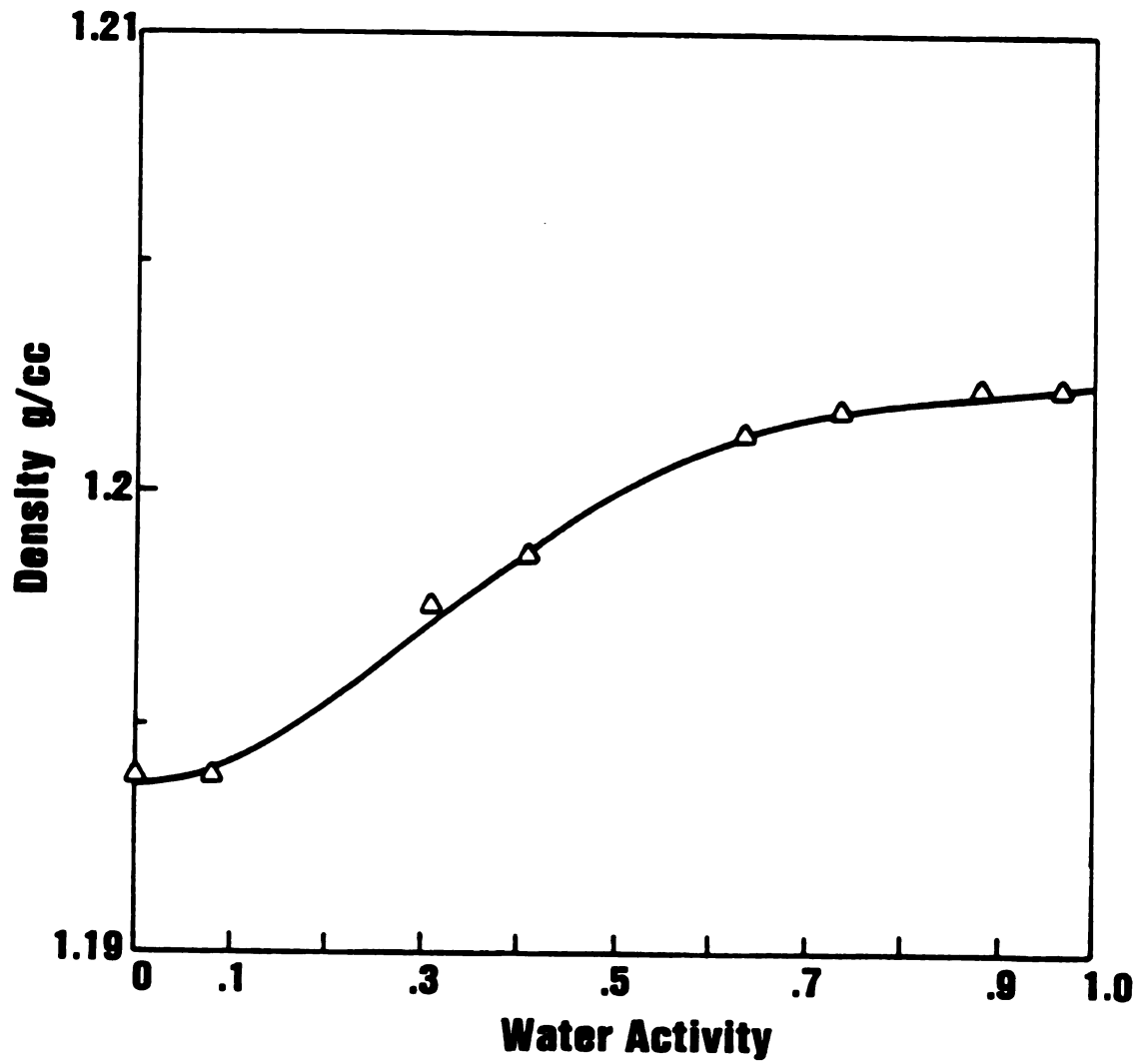


Figure 9. Density as a function of activity.

Proposed Mechanism for Effects of Water Sorption on Physical Properties of Amorphous Polyamide

At water activities less than 0.10, water preferentially chemisorbs to amide bonds, although a low mole fraction of the total hydrogen bonding sites on the polymer are occupied. The chemisorption process can be detected by observing the wave shift in the amide group absorbance. The filling of these "open" positions reduces the permeability of the polymer system to other, nonchemisorbing, species, such as oxygen. Chemisorption is essentially completed at  $a_1 = 0.1$  (about 1 vol % water). There is no measurable change in system density at this water activity. As with other dual mode sorption systems, polymer history and relaxations probably affect the Langmuir sorption capacity,  $C'_H$ , although such data have not been taken in this study.

At higher water activities, the permeability of oxygen and water change little, even though water clustering is predicted. System density increases nonlinearly as water activity increases. A change in the  $T_g$  of the system with respect to water activity coincides with the clustering predictions as does the inflection point in the density-activity curve. Clustering may be associated with the increase in density (and decrease in system volume). The effects of water sorption on transport properties will be treated in another paper. The dual mode sorption model with a Flory-Huggins term to represent non-specific sorption predicts clustering at activities similar to those determined by numerical analysis of the data.

LITERATURE CITED

- 1) P. Blatz and C. Talkowsky, Personnel Communication, (1987).
- 2) A.S. Michaels, W.R. Vieth and J.A. Barrier, J. Appl. Phys., Solution of Gases in Poly (Ethylene Terephthalate), 34(1), (1963), 13.
- 3) W.R. Vieth, J.M. Howell and J.H. Hsieh, Dual Sorption Theory, J. Membrane Sci., 1, (1976), 177.
- 4) T. Uragami, H.B. Hopfenberg, W.J. Koros, D.K. Yang, V.T. Stannett and R.T. Chern, Dual-Mode Analysis of Subatmospheric -Pressure CO<sub>2</sub> Sorption and Transport in Kapton H Polyamide Films, J. Appl. Polym. Sci., 24, (1986), 779.
- 5) R.T. Chern, W.J. Koros, E.S. Sanders and R. Yui, J. Membrane Sci., Second Component "Effect in Sorption and Permeation of Gases in Glassy Polymers," 15, (1983), 157.
- 6) W.J. Koros and E.S. Sanders, J. Polym. Sci., Multicomponent Gas Sorption in Glassy Polymers, 72, (1985), 141.
- 7) V. Stannett, M. Haider, W.J. Koros and H.B. Hopfenberg, Poly. Eng. Sci., Sorption and Transport of Water Vapor in Glassy Poly (Acrylonitrile), 20, (1980), 300.

- 8) G.R. Mauze and S.A. Stern, J. Membrane Sci., The Solution and Transport of Water Vapor in Poly (Acrylonitrile): A Reexamination, 12, (1982), 51.
- 9) A.R. Berens, Angew. Makromol. Chem., The Solubility of Vinyl Chloride in Poly (Vinyl Chloride), 47, (1985), 97.
- 10) G.R. Mauze and S.A. Stern, J. Membrane Sci., The Dual-Mode Solution of Vinyl Chloride Monomer in Poly (Vinyl Chloride), 18, (1984), 99.
- 11) D.K. Yang, W.J. Koros, H.B. Hopfenberg and V.T. Stannett, J. Appl. Polym. Sci., Sorption and Transport Studies of Water in Kapton Polyamide I, 30, (1985), 1035.
- 12) A. Sfirakis and C.E. Rogers, Polym. Eng. Sci., Effects of Sorption Modes on Transport and Physical Properties of Nylon 6, 20, (1980), 294.
- 13) J.A. Barrie, P.S. Sahoo and P. Johncock, J. Membrane Sci., The Sorption and Diffusion of Water in Epoxy Resins, 18, (1984), 197.
- 14) A. Apicella, R. Tessieri and C. DeCataldis, J. Membrane Sci., Sorption Modes of Water in Glassy Epoxies, 18, (1984), 211.

- 15) P.J. Flory, J. Chem. Phys., Thermodynamics of High Polymer Solutions, 10, (1942), 51.
- 16) P.J. Flory, Principles of Polymer Chemistry, Cornell University Press, Ithaca, NY, (1953).
- 17) M.L. Huggins,, Ann. NY Acad. Sci., Thermodynamic Properties of Solution of Long-Chain Compounds, 42, (1942), 1.
- 18) J.M. Prausnitz, R.N. Lichtenthal, and E. Gomez deAzevedo, Molecular Thermodynamics of Fluid-Phase Equilibria, 2nd Ed., Prentice-Hall, Inc., NJ, (1986).
- 19) A.R. Berens, J. American Water Works Assoc., Prediction of Organic Chemical Permeation through PVC Pipe, Nov., (1985), 57.
- 20) V.T. Stannett, G.R. Ranade and W.J. Koros, J. Membrane Sci., Characterization of Water Vapor Transport in Glassy Polyacrylonitrile by Combined Permeation and Sorption Techniques, 10, (1982), 219.
- 21) R. Puffr and J. Sabenda, J. Polym. Sci., On the Structure and Properties of Polyamides XXVII, The Mechanism of Water Sorption in Polyamides, Part C, 16, (1967), 79.

- 22) G. Skirrow and K.R. Young, Polymer, Sorption Diffusion and Conduction in Polyamide-Penetrant Systems: I Sorption Phenomena, 15, (1974), 771.
- 23) M.T. Aronhime, X. Peng and J.K. Gillhan, J. Appl. Polym. Sci., Effect of Time-Temperature Path of Cure on the Water Absorption of High T<sub>g</sub> Epoxy Resins, 32, (1986), 3589.
- 24) B.H. Zimm and J.L. Lundberg, J. Phys. Chem., Sorption of Vapors by High Polymers, 60, (1956), 425.
- 25) J.L. Lundberg, J. Macromol. Sci. Phys., Clustering Theory and Vapor Sorption by High Polymers, 4, (1969), 693.
- 26) T.A. Orofino, H.B. Hopfenberg and V.T. Stannett, J. Macromol. Sci. Phys. Ed., Characterization of Penetrant Clustering in Polymers, 4, (1969), 777.
- 27) R.J. Hernandez, L.A. Baner and J.R. Giacini, J. Plast. Films & Sheeting, The Evaluation of the Aroma Barrier Properties of Polymer Films, 2, (1986), 187.
- 28) J.V. Beck and K.J. Arnold, Parameter Estimation in Engineering and Science, J. Wiley and Sons, NY, (1977).

- 29) D.J. Skronovek, S.E. Howe, P.C. Painter and M.M. Coleman, Macromolecules, Hydrogen Bonding in Polymers: Infrared Temperature Studies of an Amorphous Polyamide, 18, (1985), 2218.
- 30) D.S. Trifan and J.R. Terenzi, J. Polym. Sci., Extends of Hydrogen Bonding in Polyamides and Polyurethanes, 28, (1958), 443.
- 31) Y.S. Papir, S. Kapur and C.E. Rogers, J. Polym. Sci., Effect of Orientation, Anisotropy, and Water on the Relaxation Behavior of Nylon 6, from 4.2 to 300°K, A-2, 10, (1972), 1305.
- 32) E.L. McKague, J.D. Reynolds and J.E. Halkias, J. Appl. Polym. Sci., Swelling and Glass Transition Relations for Epoxy Matrix Material in Humid Environments, 22, (1978), 1643.

## CHAPTER III

### EFFECT OF WATER CONTENT ON THE PERMEABILITY, SOLUBILITY, AND DIFFUSION OF OXYGEN IN NYLON 6I/6T.

#### INTRODUCTION

In general, physical properties of hydrophylic polymers such as polyamides are affected by the presence of water within the polymer matrix. Nylon 6I/6T, a totally amorphous polyamide which was recently developed, is synthesized from hexamethylenediamide and a 70/30 (weight percent) mixture of isophthalic and terephthalic acids. Preliminary studies on the effect of water sorption on the barrier properties of this polymer showed atypical behavior, as compared to semicrystalline Nylons under the same conditions. For example, oxygen permeability in Nylon 66 increases as a function of moisture content of the polymer, while the permeability of oxygen in Nylon 6I/6T shows a decrease in value, with increasing water content of the polymer. Further, the tensile modulus for Nylon 66 decreases as a function of moisture content, while the tensile modulus for Nylon 6I/6T increases with increasing moisture content.

The behavior of this amorphous polyamide has lead Hernandez et al. [1] to study the mechanism of water sorption into this polymer.

The authors proposed a dual-mode sorption model, based on a Langmuir and Flory-Huggins mechanism. At water activities below 0.1, water preferentially chemisorbs to amide bonds, although, only a low mole fraction of the total hydrogen bonding sites on the polymer are occupied (2.3%). Chemisorption is essentially completed at water activity  $a_1 = 0.1$ , and represented about 4% of the total water absorbed. At the same time, randomly non-chemisorbed water molecules dissolve within the polymer matrix are described by Flory-Huggins equation. At higher water activities,  $a_1 < 0.3-0.4$  the model predicts that water molecules start clustering among themselves. This mechanism results in an increased capacity of the polymer to accommodate water molecules. The model is given by:

$$V_1 = V_1^L + V_1^{FH} \quad (1)$$

where  $V_1$  is the total volume fraction of water within the polymer, and the superscripts L and FH refer to Langmuir and Flory-Huggins water sorption contributions, respectively. These contributions are expressed as:

$$V_1^L = \frac{K a_1}{1 + B a_1} \quad (2)$$

and

$$a_1 = \exp [\ln v_1^{FH} + (1-v_1^{FH}) + \chi (1-v_1^{FH})^2] \quad (3)$$

where  $a_1$  is water activity,  $\chi$  is the Flory-Huggins interaction parameter, and  $K$  and  $B$  are parameters of the Langmuir equation.

Equation (3) can be written in implicit form as:

$$v_1^{FH} = FH(a_1, \chi) \quad (4)$$

Applying cluster function to equation (1), the following expression is obtained [1]:

$$\frac{G_{11}}{v_1} = \frac{(1-v_1)}{v_1^2} \left[ \frac{K a_1}{(1+B a_1)} + \frac{v_1^{FH}}{1-v_1^{FH}(1+2\chi v_1^{FH})} \right] - \frac{1}{v_1} \quad (5)$$

Where  $G_{11}/v_1$  is the cluster function.

### Oxygen permeability as a function of polymer water activity

When oxygen permeability experiments were carried out on films of Nylon 6I/6T as a function of water content, it was found that permeability values decreased with an increase in

water content, with the largest relative percent decrease being observed at low water activity values,  $a_1 < 0.2$ . Similar results were reported by Chern et al., [2], for  $\text{CO}_2$  permeability through Kapton Polyimide at  $60^\circ\text{C}$ , for upstream pressure levels up to 240 psia (16.33 atm), with and without water vapor in the feed stream. The authors found that  $\text{CO}_2$  permeability was depressed by the presence of water molecules (experiments were carried out at 0, 5.5 and 9.3% relative humidity). These results suggested that competition between the two species for Langmuir sorption sites takes place [2].

The effect of a low partial pressure of water and pentane on the permeability of  $\text{H}_2$  and  $\text{CH}_4$  through several polyimide films has been measured by Pye et al., [3]. These investigators reported a decrease in the flux or permeability for  $\text{H}_2$  and  $\text{CH}_4$ , when the experiments were performed at values of 50% of water vapor.

#### Oxygen solubility and diffusion coefficient

In the present study, a series of experiments was carried out to characterize the effect of water content of Nylon 6I/6T on the permeability of oxygen, as well as on the solubility and diffusion coefficient of oxygen. The experimental conditions covered water activity values from 0 to 1 and temperatures of 11.9, 22.0 and  $40.3^\circ\text{C}$ . Upstream oxygen pressure was maintained at 1 atm, while the

downstream oxygen partial pressure value was approximately zero, as a nitrogen carrier gas was flowed continually through the downstream cell chamber. From permeability experiments, values of the solubility and diffusion coefficient of oxygen were calculated [4]. Solubility data showed that oxygen competes with water molecules for Langmuir active sites.

A semiempirical model is presented, based on the depression of oxygen solubility, and is described in terms of the Langmuir component of eqn. (1):

$$V = V^* - F \frac{K a_1}{1 + B a_1} \quad (6)$$

Where  $V$  is the solubility of oxygen in the polymer, expressed as cc  $O_2$  (of critical volume)/ cc polymer-water system,  $V^*$  is the solubility of oxygen in the polymer at dry conditions and  $F$  is a empirical constant that relates sorption values of oxygen and water associated with Langmuir sorption mode, and is defined by:

$$F = \frac{V^* - V_{eq.}}{V_{1 eq.}^L} \quad (7)$$

Where  $V^*$  is the solubility of oxygen, expressed as volume fraction of liquid oxygen (at critical conditions) in the dry polymer,  $V_{eq}$  is the solubility of oxygen, expressed as volume fraction of oxygen liquid (at critical conditions) at water activity  $a_1 = 1$ , and  $V_{1 eq}^L$  is the volume fraction of liquid water given by the Langmuir mode at  $a_1=1$ , according to eqn. 2.

Values of the diffusion coefficient of oxygen increased initially and then showed a plateau as a function of water activity, suggesting that its numerical values depend both on the effect of plasticization of the polyamide by the water molecules and by the clusters of water.

## EXPERIMENTAL METHODS

### Polymer films

An amorphous polyamide, known as Nylon 6I/6T, was provided by the E.I. Du Pont De Nemours and Co. The polymer was synthesized from hexamethylenediamine and a mixture of isophthalic (70%) and terephthalic (30%) acids. Since the acid isomers were randomly placed into the polymer backbone, resulting in structural irregularity, no crystallization of the polymer matrix was observed. No evidence of crystalline melting point was found, by performing differential scanning calorimeter (DSC) analysis.

### Equilibrium Sorption Data

Equilibrium sorption data was taken on polymer films using a Cahn Electrobalance Model RG, (Cahn Instruments Inc., Cerrito, California). A stream of nitrogen gas adjusted to specific values of water activities provided the source of water vapor in equilibrium with the polymer films. The apparatus and its operation were described in Chapter I. Closed containers with salt solutions were also used to obtain equilibrium sorption values.

Film samples of  $5.1 \times 10^{-5}$  m thickness (2 mils) dried under vacuum at  $100^{\circ}\text{C}$  for two hours before each run, were used in each experiment.

### Oxygen Permeability Studies

Oxygen permeability studies were performed using a continuous gas flow system similar to the one described in Chapter I. These studies were carried out on an Ox-Tran 100 Permeability Tester (Modern Controls, Inc., Elk River, Minnesota). This apparatus was modified to allow the two streams, oxygen and carrier gas, to be adjusted to specific water vapor activities. An schematic of the modified apparatus is shown in Figure (1). As shown, each stream is formed by mixing a wet and a dry gas component to obtain the required activity value. Water activities were measured using hygrometer sensors (Hygrodynamic Co., Silver, Spring, Maryland). Samples of  $2.93 \times 10^{-5}$  m thickness (1.15 mils), were dried under vacuum at  $100^{\circ}\text{C}$  before each run. The equilibration process between the polymer film and the gas phase, at the selected values of water activities, was done with the sample film mounted into the permeation cell. The required time to reach equilibrium was previously determined by gravimetric method, using the Cahn electrobalance. Although time consuming, this procedure avoided sample handling and assured correct conditions of tests.

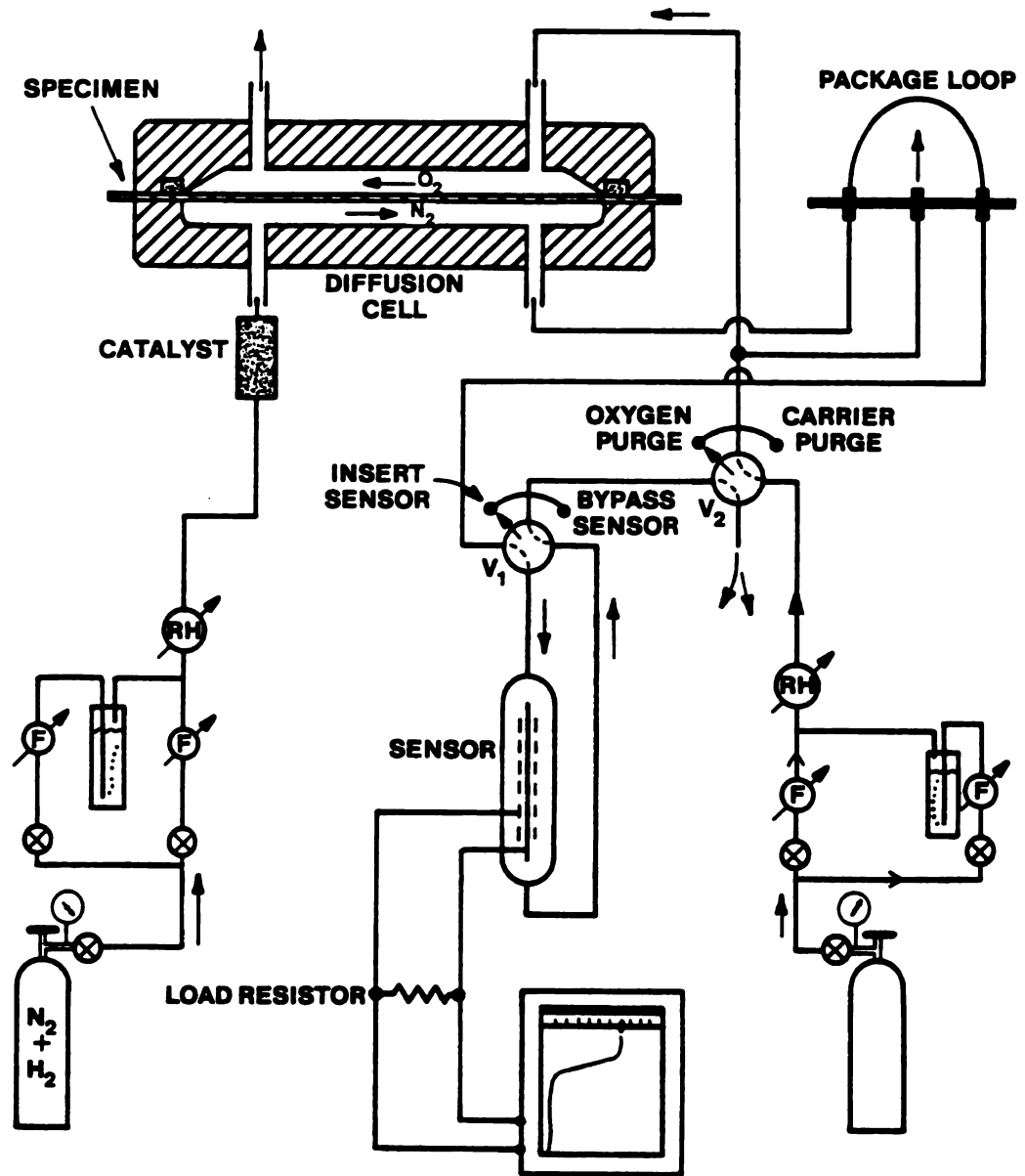


Figure 1. Oxygen permeability apparatus.

## RESULTS AND DISCUSSION

Equilibrium Sorption Isotherms

Values of the equilibrium sorption of water in Nylon 6I/6T at 5, 23 and 42°C, expressed as fraction volume, are presented as a function of water activity in Tables 1, 2 and 3, respectively. Density data were only available at 23°C and these were used to calculate the volume fraction values.

Figure 2 presents a plot of the three isotherms and, as shown, the solubility of water in the polymer decreases when temperature increases. The apparent shape of the three isotherms indicates that they follow the Langmuir-Flory-Huggins model, given by eqn. (1).

As outlined in Chapter II, equilibrium sorption data was treated to obtain the parameters of the model. Table 4 shows the values for  $\chi$ , K and B at 5, 23 and 42°C.

An Arrhenius plot of K and B is presented in Figure 3, and the following expressions correlate the constants B and K with the temperature:

$$B = 15.7 \times \exp(-0.232/T) \quad (8)$$

$$K = 2.05E-03 \times \exp(0.9135/T) \quad (9)$$

TABLE 1. Water/polymer isotherm at 5°C.

	Experimental	Calculated	Calculated
Water	Volume	Flory-Huggins	Langmuir
Activity	Fraction	Component	Component
$A_w$	$V_1 \times 100$	$V_1^{FH} \times 100$	$V_1^L \times 100$
0	0	0	0
0.096	1.21	0.692	0.51
0.185	1.90	1.38	0.52
0.36	3.37	2.84	0.53
0.402	3.76	2.84	0.53
0.60	5.78	5.24	0.53
0.685	6.80	6.23	0.57
0.83	8.72	8.17	0.55
0.91	9.98	9.42	0.56
0.975	11.15	10.57	0.58

TABLE 2. Water/polymer isotherm at 23°C

Water Activity $A_w$	Experimental Volume Fraction $V_1 \times 100$	Calculated Flory-Huggins Component $V_1^{FH} \times 100$	Calculated Langmuir Component $V_1^L \times 100$
0.046	0.56	0.313	0.329
0.560	0.781	0.383	0.340
0.072	0.893	0.494	0.353
0.080	0.935	0.551	0.357
0.090	0.992	0.622	0.362
0.110	1.113	0.764	0.369
0.155	1.433	1.093	0.378
0.189	1.526	1.347	0.383
0.252	1.970	1.835	0.388
0.269	1.884	1.970	0.389
0.308	2.583	2.287	0.391
0.041	3.545	3.161	0.394
0.440	4.142	3.430	0.395
0.565	4.839	4.640	0.396
0.580	5.272	4.795	0.397
0.585	5.007	4.847	0.397
0.635	5.789	5.381	0.398
0.735	7.022	6.538	0.399
0.790	7.998	7.235	0.399
0.860	8.791	8.195	0.399
0.880	9.132	8.487	0.400
0.963	9.995	9.800	0.400

TABLE 3. Water/polymer isotherm at 42°C.

	Experimental	Calculated	Calculated
Water	Volume	Flory-Huggins	Langmuir
Activity	Fraction	Component	Component
$A_w$	$V_1 \times 100$	$V_1^{FH} \times 100$	$V_1^L \times 100$
0	0	0	0
0.078	0.67	0.505	0.165
0.265	2.00	1.820	0.18
0.395	3.01	2.838	0.172
0.48	3.74	3.561	0.179
0.57	4.56	4.383	0.177
0.777	6.75	6.567	0.183
0.82	7.27	7.086	0.189
0.91	8.46	8.27	0.19

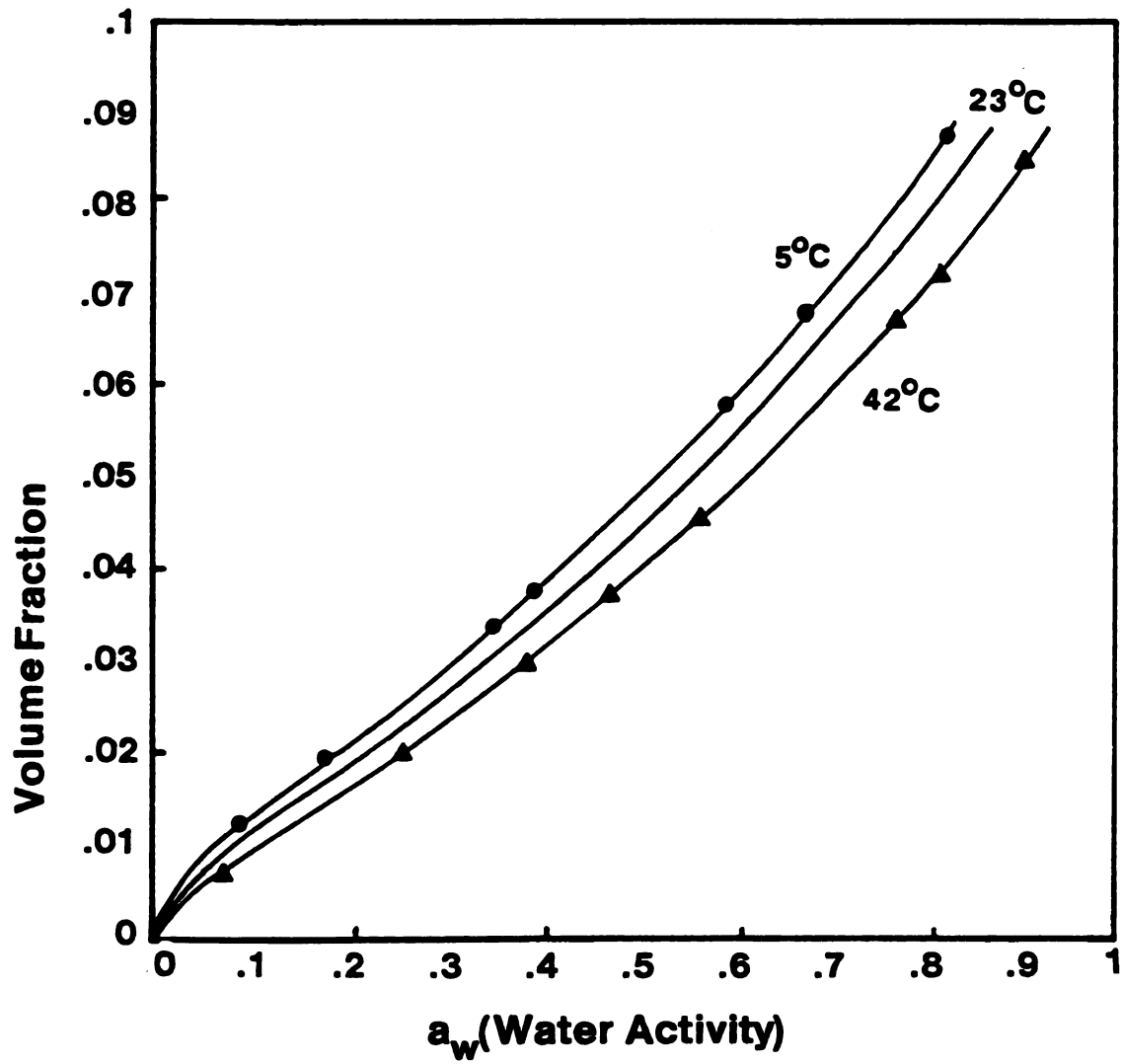


Figure 2. Water sorption isotherms at 5 °C, 23 °C and 42 °C.

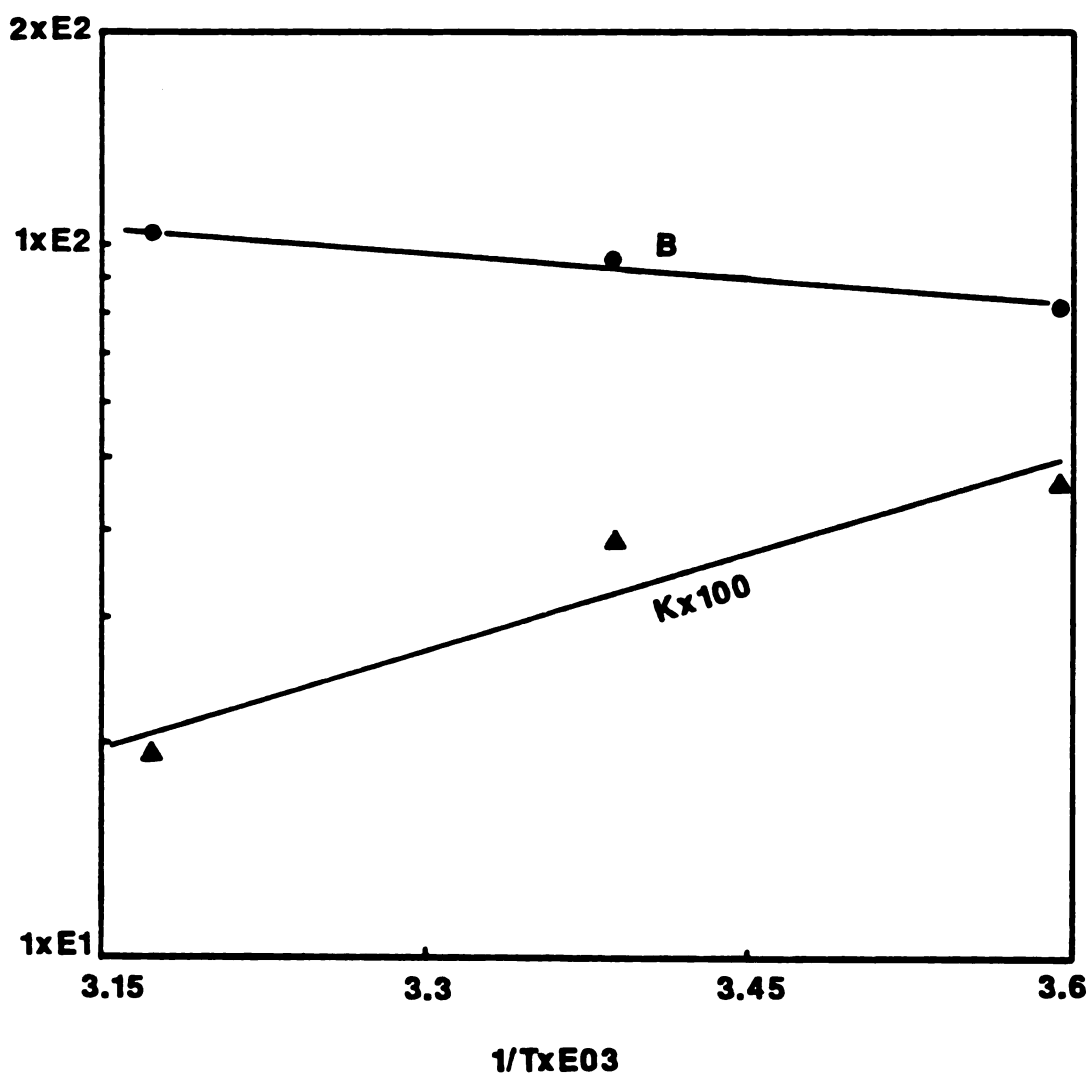


Figure 3. Values of  $K$  and  $B$  of the Langmuir equation.

The clustering function values were calculated from the equilibrium sorption values. The onset of the cluster formation was taken to be when the value of  $G_{11}/V_1 = -1$ , [5]. Table 5 shows the corresponding values of water activity for the onset of clustering at 5, 23 and 42°C. The computer program used to calculate the cluster function values, as well as the output are included in Appendix A.

#### Calculation of Oxygen Solubility

Oxygen permeability experiments were conducted at 11.9, 22 and 40.3°C. Diffusion coefficient and solubility values were obtained from these experiments according to the procedure outlined in Chapter I. Permeability experimental data obtained for this study are tabulated in Appendix B. The diffusion coefficient was calculated from a least-squares linear analysis of values from the unsteady state region for each permeability run. Values of  $4Dt/L^2$  were used as the dependent variable versus time. The corresponding values of the correlation coefficient were also calculated, to indicate the goodness of fit. Solubility values were calculated from the expression,

$$S = P/D \quad (10)$$

Where P, S and D stand for permeability, solubility and diffusion coefficient, respectively. The solubility of oxygen is expressed as S in cc O<sub>2</sub> (STP)/cc polymer-water system or V in cc (liquid O<sub>2</sub> at its critical specific volume)/cc polymer-water system.

TABLE 4. Value of  $\chi$ , K and B as a function of temperature.

Parameter	5°C	22°C	42°C
$\chi$	1.66	1.70	1.76
K	0.46	0.385	0.19
B	81.36	95.15	102.0

TABLE 5. Water activity values at the onset of cluster formation.

Temperature °C	Water Activity
5	0.42
22	0.37
42	0.28

Conditions for Applying Eqn. 10

As previously discussed in Chapter I, when eqn. 10 is applied to calculate solubility values from permeability and diffusion coefficients, it is assumed that the permeant/polymer system follows the Henry's law of solubility, [6]. For this work, which was intended to study the effect of water activity on the diffusion of oxygen, it is necessary to show that the oxygen diffusion coefficient is independent of the oxygen pressure in the range up to 1 atmosphere.

To show that the solubility of oxygen in Nylon 6I/6T follows a Henry's law behavior and that the oxygen diffusion coefficient was independent of the pressure (in the range of the experimental conditions of this work), permeability experiments were conducted in the range of 0 to 1 atmosphere oxygen. Summarized in Table 6 are the values of the oxygen solubility and diffusion coefficient in Nylon 6I/6T at 0.2, 0.366, 0.50, 0.745 and 1.0 atm of pressure and a temperature of 24°C. As shown, D remains constant through the experimental range of pressure.

For better illustration, Figure 4 presents a plot of the oxygen solubility values. The solubility of oxygen in Nylon 6I/6T as a function of oxygen partial pressure is given by:

$$S = 0.144 \times p \quad (11)$$

TABLE 6. Solubility of Oxygen in Nylon 6I/6T as a function of pressure at 24°C.

---

Pressure atm	D x E9 (a)	S x 10 (b)	V x E4 (c)
0.2	1.08	0.277	0.91
0.366	1.11	0.530	1.73
0.50	1.04	0.750	2.53
0.745	1.18	1.073	3.52
1.0	1.13	1.44	4.71

---

(a)- in (cm<sup>2</sup>/sec)

(b)- in (cc O<sub>2</sub>/cc polymer)

(c)- in (cc O<sub>2</sub> liq./cc polymer)

D = 1.11 x 10E09

Standard error = 5%

---

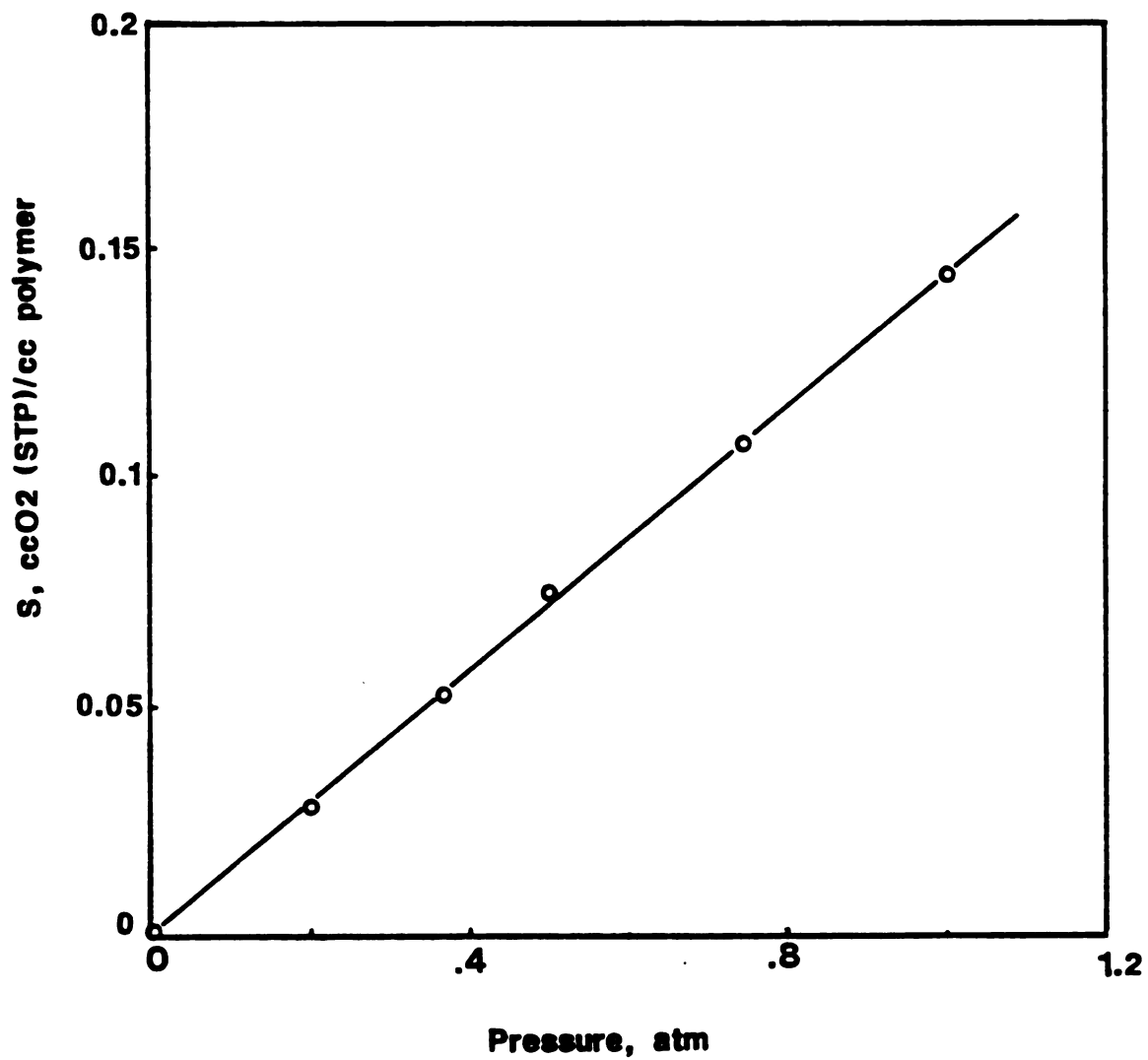


Figure 4 . Solubility of oxygen as a function of partial pressure at 24 °C.

where  $S$  is the solubility in cc O<sub>2</sub> (STP)/cc polymer and  $p$  is the pressure in atm.

### Permeability Data

Tables 7, 8 and 9 present the values of permeability, diffusion coefficient and solubility of oxygen in Nylon 6I/6T at 11.9, 22 and 40.3°C, respectively. Figures 5, 6 and 7 illustrate the effect of temperature on the permeability coefficient, the diffusion coefficient and the solubility of oxygen in Nylon 6I/6T, as a function of water activity. Figures 8, 9 and 10 show the simultaneous change of the diffusion coefficient and the solubility of oxygen as a function of water activity at 11.9, 22 and 40.3°C.

As shown in these figures, oxygen permeability values decreased as a function of water activity. The values of oxygen permeability were factored into a solubility and a mobility term according to eqn. 11. The solubility term decreased 5 times and the  $D$  values increased by 2 as a function of water activity (average values for all temperatures). From these findings it became apparent that the increase in the diffusion coefficient was not enough to compensate for the depression of the oxygen solubility values, and the result was a depression in the permeability values. An attempt is made here to interpret these results in the framework of the dual-mode sorption model presented in Chapter II.

TABLE 7. Diffusion, solubility and permeability values of oxygen at 11.9°C.

Water Activity	D x E10 (a)	S x 10 (b)	P (c)	V x E4 (d)
0	3.06	3.46	31.3	11.33
0.06	3.65	1.67	18.1	5.47
0.175	3.65	1.34	14.3	4.39
0.32	3.70	1.13	12.4	3.70
0.452	4.03	0.85	11.4	2.78
0.594	4.84	0.72	10.4	2.36
0.74	4.9	0.73	10.6	2.39
0.753	4.91	0.71	10.3	2.32
0.881	4.90	0.69	10.0	2.26

(a)- in (cm<sup>2</sup>/sec)

(b)- in (cc O<sub>2</sub>/cc polymer)

(c)- in (cc O<sub>2</sub>/m<sup>2</sup>.day)

(d)- in (cc O<sub>2</sub> liq./cc polymer)

TABLE 8. Diffusion, solubility and permeability values of oxygen at 22.0°C.

Water Activity	D x E10 (a)	S x 10 (b)	P (c)	V x E4 (d)
0	5.54	2.97	48.8	9.71
0.048	7.19	1.58	33.7	5.13
0.153	7.36	1.21	26.3	3.96
0.275	7.90	1.04	24.4	3.40
0.445	9.34	0.774	21.4	2.53
0.545	9.54	0.71	20.2	2.32
0.75	9.89	0.67	19.52	2.19

(a)- in (cm<sup>2</sup>/sec)  
(b)- in (cc O<sub>2</sub>/cc polymer)  
(c)- in (cc O<sub>2</sub>/m<sup>2</sup>.day)  
(d)- in (cc O<sub>2</sub> liq./cc polymer)

TABLE 9. Diffusion, solubility and permeability values of oxygen at 40.3°C.

Water Activity	D x E10 (a)	S x 10 (b)	P (c)	V x E4 (d)
0	11.5	2.56	87.6	8.37
0.040	13.6	1.50	60.7	4.91
0.096	12.5	1.3	50	4.25
0.15	14.38	1.10	48.5	3.6
0.253	17.54	0.87	45.1	2.84
0.392	22.25	0.65	42.6	2.13
0.535	24.41	0.52	37.3	1.7
0.67	27.42	0.46	37.6	1.5
0.81	27.67	0.45	36.5	0.1.47

(a)- in (cm<sup>2</sup>/sec)

(b)- in (cc O<sub>2</sub>/cc polymer)

(c)- in (cc O<sub>2</sub>/m<sup>2</sup>.day)

(d)- in (cc O<sub>2</sub> liq./cc polymer)

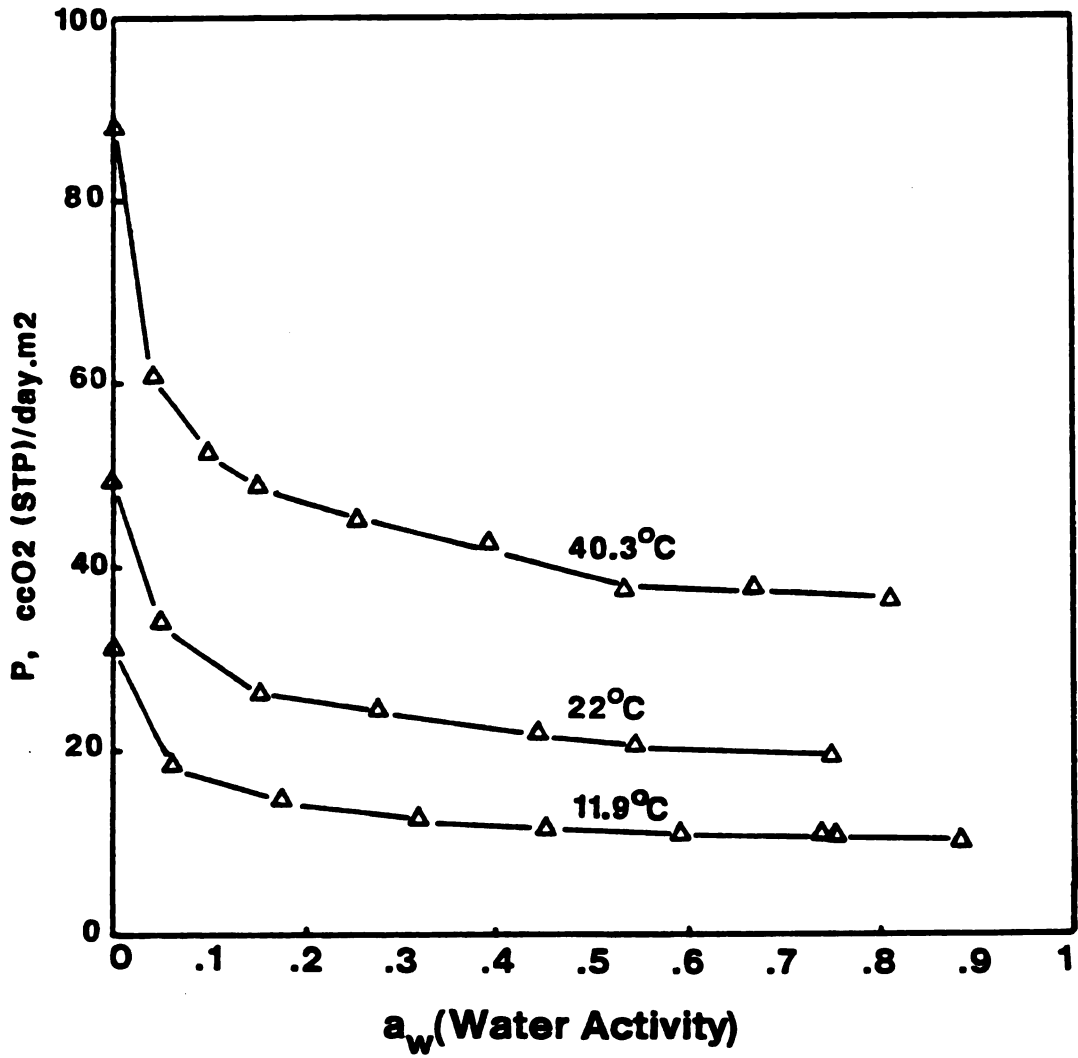


Figure 5. Oxygen permeability values at 11.9°C, 22.0°C and 40.3°C.

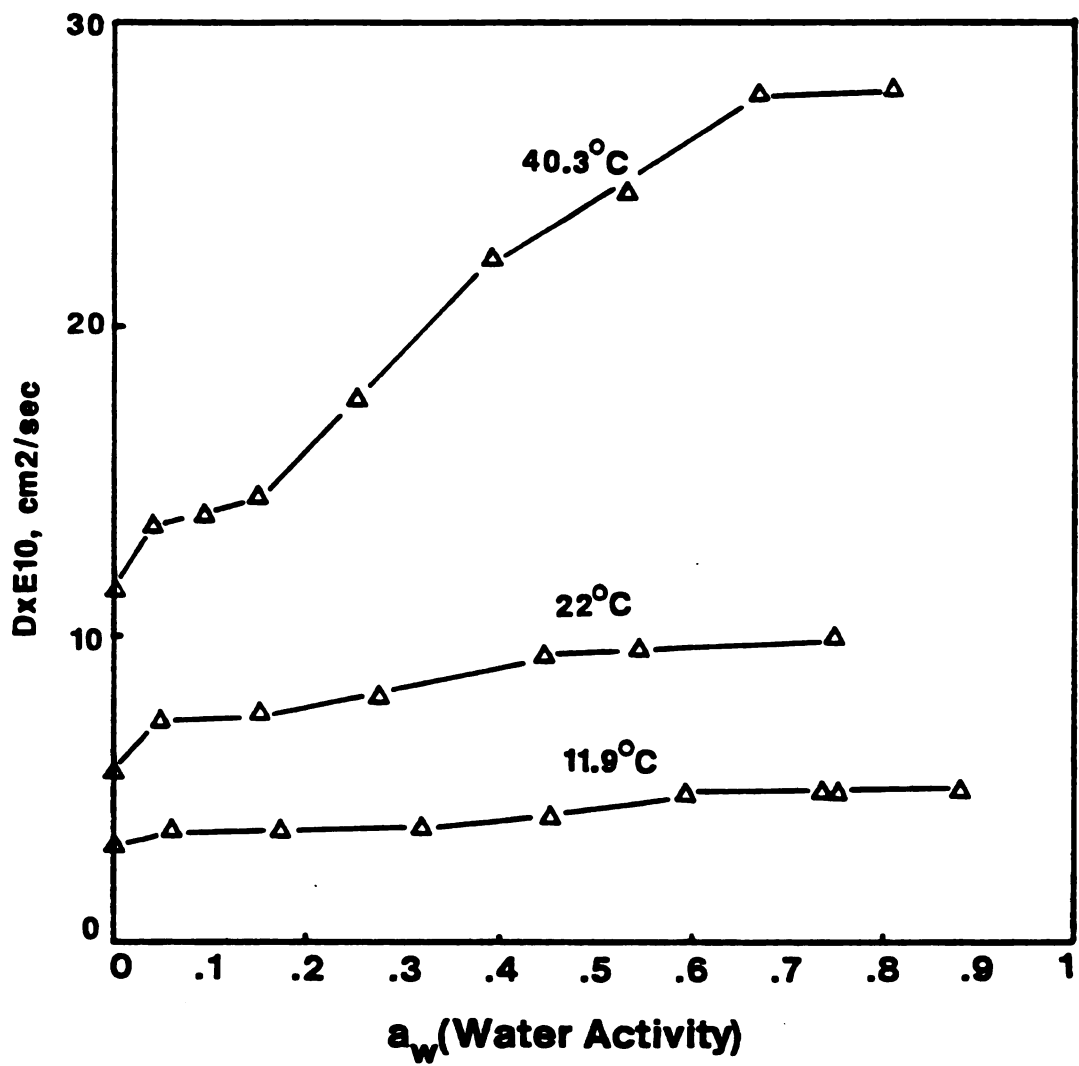


Figure .6. Diffusion coefficient values at 11.9°C, 22.0°C and 40.3°C.

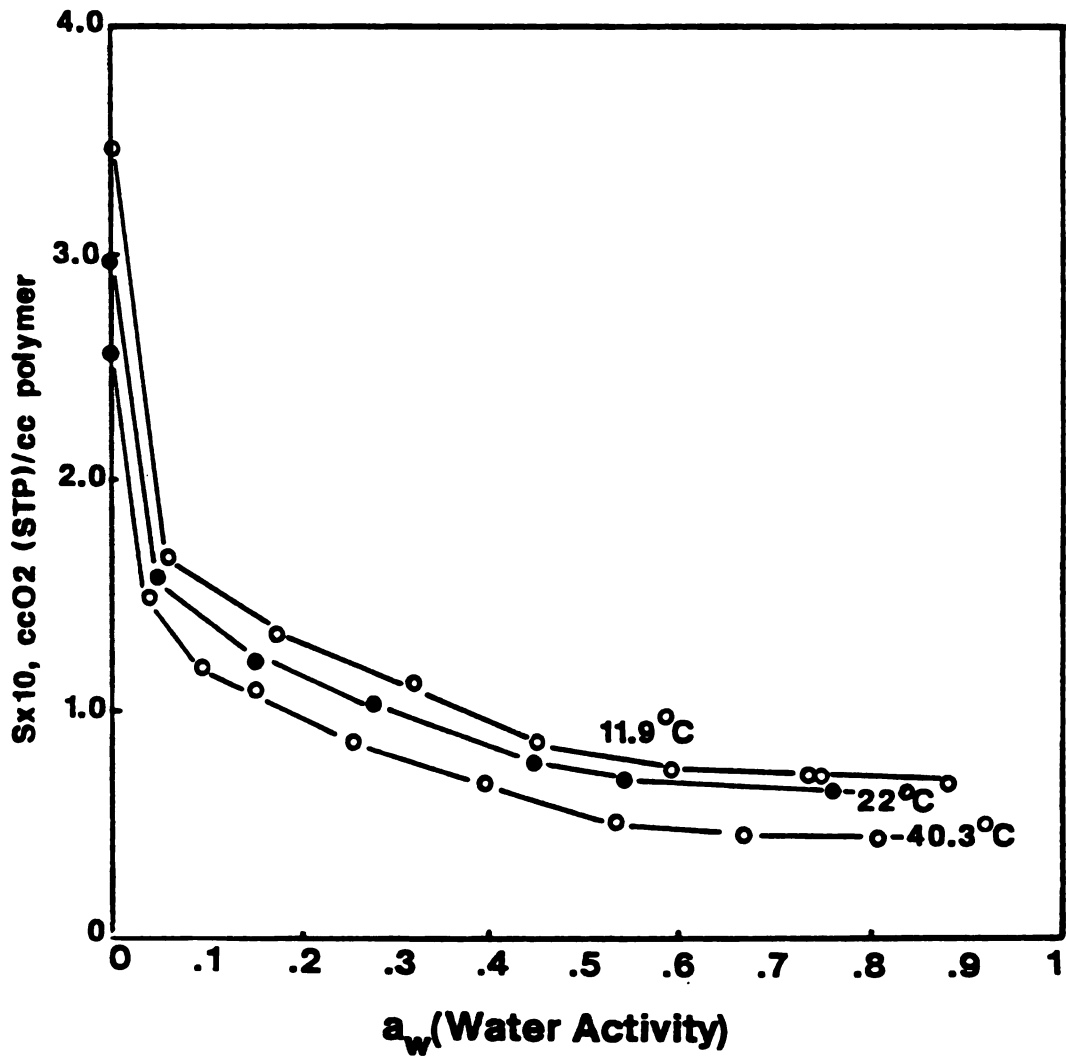


Figure 7. Oxygen solubility values at 11.9°C, 22.0°C and 40.3°C.

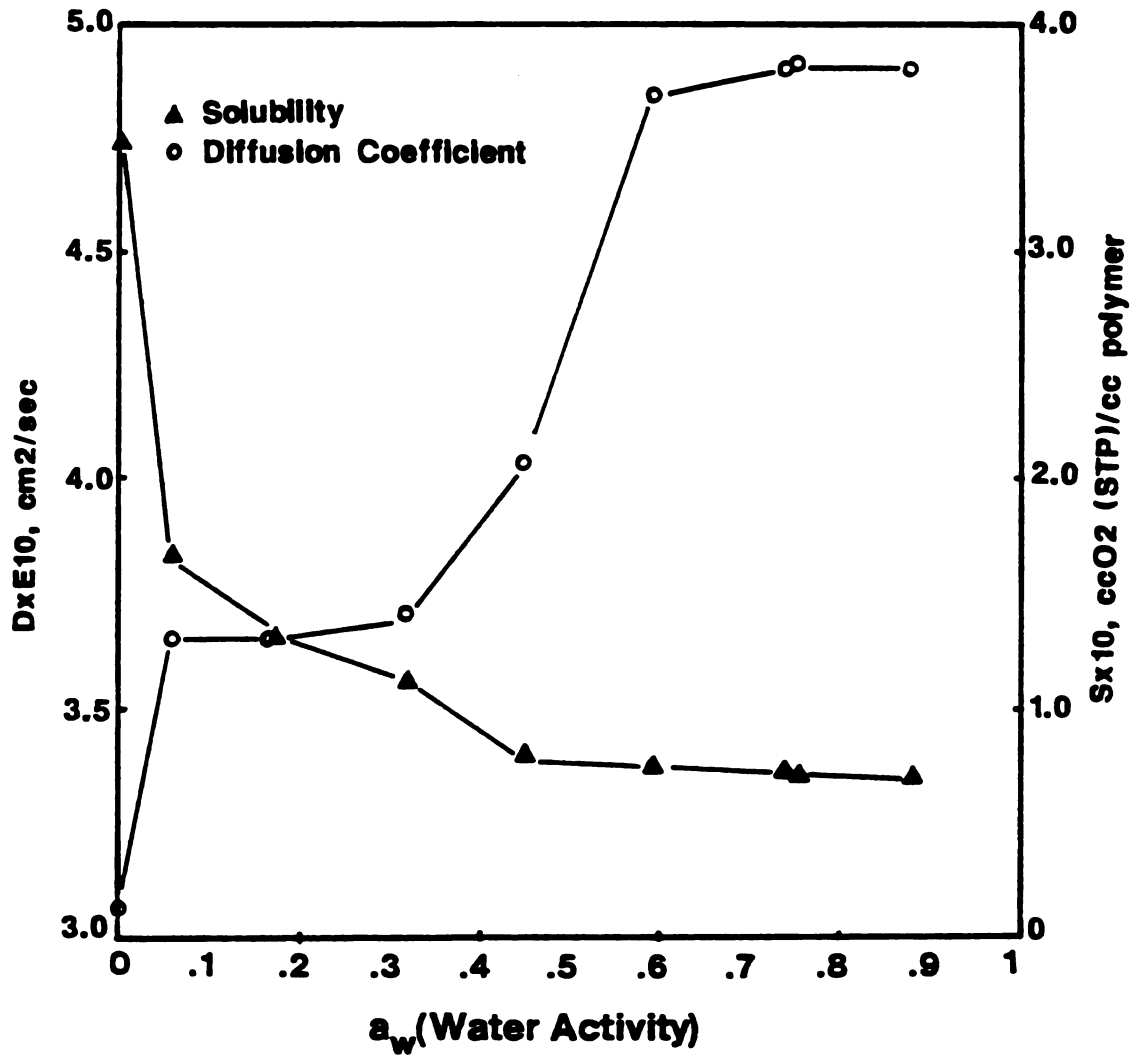


Figure 8. Solubility and diffusion coefficient of oxygen at 11.9°C.

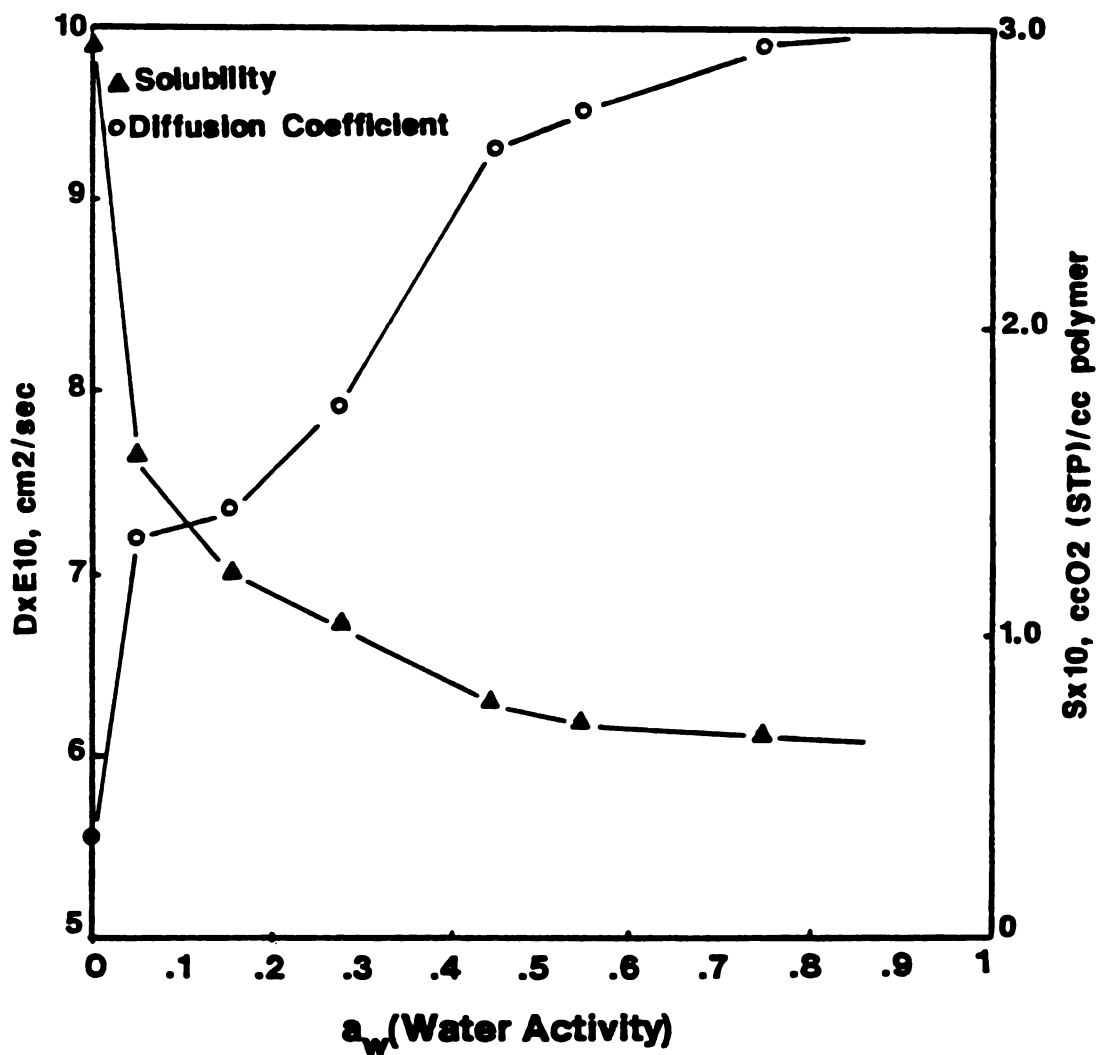


Figure 9. Solubility and diffusion coefficient of oxygen at 22.0 C.

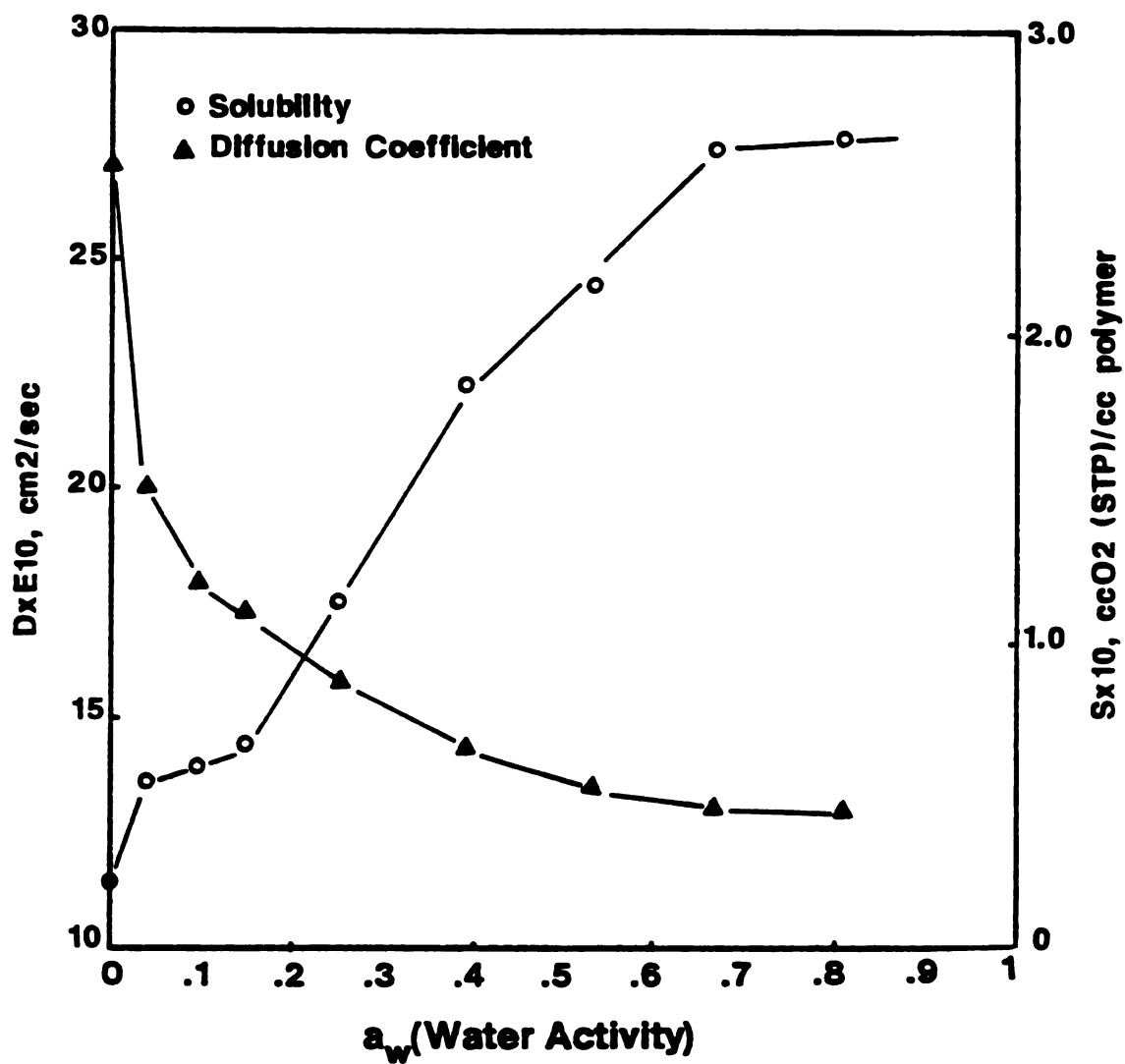


Figure 10. Solubility and diffusion coefficient of oxygen at 40.3°C.

Oxygen solubility

Equation (6) was applied to model the solubility of oxygen in Nylon 6I/6T, as a function of water activity at 11.9, 22.0 and 40.3°C.

The values of the constants necessary for eqn. (6) are presented in Table 10.

---

TABLE 10. Values of the constants for Eqn 6.

---

Temperature	F	K	B
°C	$\frac{\text{cc O}_2(\text{Liq})}{\text{cc water}}$	$\frac{\text{cc water}}{\text{cc polymer}}$	$a_1^{-1}$
11.9	.187	.42	86.7
22.0	.188	.385	95.15
40.3	.373	.19	102

---

Numerical values of F indicate that at the same temperature the volume fraction of liquid oxygen associated with active sites within the polymer is only 0.19-0.37 of the volume fraction of the chemiabsorbed water. The value of the constant F at 40.3°C appears to be somewhat higher than the

other two values. This lack of trend may be due to the numerical error associated with the values of the constants of the Langmuir equation that describe the chemisorbed molecules of water into the polymer. As shown in Chapter II, the sensibility coefficients of the parameters K and B indicated the importance of the values at low water activity when calculating these constants. In order to get better values for the constants, K and B, more data at low water activity values may be required.

Tables 11-13 present experimental and calculated (using eqn. 6) values of oxygen solubility at 11.9, 22.0 and 40.3°C respectively. For better illustration, the tabulated data is presented graphically in Figures 11-13 where oxygen solubility is plotted as a function of water activity of the polyamide. The experimentally determined solubility values are also included to show the validity of the model.

As shown, good agreement between calculated and experimental data is observed, except in the range of 0.1 to 0.3 of water activity, where the model predicted a lower solubility than that found experimentally.

These findings indicate that the solubility of oxygen in Nylon 6I/6T is comprised of two components: one, simple dissolution of O<sub>2</sub> molecules within the polymer matrix and not affected by the presence of water molecules, and second, O<sub>2</sub> molecules related to active sites of the polymer and able to be easily displaced by water molecules. The simple dissolved molecules contribution is about 20% of the

total oxygen solubility (20% at 11.9°C, 21% at 22.0°C and 18% at 40.3°C). The fact that 80% of the total dissolved oxygen was displaced by molecules of water associated with active sites of the polymer matrix, indicates the importance of these active sites in the mechanism of the solubility of oxygen within the Nylon 6I/6T. Polarity and molecular size may be important factors in determining the final equilibrium sorption values of water and oxygen molecules within the polymer matrix.

TABLE 11. Experimental and calculated solubility of oxygen at 11.9°C.

Aw	Experimental	Calculated
	(cc O <sub>2</sub> (Liq) per cc of polymer-water) x E4	
0	11.32	11.32
0.06	5.41	3.73
0.175	4.39	2.81
0.32	3.70	2.59
0.452	2.59	2.49
0.594	2.42	2.42
0.74	2.39	2.39
0.753	2.26	2.31
0.881	2.26	2.31

$$F = \frac{V^* - V_{eq.}}{V_1^L eq.} = \frac{(11.36-3.26) \times 10^{-4}}{0.00484} = 0.187$$

TABLE 12. Experimental and calculated solubility of oxygen at 22.0°C.

Aw	Experimental (cc O <sub>2</sub> (Liq) per cc of polymer) X E4	Calculated
0	9.72	9.72
0.048	5.15	3.43
0.153	3.96	2.53
0.275	3.41	2.31
0.445	2.53	2.21
0.545	2.32	2.18
0.75	2.19	2.15

$$F = \frac{V^* - V_{eq.}}{V_1^L eq.} = \frac{(9.72-2.19) \times E-4}{0.004} = 0.188$$

TABLE 13. Experimental and calculated solubility of oxygen at 40.3°C.

Aw	Experimental (cc O <sub>2</sub> (Liq) per cc of polymer) x E4	Calculated
0	8.34	8.34
0.04	4.91	2.78
0.096	3.92	2.06
0.15	3.60	1.86
0.253	2.80	1.70
0.392	2.12	1.60
0.535	1.70	1.57
0.67	1.50	1.54
0.81	1.47	1.50

$$F = \frac{V^* - V_{eq.}}{V_{1 eq.}^L} = \frac{(8.34-1.47) \times E-4}{0.00185} = 0.373$$

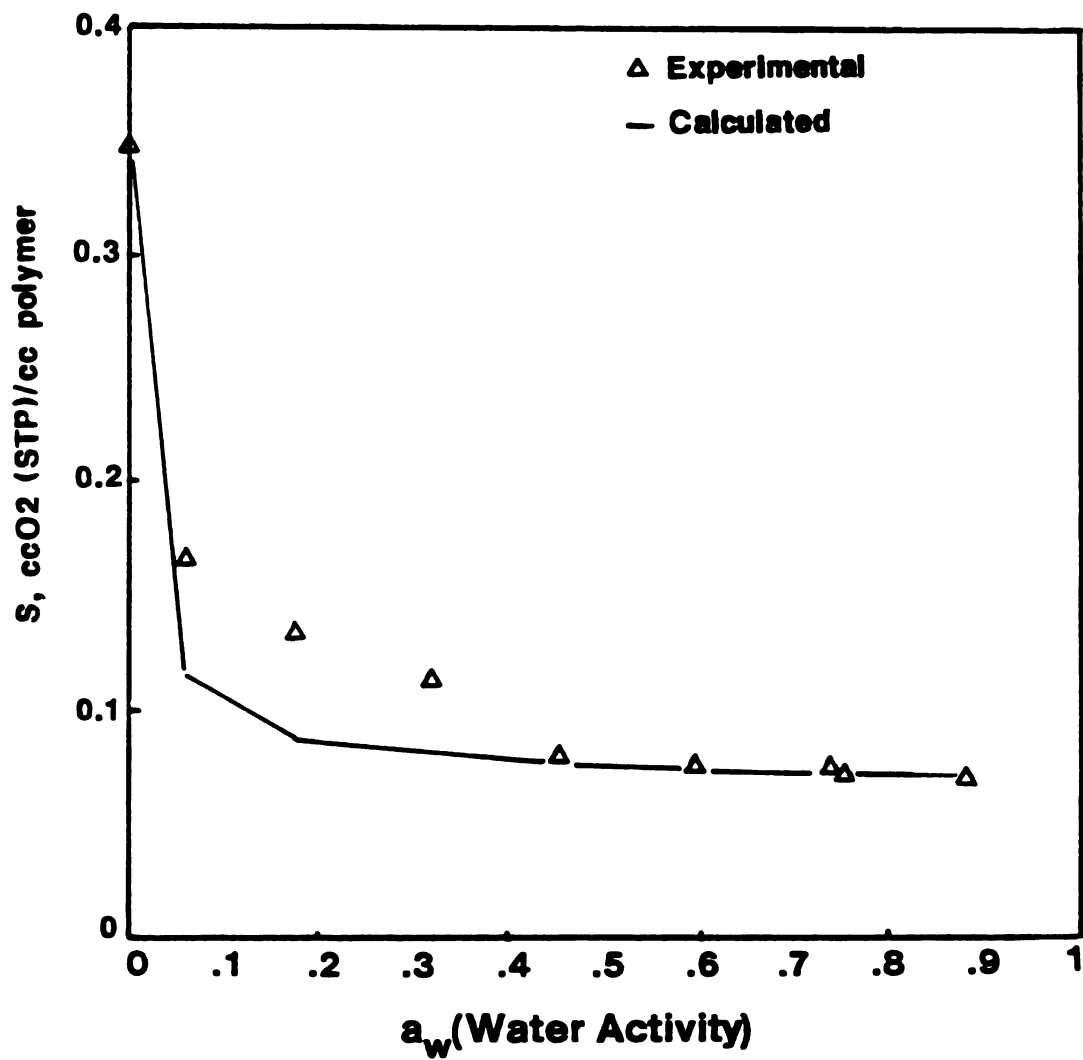


Figure 11. Oxygen solubility at 11.9°C as function of  $a_w$ .

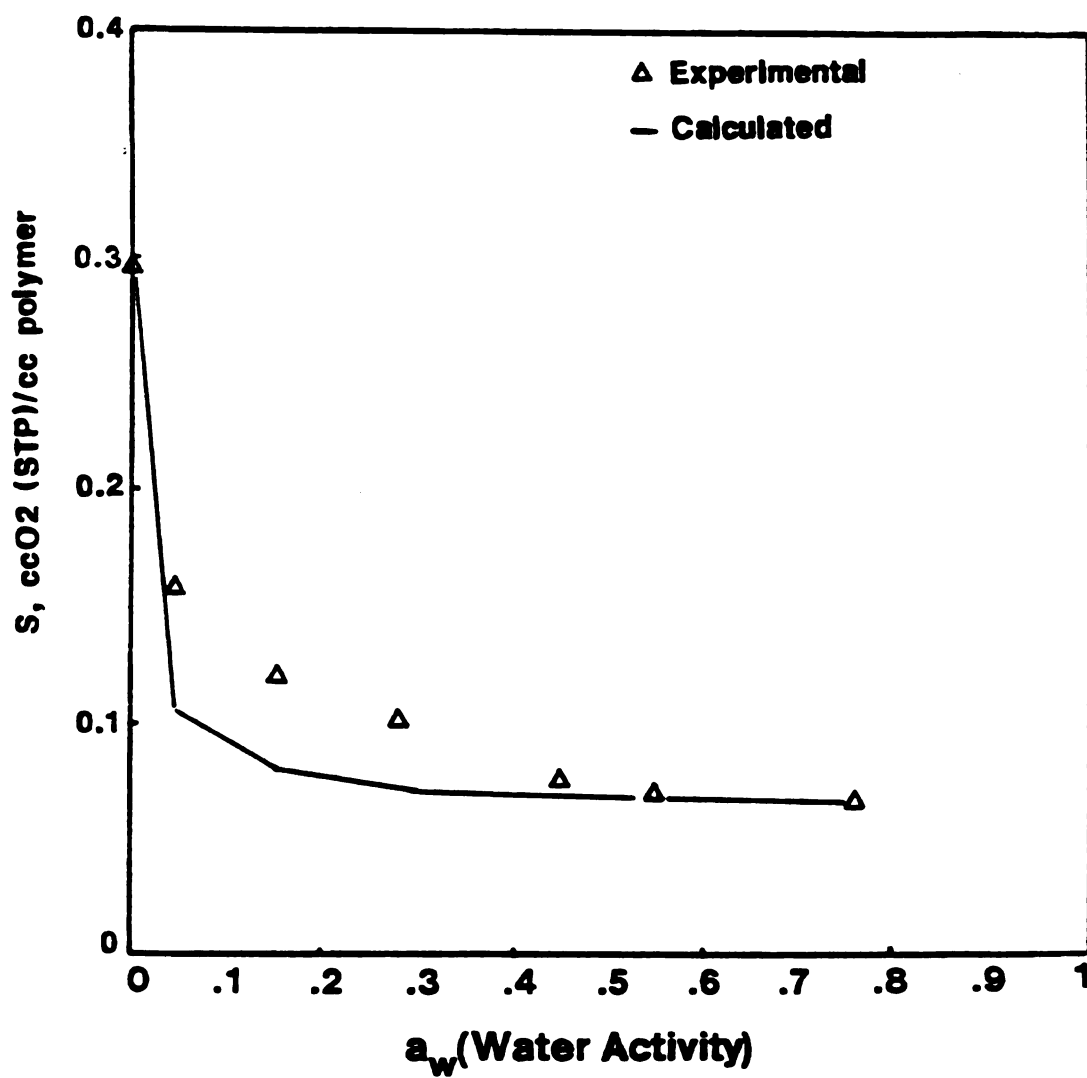


Figure 12. Oxygen solubility at 22.0°C as function of a<sub>w</sub>.

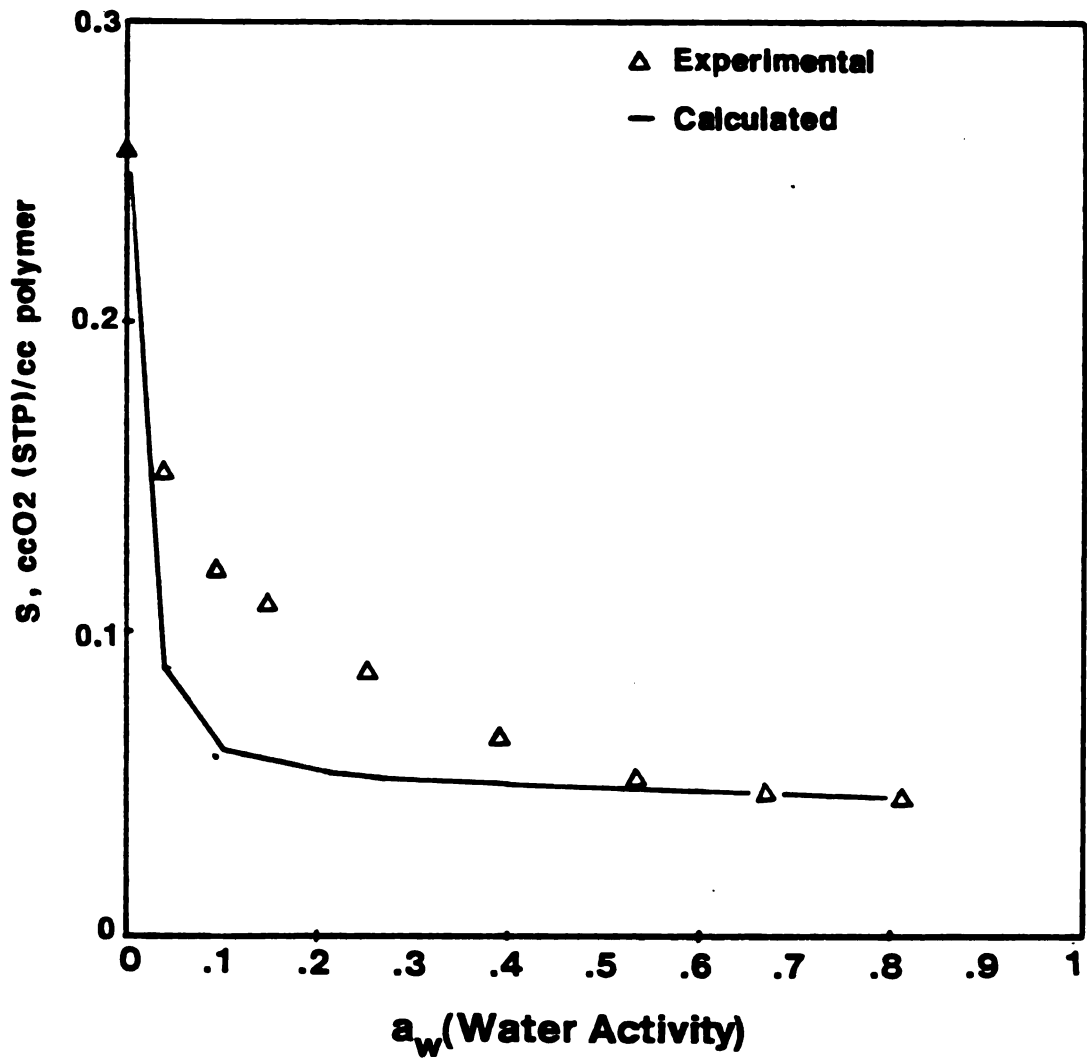


Figure 13. Oxygen solubility at 40.3°C as function of a<sub>w</sub>.

### Oxygen diffusion coefficient

Values of the oxygen diffusion coefficient  $D$  in the amorphous polyamide/water system were presented in Figures 8-10 as a function of water activity  $a_1$ , for three temperatures. As shown, the general trend in the change of  $D$  values as function of  $a_1$  was similar in the three cases. In general, the diffusion coefficient increased with increasing water activity up to a value of 0.5-0.6 activity, after that,  $D$  values showed a plateau. The value of water activity at which the diffusion coefficient approached a constant value (0.5-0.6), was immediately above the value of  $a_1$  at which the clustering of water within the polyamide was predicted (0.3-0.4). This behavior was observed for all temperatures except at 11.9 °C where  $D$  showed constant values for  $0.05 < a_1 < 0.20$ .

The observed increase in  $D$  the region of low water activity ( $a_1 < 0.5$ ), may be attributed to a plasticization of the polyamide chain backbone by sorbed water. This plasticization effect would tend to increase the mobility of oxygen molecules within the polymer bulk phase. This is consistent with the behavior of the glass transition temperature of the system polymer/water. As shown in Figure 8 Chapter II, the glass transition temperature of Nylon 6I/6T had a sharp decrease in its value for  $0 < a_1 < 0.5$ . For values of water activity larger than 0.5 the slope of  $T_g$  versus  $a_1$  changed at a lower value.

The plateau shown by the oxygen diffusion coefficient for values of  $a_1$  above 0.4-0.5 suggests that clusters of molecules of water formed within the polymer, may have a retardant effect on the mobility of oxygen molecules.

A better appreciation of the effect of the distribution of water molecules within the polymeric matrix on the mobility of oxygen molecules can be obtained by analyzing the activation energy of the oxygen diffusion process as a function of water activity. The activation energy is related to the diffusion coefficient by the following equation:

$$E_D = - RT \ln \frac{D}{D_0} \quad (12)$$

Where  $E_D$  is the activation energy,  $D_0$  is a pre-exponential term,  $R$  is the gas constant and  $T$  is the absolute temperature. Figure 14 presents a plot of the activation energy of the diffusion process of oxygen as a function of water activity in equilibrium with Nylon 6I/6T. Values of the activation energy at selected values of  $a_1$  and a plot of  $E_D$  vs.  $D_0$  (to show consistency of the data) are presented in Appendix B.

As shown in Figure 14, values of the activation energy shifted from the region of low water activity values,

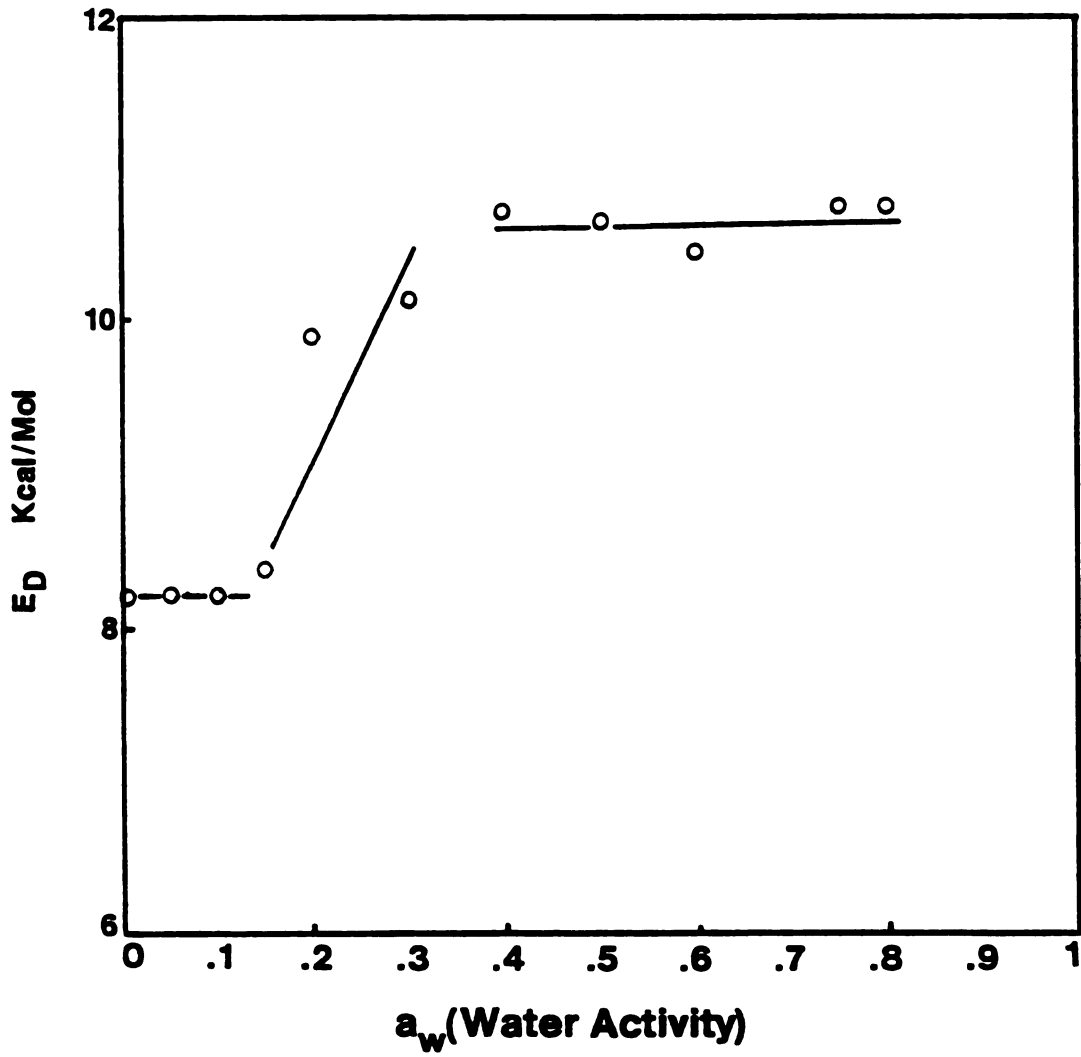


Figure 14. Activation energy as a function of water activity.

$0 < a_1 < 0.15$ , (about 8.2 Kcal/mole) to a higher value (about 10.7 Kcal/mole) for  $a_1 > 0.4$ . The change of  $E_D$  values took place for the range  $0.15 < a_1 < 0.4$ .

An increase in the activation energy is interpreted as an increase in the energy required by the oxygen molecules to overcome the intermolecular forces within the polymer, to move from one position to another [7-9]. The fact that oxygen molecules require more energy to diffuse through the polymer water-system for  $a_1 > 0.4$  may be a indication that clusters of water molecules opposes the passage of oxygen molecules, creating a more tortuouse path to the diffusing molecule [8]. If this is true, the oxygen diffusion coefficient studies as a function of water activity may be considered as a experimental proof of the clustering of water molecules within the polymer.

## CONCLUSIONS

Results from the study of oxygen solubility and diffusivity complemented the Fourier Transform Infrared spectroscopy, temperature relaxation and density studies that were performed on the polyamide water system. Further, these results provided additional supportive evidence for the dual-mode sorption model proposed in Chapter II. Water is rapidly chemisorbed to dry Nylon 6I/6T, bounded to amide groups through hydrogen bonds. Saturation of the amide actives sites is completed before water activity reaches a

value of 0.1. There is also a simultaneous process of dissolution of water non-chemisorbed and randomly distributed within the polymer. This water is easily removed from the polymer and does not present hysteresis during the desorption process. When water activity reaches a value between 0.3 and 0.4 molecules of water tend to self associate forming clusters of molecules. The degree to which molecules of water preferentially self associate rather than exist as loosely dissolved within the polymer is not known. However, it appears to be large enough to result in a increase in the activation energy for the diffusion process of oxygen molecules. Techniques such Nuclear Magnetic Resonance spectroscopy and isotopes tracers studies may help to elucidate this important question.

#### SUMMARY

The sorption of water molecules by a glassy amorphous polyamide, Nylon 6I/6T, showed a depression in the oxygen permeability values as a function of polymer moisture content. The oxygen permeability behavior was analysed in terms of the multiplicative effect of a mobility and a solubility term. The analysis of the solubility values of the oxygen within the polymer-water system, provided a complementary framework for the dual sorption model presented in Chapter II. The model provided a theoretical

basis for interpreting transport behavior in polymer-vapor-gas systems. This may prove important in relation with the new generation of materials that are characterized by high glass transition temperature, molecular backbone rigidity and eventually made of polar groups such as Nylon 6I/6T.

## REFERENCES

1. Hernandez, R. J., J. R. Giacin and E. A. Grulke, The sorption of Water by an Amorphous Polyamide, submitted to the Journal Membrane Science.
2. Chern, R. T., W. J. Koros, E. S. Sanders and R. Yui, "Second Component" Effect in Sorption and Permeation in Glassy Polymers, J. Membrane Sc., 15 (1983) 157-169.
3. Pye, D. G., M. M. Moehr and M. Panar, Measurement of gas Permeability of Polymer, II. Apparatus for Determination of the Permeability of Mixed gases, J. Applied Sc., 20 (1976) 287-301.
4. Hernandez, R. J., J. R. Giacin and A. L. Baner, The Evaluation of the Aroma Barrier Properties of Polymer Films, J. Plastic Film Sheeting, 2 (1986) 187-211.
5. Lundberg, J. L., Clustering Theory and Vapor Sorption by High Polymers, 4 B3 (1969) 263-711.
6. Crank, J. and G. S. Park, Diffusion in Polymers, Academic Press, London, (1968).

7. DiBenedetto, A. T. and D. R. Paul, An Interpretation of Gaseous Diffusion Through Polymers Using Fluctuation Theory, J. Polym. Sc.: Part A, 2 (1964) 1001-1015.
8. Paul D. R. and A. T. DiBenedetto, Diffusion in Amorphous Polymers, J. Polym. Sc.: Part C, 10 (1965) 17-44.
9. Kumins, C. A., Transport Through Polymer Films, J. Polym. Sc.: Part C, 10 (1965) 1-9.

APPENDIX A

```

100 REM BOX KANAMAZU METHOD FOR FLORY HUGGINS MODEL
110 CLS: DIM A1(20),V1(20),ETA(20),X(20)
120 INPUT "HOW MANY POINTS?", N
130 INPUT "HOW MANY ITERATIONS?", ITE
140 INPUT "ENTER THE FIRST ESTIMATE OF CHI", B
150 PRINT "ENTER FIRST A1'S AND THEN V1'S"
160 A1(1)=.056:A1(2)=.08:A1(3)=.11 : A1(4)=.189 :A1(5)=.252
165 A1(6)=.308
170 A1(7)=.41 : A1(8)=.44 :A1(9)=.565 : A1(10)=.585
175 A1(11)=.635 : A1(12)=.735
180 A1(13)=.79 :A1(14)=.86 :A1(15)=.88 : A1(16)=.963 : A1(17)=.58
190 V1(1)=.0076 : V1(2)=8.000001E-03 : V1(3)=.0109 :V1(4)=.0139
191 V1(5)=.0912
195 REM
200 V1(6)=.02515 : V1(7)=.03442 : V1(8)=.04016 :V1(9)=.05097
205 V1(10)=.04843
210 V1(11)=.05591 : V1(12)=.06768 :V1(13)=.07696:V1(14)=.0845:
V1(15)=.0877 :V1(16)=.0955:V1(17)=.0109
215 PRINT " H", " S1", " CHI"
220 RL =0!
225 RL=RL+1
230 XTX=0! : XTY=0! :SO=0! :S1=0!
240 REM EQUATION FOR THE MODEL
250 FOR K=1 TO N
255 V2=1 -V1(K)
260 ETA(K)=V1(K)*EXP(V2+B*V2*V2)
270 NEXT K
280 REM EQUATION FOR THE SENSITIVITY COEFF
290 FOR K=1 TO N
295 V2=1!-V1(K)
300 X(K)=V1(K)*V2*V2*EXP(V2+B*V2*V2)
310 NEXT K
315 REM CALCULATE SO, XTX, XTY
320 FOR K=1 TO N
330 SO=SO+(A1(K)-ETA(K))*(A1(K)-ETA(K))

```

```
340 XTX=XTX+X(K)*X(K)
350 XTY=XTY+X(K)*(A1(K)-ETA(K))
360 NEXT K
370 DELTAB=XTY/XTX
380 REM CALCULATE G
390 G=DELTAB*DELTAB*XTX
400 IF (G<0!) OR (G=0!) GOTO 670
410 H=1!
420 B=B+DELTAB*H
430 REM CALCULATE ETA'S WITH B'S
440 FOR K=1 TO N
445 V2=1!-V1(K)
450 ETA(K)=V1(K)*EXP(V2+B*V2*V2)
460 NEXT K
560 REM CALCULATE S1
570 FOR K=1 TO N
580 S1 =S1+(A1(K)-ETA(K))*(A1(K)-ETA(K))
590 NEXT K
600 JJ=SO-(2-(1/1.1))*G
610 IF (S1<JJ) OR (S1=JJ) GOTO 640
615 B=B-DELTAB*H
620 H=G/(S1-SO+2!*G)
630 B=B+H*DELTAB
640 PRINT H,S1,B
650 IF (RL<ITE+1) GOTO 225
660 IF (RL=ITE) GOTO 680
670 PRINT "G=",G
680 END
```

```

90  REM CALCULATES VALUES OF THE CLUSTER FUNCTION
100 REM CALCULATES VOLUME FRACTION FOR FLORY-HUGGINS MODEL
110 REM (USING NEWTON -RAWSON METHOD) AND THE LANGMUIR
112 REM CONTRIBUTION
115 REM GIVEN BY PARAM(1)*ACTIVITY/1+PARAM(2)*ACTIV.
118 DIM A(100),W(100),V(100)
121 FOR I=1 TO 100
122 A(I)=.01*I
125 NEXT I
130 INPUT "ENTER VALUE OF CHI      ",CHI
132 INPUT "ENTER VALUE OF PARAM(1)  ",K
133 INPUT "ENTER VALUE OF PARAM(2)  ",B
135 LPRINT "CHI VALUE USED=";CHI
136 LPRINT "PARAM (1),K =          ";K
137 LPRINT "PARAM (2),B =          ";B
140 LPRINT "ACTIVITY "; "          V1      "; " CLUSTER FUNCTION"
150 FOR I=1 TO 100
155 REM FIRST GUESS FOR VOLUME FRACTION : X=A(I)/10
160 FOR II =1 TO 4
170 Z=1-X
180 Y=Z+CHI*Z*Z
190 F=X*EXP(Y)-A(I)
200 FP=EXP(Y)*(1-X*(2*CHI*Z+1))
210 X=X-F/FP
215 W(I)=X
220 NEXT II
225 V(I)=W(I)+K*A(I)/(1+B*A(I))
230 NEXT I
235 FOR I=2 TO 99 STEP 2
240 X1=(A(I+1)/V(I+1))-A(I-1)/V(I-1)
245 X2=A(I+1)-A(I-1)
250 DER=X1/X2
255 CLUST=-(1-V(I))*DER-1
260 LPRINT A(I),V(I),CLUST
265 NEXT I
270 END

```

```
5  REM THIS PROGRAM CALCULATES THE DIFFUSION COEFFICIENT FROM
6  REM PERMEABILITY CONTINUOUS FLOW EXPERIMENTS.
7  REM PROGRAM WRITTEN BY RUBEN J. HERNANDEZ. JAN/1988
10 DIM F(50),T(50),X(50),DF(50)
30 REM TIME SHOULD BE IN MINUTES TO GIVE THE UNITS
31 REM OF THE DIFFUSION COEFFICIENT IN cm2/sec
32 PRINT "ENTER RELATIVE HUMIDITY IN PERCENT"
33 INPUT HUM
35 PRINT "ENTER THE RUN IDENTIFICATION NUMBER"
36 REM
37 INPUT SUN
38 PRINT "ENTER THE TEMPERATURE AT STEADY STATE "
39 INPUT W
40 PRINT "ENTER THE NUMBER OF DATA POINTS"
50 INPUT D
60 PRINT "ENTER THE FLOW F(in mV) AND TIME T(min) STARTING FROM ZERO"
70 FOR I=1 TO D
80 PRINT "ENTER TIME"
90 INPUT T(I)
100 PRINT "ENTER FLOW"
110 INPUT F(I)
120 NEXT I
160 PRINT "ENTER YOUR GUESS FOR X"
170 INPUT GUESS
180 PRINT "ENTER STEADY STATE VALUE OF FLOW"
190 INPUT FI
195 REM NEWTON-RAWSON METHOD
200 FOR I=1 TO D
205 DF(I)=F(I)/FI
210 A=.44313*F(I)/FI
220 X=GUESS
230 FOR J=1 TO 7
240 B=SQR(X)
250 C=EXP(-X)
260 L=1/B
270 H=(.5*L-B)*C
280 E=(B*C)-A
290 X=X-(E/H)
300 NEXT J
310 X(I)=X
320 GUESS=X
330 NEXT I
```

```

380 REM LINEAR REGRESSION
390 ST=0
400 SX=0
410 SXT=0
420 STSQ=0
430 SXSQ=0
440 FOR I=1 TO D
445 X(I)=1!/X(I)
450 ST=ST+T(I)
460 SX=SX+X(I)
470 SXT=SXT+(X(I)*T(I))
480 SXSQ=SXSQ+(X(I)*X(I))
490 STSQ=STSQ+(T(I)*T(I))
500 NEXT I
510 SLOPE=(ST*SX-D*SXT)/(ST*ST-D*STSQ)
520 DUM1=(D*SXT)-(SX*ST)
530 DUM2=(D*STSQ)-(ST*ST)
540 DUM3=(D*SXSQ)-(SX*SX)
550 DUM4=SQR(DUM2*DUM3)
560 R=DUM1/DUM4
562 LPRINT "RUN NUMBER: " SUN
563 LPRINT
564 LPRINT "TIME (MIN) ", "FLOW (mV)", " 1/X", "FLOW PERCENT"
570 FOR I=1 TO D
600 LPRINT T(I),F(I),X(I),DF(I)
610 NEXT I
620 LPRINT
630 LPRINT
635 DIFF=(3.555E-08)*SLOPE
636 LPRINT "DIFFUSION COEFFICIENT (cm2/sec.) =" DIFF
637 LPRINT
638 LPRINT "PERMEABILITY COEFFICIENT (cm3/m2.day) =" FI*12.5156
639 LPRINT
640 LPRINT "SOLUBILITY (cc O2/cc polymer) =" (4.22994E-11)*FI/DIFF
642 LPRINT
645 LPRINT "CORRELATION COEFFICIENT =" R
646 LPRINT
647 LPRINT "TEMPERATURE (C) =" W : LPRINT
648 LPRINT "WATER ACTIVITY, aw =" HUM/100 : LPRINT
649 LPRINT "STEADY STATE FLOW, mV =" FI
650 REM THE VALUE OF THE DIFF. COEFF. IS FOR TIME IN MINUTES
655 REM THE THICKNESS IS L=2.93E-03 cm.
659 END

```

```

100 REM CALCULATES VOLUME FRACTION FOR FLORY-HUGGINS MODEL
110 REM (USING NEWTON -RAPHSON METHOD) AND THE LANGMUIR CONTRIBUTION
115 REM GIVEN BY PARAM[1]*ACTIVITY/1+PARAM[2]*ACTIV.
118 DIM A(30),W(30)
121 A(1)=0! : A(6)=.046:A(7)=.056:A(8)=.072:A(9)=.08:A(10)=.0901
111=.11:A(12)=.155:A(13)=.189:A(14)=.252:A(15)=.269:A(16)=.308:
7)=.41:A(18)=.44:A(19)=.565:A(20)=.58:A(21)=.585:A(22)=.635:A(23)
35:A(24)=.79
122 A(2)=.01 : A(3)=.02 : A(4)=.03 : A(5)=.04
130 INPUT "ENTER VALUE OF CHI ",CHI
132 INPUT "ENTER VALUE OF PARAM(1) ",K
133 INPUT "ENTER VALUE OF PARAM(2) ",B
135 LPRINT "CHI VALUE USED=";CHI
136 LPRINT "PARAM 1= ";K
137 LPRINT "PARAM 2 = ";B
140 LPRINT "ACTIVITY "; " LANG. "; " F-H "; " TOTAL "
150 FOR I=1 TO 27
155 REM FIRST GUESS FOR VOLUME FRACTION : X=A(I)/10
160 FOR II =1 TO 4
170 Z=1-X
180 Y=Z+CHI*Z*Z
190 F=X*EXP(Y)-A(I)
200 FP=EXP(Y)*(1-X*(2*CHI*Z+1))
210 X=X-F/FP
215 W(I)=X
220 NEXT II
225 V=W(I)+K*A(I)/(1+B*A(I))
230 LPRINT A(I),V-W(I),W(I),V
235 NEXT I
240 END
260 END

```

CHI VALUE USED= 1.66  
 PARAM (1),K = .46  
 PARAM (2),B = 81.36

ACTIVITY	V1	CLUSTER FUNCTION	5 °C
.02	4.909319E-03	-90.90162	
.04	7.15727E-03	-64.81381	
.06	8.967592E-03	-48.22278	
.08	1.063685E-02	-37.01073	
9.999999E-02	.0122507	-29.07661	
.12	1.384331E-02	-23.25473	
.14	1.543119E-02	-18.85523	
.16	1.702347E-02	-15.44847	
.18	1.862575E-02	-12.75571	
.2	2.024176E-02	-10.5894	
.22	2.187418E-02	-8.81987	
.24	2.352508E-02	-7.354772	
.26	2.519619E-02	-6.127185	
.28	2.688893E-02	-5.087882	
.3	2.860463E-02	-4.199164	
.32	3.034454E-02	-3.432935	
.34	.0321098	-2.766167	
.36	3.390159E-02	-2.182774	
.38	3.572106E-02	-1.667958	
.4	3.756939E-02	-1.210921	
.42	3.944775E-02	-.8029108	
.44	.0413574	-.436193	
.46	4.329963E-02	-.1050007	
.48	4.527576E-02	.1956189	
.5	4.728722E-02	.4702143	
.52	4.933547E-02	.7221345	
.54	5.142208E-02	.9541478	
.56	5.354873E-02	1.169004	
.58	5.571716E-02	1.369228	
.6	5.792922E-02	1.556429	
.62	6.018697E-02	1.732119	
.64	6.249248E-02	1.89784	
.66	6.484811E-02	2.055503	
.68	6.725629E-02	2.204984	
.7	6.971966E-02	2.348459	
.72	7.224111E-02	2.486567	
.74	7.482374E-02	2.619742	
.76	.0774709	2.749503	
.78	8.018624E-02	2.875573	
.8	8.297378E-02	2.99972	
.82	8.583789E-02	3.12211	
.84	8.878334E-02	3.243133	
.8599999	9.181541E-02	3.364202	
.88	9.493999E-02	3.485315	
.9	9.816351E-02	3.607294	
.9199999	.1014932	3.730898	
.94	.1049372	3.856965	
.96	.1085045	3.986406	
.9799999	.1122056	4.12035	

CHI VALUE USED= 1.7

PARAM (1),K = .385

PARAM (2),B = 95.15

ACTIVITY V1 CLUSTER FUNCTION 23 °C

.02	4.004555E-03	-109.8264
.04	5.924888E-03	-72.53325
.06	7.548856E-03	-51.0288
.08	9.084456E-03	-37.49783
9.999999E-02	1.058944E-02	-28.43002
.12	1.208647E-02	-22.05536
.14	1.358643E-02	-17.40221
.16	1.509535E-02	-13.90056
.18	1.661697E-02	-11.19784
.2	1.815385E-02	-9.067458
.22	1.970787E-02	-7.356995
.24	2.128052E-02	-5.962404
.26	2.287309E-02	-4.808938
.28	2.448669E-02	-3.843528
.3	2.612237E-02	-3.026233
.32	2.778114E-02	-2.32777
.34	2.946397E-02	-1.725049
.36	3.117185E-02	-1.201051
.38	3.290575E-02	-.7411583
.4	.0346667	-.3353634
.42	3.645574E-02	2.531791E-02
.44	3.827395E-02	.3484278
.46	4.012246E-02	.6389959
.48	4.200245E-02	.9025192
.5	4.391517E-02	1.142076
.52	4.586192E-02	1.362017
.54	.0478441	1.563781
.56	4.986316E-02	1.751476
.58	5.192066E-02	1.925771
.6	5.401825E-02	2.088488
.62	5.615769E-02	2.241869
.64	5.834089E-02	2.386677
.66	.0605698	2.523843
.68	6.284664E-02	2.655386
.7	6.517371E-02	2.781028
.72	6.755351E-02	2.902389
.74	.0699887	3.020126
.76	7.248222E-02	3.134567
.78	7.503723E-02	3.246629
.8	7.765715E-02	3.356855
.82	8.034578E-02	3.466034
.84	8.310711E-02	3.574474
.8599999	8.594568E-02	3.68273
.88	8.886645E-02	3.79195
.9	.0918748	3.901837
.9199999	9.497685E-02	4.013824
.94	9.817922E-02	4.127654
.96	.1014896	4.245092
.9799999	.1049162	4.366406

CHI VALUE USED= 1.76

PARAM (1),K = .19

PARAM (2),B = 102

ACTIVITY	V1	CLUSTER FUNCTION	42 °C
.02	2.523137E-03	-135.1841	
.04	4.057181E-03	-73.0991	
.06	5.465441E-03	-45.03116	
.08	6.842509E-03	-29.96472	
9.999999E-02	8.214356E-03	-20.94153	
.12	9.591216E-03	-15.1085	
.14	1.097809E-02	-11.11884	
.16	1.237786E-02	-8.267276	
.18	1.379239E-02	-6.157206	
.2	1.522304E-02	-4.550576	
.22	1.667089E-02	-3.297645	
.24	1.813686E-02	-2.300347	
.26	1.962179E-02	-1.492445	
.28	2.112646E-02	-.8276245	
.3	2.265163E-02	-.2731706	
.32	2.419806E-02	.1951207	
.34	2.576649E-02	.5948483	
.36	2.735772E-02	.9403656	
.38	2.897253E-02	1.240473	
.4	3.061176E-02	1.505156	
.42	3.227627E-02	1.739242	
.44	3.396694E-02	1.948834	
.46	3.568473E-02	2.136946	
.48	.0374306	2.307936	
.5	3.920563E-02	2.464288	
.52	4.101084E-02	2.607499	
.54	4.284744E-02	2.740478	
.56	4.471666E-02	2.864259	
.58	4.661973E-02	2.980225	
.6	4.855809E-02	3.089716	
.62	5.053315E-02	3.193428	
.64	5.254651E-02	3.292421	
.66	5.459977E-02	3.387795	
.68	5.669473E-02	3.479759	
.7	.0588333	3.568708	
.72	.0610175	3.655758	
.74	6.324952E-02	3.741069	
.76	6.553169E-02	3.825558	
.78	6.786656E-02	3.908974	
.8	7.025688E-02	3.992309	
.82	7.270565E-02	4.0757	
.84	7.521605E-02	4.15959	
.8599999	7.779161E-02	4.244279	
.88	8.043621E-02	4.330721	
.9	8.315405E-02	4.418622	
.9199999	8.594977E-02	4.508579	
.94	8.882847E-02	4.601832	
.96	9.179582E-02	4.697719	
.9799999	9.485813E-02	4.797932	

APPENDIX B

RUN NUMBER: 1 A

TIME (MIN)	FLOW (mV)	1/X	FLOW PERCENT
30	.62	.3695568	.248
36	.86	.4353971	.344
42	1.09	.5031636	.436
46	1.21	.5416824	.4840001
50	1.33	.5832294	.532
54	1.43	.6207683	.572
58	1.51	.6531465	.604
62	1.6	.6926031	.64
66	1.67	.7259575	.668
70	1.74	.7621256	.696
75	1.8	.7957972	.72
80	1.86	.8324215	.744
85	1.91	.8656294	.764
90	1.95	.8942747	.78
100	2.06	.9853724	.824

DIFFUSION COEFFICIENT (cm<sup>2</sup>/sec.) = 3.056011E-10

PERMEABILITY COEFFICIENT (cm<sup>3</sup>/m<sup>2</sup>.day) = 31.289

SOLUBILITY (cc O<sub>2</sub>/cc polymer) = .3460344

CORRELATION COEFFICIENT = .9960481

TEMPERATURE (C) = 11.9

WATER ACTIVITY, aw = 0

STEADY STATE FLOW, mV = 2.5

RUN NUMBER: 1D

TIME (MIN)	FLOW (mV)	1/X	FLOW PERCENT
20	.08	.2242855	5.517241E-02
25	.175	.2805958	.1206897
30	.29	.3370263	.2
35	.41	.3930966	.2827586
40	.53	.4506895	.3655172
45	.63	.5019877	.4344828
50	.725	.5551573	.5
55	.805	.6046123	.5551724
60	.88	.6561946	.6068965
65	.95	.710357	.6551725
70	1	.753656	.6896551
75	1.05	.801886	.7241379
85	1.14	.9059511	.7862068
94	1.2	.99379	.8275863

DIFFUSION COEFFICIENT (cm<sup>2</sup>/sec.) = 3.694086E-10

PERMEABILITY COEFFICIENT (cm<sup>3</sup>/m<sup>2</sup>.day) = 18.14762

SOLUBILITY (cc O<sub>2</sub>/cc polymer) = .166484

CORRELATION COEFFICIENT = .9995706

TEMPERATURE (C) = 11.9

WATER ACTIVITY, a<sub>w</sub> = .06

STEADY STATE FLOW, mV = 1.45

RUN NUMBER: 1 E

TIME (MIN)	FLOW (mV)	1/X	FLOW PERCENT
25	.12	.2686466	.1052632
30	.21	.326189	.1842105
35	.3	.3798029	.2631579
40	.39	.4340633	.3421053
45	.48	.4916768	.4210527
50	.55	.5404004	.4824562
55	.62	.594054	.5438597
60	.68	.6453394	.5964912
65	.73	.6930058	.6403509
70	.77	.7352706	.6754386
75	.815	.78843	.7149123
80	.85	.8350044	.7456141
85	.88	.879576	.7719298
90	.91	.9296001	.7982457
100	.965	1.041357	.8464912

DIFFUSION COEFFICIENT (cm<sup>2</sup>/sec.) = 3.595235E-10

PERMEABILITY COEFFICIENT (cm<sup>3</sup>/m<sup>2</sup>.day) = 14.26778

SOLUBILITY (cc O<sub>2</sub>/cc polymer) = .1341256

CORRELATION COEFFICIENT = .9995285

TEMPERATURE (C) = 11.9

WATER ACTIVITY, a<sub>w</sub> = .175

STEADY STATE FLOW, mV = 1.14

RUN NUMBER: 5

TIME (MIN)	FLOW (mV)	1/X	FLOW PERCENT
25	9.529999E-02	.2681289	.1046103
30	.1737	.330636	.1906696
35	.2542	.3905649	.2790341
40	.339	.4554396	.3721185
45	.4068	.5114006	.4465423
50	.4662	.5652788	.5117454
55	.519	.6185303	.5697036
60	.572	.6789239	.6278815
65	.6145	.7341264	.6745335
75	.678	.8327998	.7442371

DIFFUSION COEFFICIENT (cm<sup>2</sup>/sec.) = 4.032022E-10

PERMEABILITY COEFFICIENT (cm<sup>3</sup>/m<sup>2</sup>.day) = 11.40171

SOLUBILITY (cc O<sub>2</sub>/cc polymer) = .0955718

CORRELATION COEFFICIENT = .9993317

TEMPERATURE (C) = 11.9

WATER ACTIVITY, a<sub>w</sub> = .452

STEADY STATE FLOW, mV = .911

RUN NUMBER: 6

TIME (MIN)	FLOW (mV)	1/X	FLOW PERCENT
30	.213	.3753858	.2566265
35	.298	.4460538	.3590362
40	.373	.5136517	.4493976
45	.447	.5891816	.5385543
50	.5	.6514816	.6024097
55	.554	.7253016	.66747
60	.596	.7929905	.7180723
65	.628	.8530728	.7566266
70	.66	.9234472	.7951808

DIFFUSION COEFFICIENT (cm<sup>2</sup>/sec.) = 4.868098E-10

PERMEABILITY COEFFICIENT (cm<sup>3</sup>/m<sup>2</sup>.day) = 10.38795

SOLUBILITY (cc O<sub>2</sub>/cc polymer) = 7.211955E-02

CORRELATION COEFFICIENT = .9998113

TEMPERATURE (C) = 11.9

WATER ACTIVITY, aw = .5940001

STEADY STATE FLOW, mV = .83

RUN NUMBER: 1 F

TIME (MIN)	FLOW (mV)	1/X	FLOW PERCENT
25	.115	.2914978	.1352941
30	.195	.3569971	.2294118
35	.28	.4251765	.3294118
40	.36	.4935652	.4235294
45	.435	.5652957	.5117647
50	.495	.6309945	.582353
55	.55	.7007728	.6470589
60	.595	.7675537	.7
65	.615	.8009851	.7235294
70	.67	.9098404	.7882353
75	.7	.9842807	.8235294
80	.72	1.042877	.8470588
90	.76	1.195295	.8941176

DIFFUSION COEFFICIENT (cm<sup>2</sup>/sec.) = 4.900779E-10

PERMEABILITY COEFFICIENT (cm<sup>3</sup>/m<sup>2</sup>.day) = 10.63826

SOLUBILITY (cc O<sub>2</sub>/cc polymer) = 7.336486E-02

CORRELATION COEFFICIENT = .9991102

TEMPERATURE (C) = 11.9

WATER ACTIVITY, aw = .74

STEADY STATE FLOW, mV = .85

RUN NUMBER: 7

TIME (MIN)	FLOW (mV)	1/X	FLOW PERCENT
30	.2136	.3775252	.2597908
35	.316	.4643096	.3843348
40	.3844	.5281584	.4675262
45	.4485	.5955592	.5454877
50	.5125	.6738917	.6233277
55	.555	.7347388	.6750183
60	.598	.8066253	.727317
65	.632	.8737842	.7686695
70	.662	.9438266	.8051569
75	.683	1.00124	.8306981

DIFFUSION COEFFICIENT (cm<sup>2</sup>/sec.) = 4.909014E-10PERMEABILITY COEFFICIENT (cm<sup>3</sup>/m<sup>2</sup>.day) = 10.29033SOLUBILITY (cc O<sub>2</sub>/cc polymer) = 7.084635E-02

CORRELATION COEFFICIENT = .9995529

TEMPERATURE (C) = 11.9

WATER ACTIVITY, a<sub>w</sub> = .753

STEADY STATE FLOW, mV = .8222

RUN NUMBER: 8

TIME (MIN)	FLOW (mV)	1/X	FLOW PERCENT
25	.13845	.3184585	.1730625
30	.22365	.3909239	.2795625
35	.30885	.4655729	.3860625
40	.3834	.5377478	.47925
43	.426	.5836809	.5325
45	.4558	.6185755	.56975
48	.49	.6621512	.6125
50	.5112	.6914581	.639
53	.54315	.7397224	.6789375
55	.5538	.7570992	.69225
60	.5964	.8348215	.7455
70	.6284	.9046042	.7855001

DIFFUSION COEFFICIENT (cm<sup>2</sup>/sec.) = 4.891418E-10

PERMEABILITY COEFFICIENT (cm<sup>3</sup>/m<sup>2</sup>.day) = 10.01248

SOLUBILITY (cc O<sub>2</sub>/cc polymer) = 6.918142E-02

CORRELATION COEFFICIENT = .9940052

TEMPERATURE (C) = 11.9

WATER ACTIVITY, aw = .881

STEADY STATE FLOW, mV = .8

RUN NUMBER: 1B

TIME (MIN)	FLOW (mV)	1/X	FLOW PERCENT
15	.69	.3211444	.1769231
18	1.18	.4066213	.3025641
20	1.34	.4351081	.3435898
23	1.64	.4912659	.4205128
25	1.82	.5274619	.4666667
28	2.11	.5914451	.5410256
30	2.26	.628141	.5794871
35	2.55	.7087757	.6538461
40	2.76	.7781929	.7076923
45	2.93	.8442052	.7512821
50	3.05	.8980966	.7820513
55	3.15	.9491737	.8076923

DIFFUSION COEFFICIENT (cm<sup>2</sup>/sec.) = 5.541952E-10PERMEABILITY COEFFICIENT (cm<sup>3</sup>/m<sup>2</sup>.day) = 48.81084SOLUBILITY (cc O<sub>2</sub>/cc polymer) = .2976707

CORRELATION COEFFICIENT = .9925459

TEMPERATURE (C) = 22

WATER ACTIVITY, a<sub>w</sub> = 0

STEADY STATE FLOW, mV = 3.9

RUN NUMBER: 2 A

TIME (MIN)	FLOW (mV)	1/X	FLOW PERCENT
14	.43	.3091848	.1598513
18	.8	.4030821	.2973978
22	1.12	.4881121	.4163569
26	1.4	.5729102	.5204461
30	1.6	.6435948	.5947955
34	1.77	.7137386	.6579926
38	1.92	.7867717	.7137546
42	2.05	.8623256	.7620818
46	2.15	.9316498	.7992565
50	2.25	1.015341	.8364312
60	2.4	1.187729	.8921933
70	2.55	1.519134	.9479554

DIFFUSION COEFFICIENT (cm<sup>2</sup>/sec.) = 7.185359E-10

PERMEABILITY COEFFICIENT (cm<sup>3</sup>/m<sup>2</sup>.day) = 33.66697

SOLUBILITY (cc O<sub>2</sub>/cc polymer) = .1583573

CORRELATION COEFFICIENT = .9958065

TEMPERATURE (C) = 22

WATER ACTIVITY, aw = .048

STEADY STATE FLOW, mV = 2.69

RUN NUMBER: 2 B

TIME (MIN)	FLOW (mV)	1/X	FLOW PERCENT
12	.2	.2605724	9.523811E-02
14	.33	.3072656	.1571429
16	.47	.3532068	.2238096
18	.61	.3983534	.2904762
20	.75	.4447045	.3571429
23	.92	.5047915	.4380953
26	1.19	.6155871	.5666668
29	1.22	.6295978	.5809524
32	1.34	.6904246	.6380953
35	1.45	.7547426	.6904763
38	1.53	.8085104	.7285715
41	1.6	.8620221	.7619048
45	1.7	.9530811	.8095239

DIFFUSION COEFFICIENT (cm<sup>2</sup>/sec.) = 7.364255E-10

PERMEABILITY COEFFICIENT (cm<sup>3</sup>/m<sup>2</sup>.day) = 26.28276

SOLUBILITY (cc O<sub>2</sub>/cc polymer) = .1206215

CORRELATION COEFFICIENT = .9973829

TEMPERATURE (C) = 22

WATER ACTIVITY, a<sub>w</sub> = .153

STEADY STATE FLOW, mV = 2.1

RUN NUMBER: 2C

TIME (MIN)	FLOW (mV)	1/X	FLOW PERCENT
12	.17	.2538611	8.717949E-02
14	.3	.3049202	.1538462
15.5	.4	.3405245	.2051282
17	.5	.3752396	.2564103
19	.63	.4207709	.3230769
21	.76	.4682719	.3897436
23	.86	.5070758	.4410257
25	.96	.5486355	.4923077
27	1.07	.5985596	.548718
29	1.17	.6489706	.6
31	1.24	.6879242	.6358974
36	1.4	.7928111	.7179487
41	1.55	.9228322	.7948718
46	1.62	1.001412	.8307693

DIFFUSION COEFFICIENT (cm<sup>2</sup>/sec.) = 7.901757E-10

PERMEABILITY COEFFICIENT (cm<sup>3</sup>/m<sup>2</sup>.day) = 24.40542

SOLUBILITY (cc O<sub>2</sub>/cc polymer) = .1043867

CORRELATION COEFFICIENT = .9994421

TEMPERATURE (C) = 22

WATER ACTIVITY, a<sub>w</sub> = .275

STEADY STATE FLOW, mV = 1.95

RUN NUMBER: 2 D

TIME (MIN)	FLOW (mV)	1/X	FLOW PERCENT
10	.075	.2120374	4.385965E-02
12	.17	.2639706	9.941521E-02
14	.295	.3180766	.1725146
16	.43	.3718956	.251462
18	.555	.4218016	.3245614
20	.685	.4762826	.4005848
22	.8	.5284098	.4678363
24	.905	.5807443	.5292397
26	1	.6334406	.5847953
28	1.08	.6830525	.631579
30	1.16	.7389876	.6783626
35	1.31	.8692451	.7660818
40	1.42	1.000543	.8304093

DIFFUSION COEFFICIENT (cm<sup>2</sup>/sec.) = 9.338639E-10

PERMEABILITY COEFFICIENT (cm<sup>3</sup>/m<sup>2</sup>.day) = 21.40168

SOLUBILITY (cc O<sub>2</sub>/cc polymer) = 7.745451E-02

CORRELATION COEFFICIENT = .9999887

TEMPERATURE (C) = 22

WATER ACTIVITY, aw = .445

STEADY STATE FLOW, mV = 1.71

RUN NUMBER: 2 E

TIME (MIN)	FLOW (mV)	1/X	FLOW PERCENT
12	.155	.2614194	9.627329E-02
14	.27	.314712	.1677019
16	.395	.3677611	.2453416
18	.525	.422862	.326087
20	.65	.478622	.4037267
22	.76	.5318381	.4720497
24	.86	.5851842	.5341615
26	.95	.6387602	.5900621
28	1.03	.6923183	.6397516
30	1.1	.745248	.6832298
34	1.22	.8549849	.757764
38	1.31	.9620561	.8136646
42	1.38	1.070902	.8571429
47	1.44	1.196458	.8944099

DIFFUSION COEFFICIENT (cm<sup>2</sup>/sec.) = 9.546139E-10

PERMEABILITY COEFFICIENT (cm<sup>3</sup>/m<sup>2</sup>.day) = 20.15012

SOLUBILITY (cc O<sub>2</sub>/cc polymer) = 7.133988E-02

CORRELATION COEFFICIENT = .9999728

TEMPERATURE (C) = 22

WATER ACTIVITY, aw = .545

STEADY STATE FLOW, mV = 1.61

RUN NUMBER: 2

TIME (MIN)	FLOW (mV)	1/X	FLOW PERCENT
10	.07	.2131914	.0448718
12	.16	.2664996	.1025641
14	.28	.3229229	.1794872
16	.405	.3774066	.2596154
18	.53	.4324036	.3397436
20	.65	.4883466	.4166667
22	.765	.5470177	.4903847
24	.86	.6009548	.5512821
26	.95	.6583942	.6089744
28	1.03	.7164725	.6602565
31	1.125	.7974862	.7211539
34	1.2	.8747756	.7692308

DIFFUSION COEFFICIENT (cm<sup>2</sup>/sec.) = 9.888553E-10PERMEABILITY COEFFICIENT (cm<sup>3</sup>/m<sup>2</sup>.day) = 19.52434SOLUBILITY (cc O<sub>2</sub>/cc polymer) = 6.673075E-02

CORRELATION COEFFICIENT = .9999458

TEMPERATURE (C) = 22

WATER ACTIVITY, a<sub>w</sub> = .75

STEADY STATE FLOW, mV = 1.56

RUN NUMBER: 1C

TIME (MIN)	FLOW (mV)	1/X	FLOW PERCENT
6	.55	.2464279	7.857143E-02
7	.95	.2918066	.1357143
8	1.4	.3370263	.2
9	1.9	.385404	.2714286
10	2.35	.4295787	.3357143
11	2.8	.4758481	.4
12	3.15	.5141279	.45
14	3.84	.5984231	.5485715
16	4.34	.6702503	.62
18	4.75	.7392545	.6785714
20	5.05	.7978894	.7214286
25	5.5	.9050119	.7857143
30	5.8	.9961334	.8285715

DIFFUSION COEFFICIENT (cm<sup>2</sup>/sec.) = 1.151891E-09

PERMEABILITY COEFFICIENT (cm<sup>3</sup>/m<sup>2</sup>.day) = 97.6092

SOLUBILITY (cc O<sub>2</sub>/cc polymer) = .257052

CORRELATION COEFFICIENT = .9846563

TEMPERATURE (C) = 40.2

WATER ACTIVITY, a<sub>w</sub> = 0

STEADY STATE FLOW, mV = 7

RUN NUMBER: 2G

TIME (MIN)	FLOW (mV)	1/X	FLOW PERCENT
6	.36	.2425544	7.422681E-02
7	.65	.2905604	.1340206
9	1.35	.3901006	.2783505
11	2	.4851021	.4123711
13	2.53	.573975	.5216495
15	2.95	.6576235	.6082475
17	3.25	.7285702	.6701031
19	3.55	.8136434	.7319588
21	3.72	.8708681	.7670103
23	3.85	.9207344	.7938145
25	3.98	.9775943	.8206186
27	4.13	1.055105	.8515464

DIFFUSION COEFFICIENT (cm<sup>2</sup>/sec.) = 1.363489E-09

PERMEABILITY COEFFICIENT (cm<sup>3</sup>/m<sup>2</sup>.day) = 60.70066

SOLUBILITY (cc O<sub>2</sub>/cc polymer) = .1504611

CORRELATION COEFFICIENT = .9949336

TEMPERATURE (C) = 40.3

WATER ACTIVITY, aw = .04

STEADY STATE FLOW, mV = 4.85

RUN NUMBER: 3

TIME (MIN)	FLOW (mV)	1/X	FLOW PERCENT
12	.25	.2323619	6.329114E-02
15	.68	.3178236	.1721519
18	1.175	.4031303	.2974683
21	1.68	.4949314	.4253164
24	2.17	.5991648	.5493671
27	2.55	.6990365	.6455696
30	2.885	.8112427	.7303798
33	3.135	.9204504	.7936709
36	3.325	1.028941	.8417721
39	3.49	1.155459	.8935442

DIFFUSION COEFFICIENT (cm<sup>2</sup>/sec.) = 1.215242E-09

PERMEABILITY COEFFICIENT (cm<sup>2</sup>/m<sup>2</sup>.day) = 49.43663

SOLUBILITY (cc O<sub>2</sub>/cc polymer) = .1374892

CORRELATION COEFFICIENT = .998459

TEMPERATURE (C) = 40

WATER ACTIVITY, a<sub>w</sub> = .096

STEADY STATE FLOW, mV = 3.95

RUN NUMBER: 4

TIME (MIN)	FLOW	1/X	FLOW PERCENT
10	.42	.2232762	5.419355E-02
13	1.3	.3147401	.1677419
16	2.49	.4195317	.3212903
19	3.62	.5278103	.4670968
22	4.67	.6516603	.6025807
25	5.5	.7809827	.7096774
28	6.1	.9076528	.7870968
31	6.6	1.055288	.8516129
34	6.9	1.180514	.8903226

DIFFUSION COEFFICIENT (cm<sup>2</sup>/sec.) = 1.437803E-09PERMEABILITY COEFFICIENT (cm<sup>3</sup>/m<sup>2</sup>.day) = 48.4995SOLUBILITY (cc O<sub>2</sub>/cc polymer) = .1140004

CORRELATION COEFFICIENT = .9980205

TEMPERATURE (C) = 40

WATER ACTIVITY, a<sub>w</sub> = .15

STEADY STATE FLOW = 7.75

R  
UN NUMBER: 5

TIME (MIN)	FLOW	1/X	FLOW PERCENT
10	.75	.2677766	.1041667
12	1.51	.3436512	.2097222
14	2.44	.4318037	.3388889
16	3.35	.5263384	.4652778
18	4.15	.6250758	.5763889
20	4.8	.7243094	.6666667
22	5.35	.8309175	.7430556
24	5.8	.9446628	.8055556
26	6.1	1.043316	.8472222
28	6.32	1.135357	.8777778

DIFFUSION COEFFICIENT (cm<sup>2</sup>/sec.) = 1.754137E-09

PERMEABILITY COEFFICIENT (cm<sup>3</sup>/m<sup>2</sup>.day) = 45.0576

SOLUBILITY (cc O<sub>2</sub>/cc polymer) = 8.681068E-02

CORRELATION COEFFICIENT = .9991106

TEMPERATURE (C) = 40

WATER ACTIVITY, *a<sub>w</sub>* = .253

STEADY STATE FLOW = 7.2

RUN NUMBER: 6

TIME (MIN)	FLOW	1/X	FLOW PERCENT
9	.93	.2925775	.1367647
10	1.45	.3460382	.2132353
11	1.95	.3958234	.2867647
12	2.51	.4532766	.3691177
13	3.01	.5083436	.4426471
14	3.55	.5743376	.5220588
15	4	.6369081	.5882353
16	4.42	.7042227	.65
17	4.76	.7675534	.7
19	5.35	.9070168	.7867647
21	5.75	1.038951	.8455882

DIFFUSION COEFFICIENT (cm<sup>2</sup>/sec.) = 2.225163E-09

PERMEABILITY COEFFICIENT (cm<sup>3</sup>/m<sup>2</sup>.day) = 42.5544

SOLUBILITY (cc O<sub>2</sub>/cc polymer) = 6.463255E-02

CORRELATION COEFFICIENT = .9987307

TEMPERATURE (C) = 40

WATER ACTIVITY, aw = .392

STEADY STATE FLOW = 6.8

RUN NUMBER: 7

TIME (MIN)	FLOW	1/X	FLOW PERCENT
7	.4	.2360046	.0671141
8	.85	.2968458	.1426175
9	1.33	.3527632	.2231544
10	1.88	.4154808	.3154363
11	2.44	.4828646	.409396
12	2.96	.5523021	.4966443
13	3.43	.6242035	.5755034
14	3.84	.6975561	.6442953
15	4.19	.7716989	.7030201
16	4.47	.8421059	.75
17	4.7	.9105256	.7885906
18	4.9	.981093	.8221477

DIFFUSION COEFFICIENT (cm<sup>2</sup>/sec.) = 2.44146E-09

PERMEABILITY COEFFICIENT (cm<sup>3</sup>/m<sup>2</sup>.day) = 37.29768

SOLUBILITY (cc O<sub>2</sub>/cc polymer) = 5.162986E-02

CORRELATION COEFFICIENT = .9993703

TEMPERATURE (C) = 40

WATER ACTIVITY, aw = .535

STEADY STATE FLOW = 5.96

RUN NUMBER: 8

TIME (MIN)	FLOW	1/X	FLOW PERCENT
7	.63	.268438	.105
8	1.13	.3290299	.1883333
9	1.73	.3968923	.2883333
10	2.36	.4709141	.3933333
11	2.97	.5509088	.495
12	3.49	.6303095	.5816666
13	2.92	.5439042	.4866667
14	4.29	.788556	.715
15	4.61	.8731919	.7683334
16	4.87	.9577005	.8116667
17	5.1	1.050848	.8499999

DIFFUSION COEFFICIENT (cm<sup>2</sup>/sec.) = 2.741845E-09

PERMEABILITY COEFFICIENT (cm<sup>3</sup>/m<sup>2</sup>.day) = 37.548

SOLUBILITY (cc O<sub>2</sub>/cc polymer) = 4.628205E-02

CORRELATION COEFFICIENT = .9788098

TEMPERATURE (C) = 40

WATER ACTIVITY, *a<sub>w</sub>* = .67

STEADY STATE FLOW = 6

RUN NUMBER: 9

TIME (MIN)	FLOW	1/X	FLOW PERCENT
7	.72	.2827206	.1234992
8	1.26	.3479984	.2161235
9	1.88	.4203497	.32247
10	2.46	.4923645	.4219554
11	3	.5677521	.5145798
12	3.49	.6475471	.5986278
13	3.9	.7271404	.6689537
14	4.26	.8117335	.7307033
15	4.55	.8951025	.780446
16	4.7	.9459649	.806175
17	5	1.072316	.8576329

DIFFUSION COEFFICIENT (cm<sup>2</sup>/sec.) = 2.767158E-09

PERMEABILITY COEFFICIENT (cm<sup>3</sup>/m<sup>2</sup>.day) = 36.48414

SOLUBILITY (cc O<sub>2</sub>/cc polymer) = 4.455934E-02

CORRELATION COEFFICIENT = .9986682

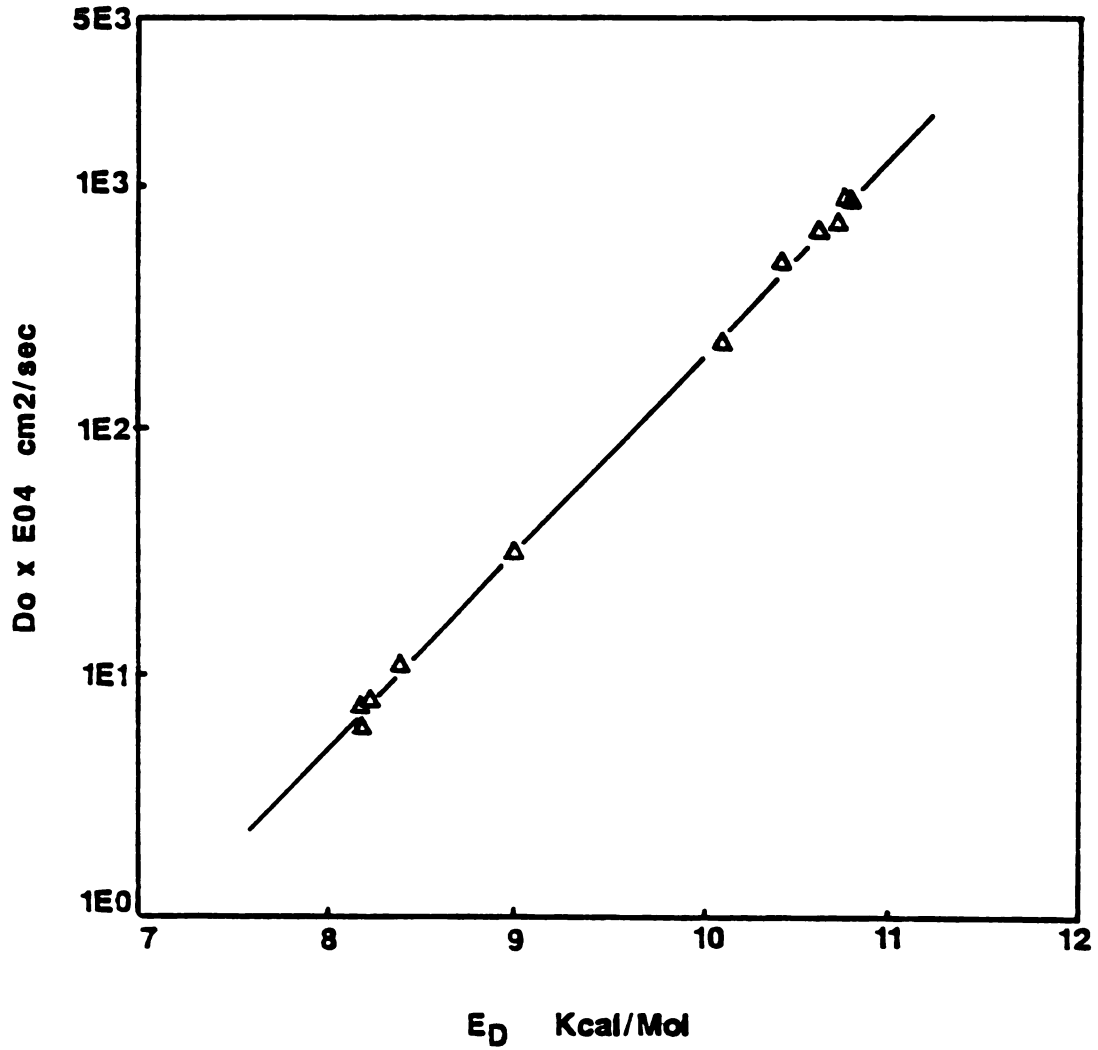
TEMPERATURE (C) = 40

WATER ACTIVITY, *a<sub>w</sub>* = .81

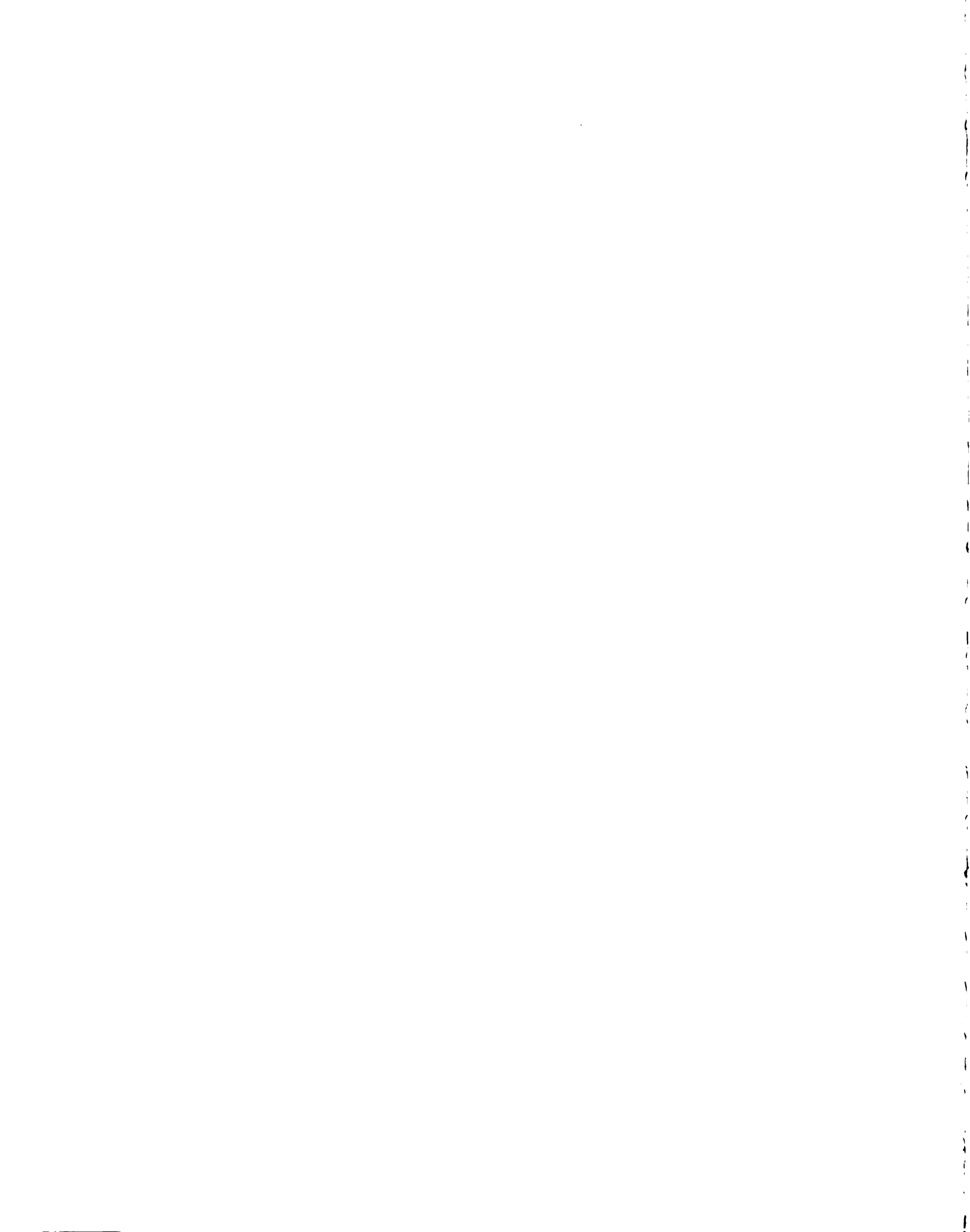
STEADY STATE FLOW = 5.83

Table of activation energy as a function of water activity.

Aw	Diffusion Coefficient xE10			- E <sub>D</sub>	D <sub>0</sub>
	cm <sup>2</sup> /sec.				
	11.9°C	22.0°C	40.3°C		
				Kcal/mol	
0	3.06	5.54	11.50	8.18	6.00E-4
0.05	3.55	7.19	13.65	8.22	7.70E-4
0.10	3.65	7.27	13.90	8.18	7.33E-4
0.15	3.65	7.36	14.38	8.39	1.07E-3
0.20	3.67	7.36	15.91	9.00	3.15E-3
0.30	3.70	8.00	19.12	10.10	2.23E-2
0.40	3.90	8.95	22.30	10.73	7.07E-2
0.50	4.30	9.45	24.08	10.64	6.50E-2
0.60	4.84	9.63	25.86	10.43	4.90E-2
0.75	4.91	9.89	27.56	10.74	8.58E-2
0.8	4.91	9.89	27.67	10.76	8.87E-2



Plot of the activation enrgy versus pre-exponential term  
for the diffusion process of oxygen in water/Nylon 6I/6T.



MICHIGAN STATE UNIV. LIBRARIES



31293005503432